

2007 - 1428

جامعة الحدود الشمالية

NORTHERN BORDER UNIVERSITY

المملكة العربية السعودية

مجلة الشمال للعلوم الأساسية والتطبيقية (JNBAS)

دورية علمية محكمة

تصدر عن

مركز النشر العلمي والتأليف والترجمة
جامعة الحدود الشمالية

المجلد الخامس – العدد الثاني

نوفمبر 2020م – ربيع الثاني 1442هـ

الموقع والبريد الإلكتروني

<http://jnbas.nbu.edu.sa>

s.journal@nbu.edu.sa & s.journal.nbu@gmail.com

طباعة - ردمد: 1658-7022 / إلكتروني - ردمد: 1658-7014

مجلة الشمال للعلوم الأساسية والتطبيقية (JNBAS)

التعريف بالمجلة

تعنى المجلة بنشر البحوث والدراسات العلمية الأصلية في مجال العلوم الأساسية والتطبيقية، باللغتين العربية والإنجليزية، كما تهتم بنشر جميع ما له علاقة بعرض الكتب ومراجعتها أو ترجمتها، وملخصات الرسائل العلمية، وتقارير المؤتمرات والندوات العلمية، وتصدر مرتين في السنة (مايو - نوفمبر).

الرؤية

الريادة في نشر البحوث العلمية المحكمة، وتصنيف المجلة ضمن أشهر الدوريات العلمية العالمية.

الرسالة

نشر البحوث العلمية المحكمة في مجال العلوم الأساسية والتطبيقية وفق معايير عالمية متميزة.

أهداف المجلة

- (1) أن تكون المجلة مرجعاً علمياً للباحثين في العلوم الأساسية والتطبيقية.
- (2) تلبية حاجة الباحثين إلى نشر بحوثهم العلمية، وإبراز جهوداتهم البحثية على المستويات المحلية والإقليمية والعالمية.
- (3) المشاركة في بناء مجتمع المعرفة بنشر البحوث الرصينة التي تؤدي إلى تنمية المجتمع.
- (4) تغطية أعمال المؤتمرات العلمية المحكمة.

شروط قبول البحث

- (1) الأصالة والابتكار وسلامة المنهج والاتجاه.
- (2) الالتزام بالمناهج والأدوات والوسائل العلمية المتبعة في مجاله.
- (3) الدقة في التوثيق والمصادر والمراجع والتخريج.
- (4) سلامة اللغة.
- (5) أن يكون البحث غير منشور أو مقدم للنشر في أي مكان آخر.
- (6) أن يكون البحث المستل من الرسائل العلمية غير منشور أو مقدم للنشر، وأن يشير الباحث إلى أنه مستل.

الإشتراك والتبادل

مركز النشر العلمي والتأليف والترجمة
جامعة الحدود الشمالية
ص.ب. 1321، عرعر، 91431
المملكة العربية السعودية.

للمراسلة

رئيس التحرير
مجلة الشمال للعلوم الأساسية والتطبيقية (JNBAS)
جامعة الحدود الشمالية
ص.ب. 1321، عرعر 91431
المملكة العربية السعودية.
هاتف: +966146615499
فاكس: +966146614439

البريد الإلكتروني: s.journal.nbu@gmail.com & s.journal@nbu.edu.sa

الموقع الإلكتروني: <http://jnbas.nbu.edu.sa>



شروط النشر

أولاً: ضوابط النص المقدم للنشر

- (1) ألا تزيد صفحاته عن (35) صفحة من القطع العادي (A4).
- (2) أن يحتوي على عنوان البحث وملخصه باللغتين العربية والإنجليزية في صفحة واحدة، بحيث لا يزيد عن (250) كلمة للملخص، وأن يتضمن البحث كلمات مفتاحية دالة على التخصص الدقيق للبحث باللغتين، بحيث لا يتجاوز عددها (6) كلمات، توضع بعد نهاية كل ملخص.
- (3) أن يذكر اسم المؤلف وجهة عمله بعد عنوان البحث مباشرة باللغتين العربية والإنجليزية.
- (4) أن تقدم البحوث العربية مطبوعة بخط (Simplified Arabic)، بحجم (14) للنصوص في المتن، وبالخط نفسه بحجم (12) للهوامش.
- (5) أن تقدم البحوث الإنجليزية مطبوعة بخط (Times New Roman) بحجم (12) للنصوص في المتن، وبالخط نفسه بحجم (9) للهوامش.
- (6) كتابة البحث على وجه واحد من الصفحة، مع ترك مسافة سطر واحد بين السطور، وتكون الحواشي 2.5 سم على الجوانب الأربعة للصفحة، بما يعادل 1.00 إنش (بوصة).
- (7) التزام الترتيب الموضوعي الآتي:
المقدمة: تكون دالة على موضوع البحث، والهدف منه، ومنسجمة مع ما يرد في البحث من معلومات وأفكار وحقائق علمية، كما تشير باختصار إلى مشكلة البحث، وأهمية الدراسات السابقة.
العرض: يتضمن التفاصيل الأساسية لمنهجية البحث، والأدوات والطرق التي تخدم الهدف، وترتب المعلومات حسب أولويتها.
النتائج والمناقشة: يجب أن تكون واضحة موجزة، مع بيان دلالاتها دون تكرار.
الخاتمة: تتضمن تلخيصاً موجزاً للموضوع، وما توصل إليه الباحث من نتائج، مع ذكر التوصيات والمقترحات.
- (8) أن تدرج الرسوم البيانية والأشكال التوضيحية في النص، وترقم ترقيماً متسلسلاً، وتكتب أسماؤها والملاحظات التوضيحية أسفلها.
- (9) أن تدرج الجداول في النص، وترقم ترقيماً متسلسلاً، وتكتب أسماؤها أعلاها، وأما الملاحظات التوضيحية فتكتب أسفل الجدول.
- (10) ألا توضع الهوامش أسفل الصفحة إلا عند الضرورة فقط، ويشار إليها برقم أو نجمة، ويكون الخط فيها بحجم (12) للعربي و (9) للإنجليزي.
- (11) لا تنشر المجلة أدوات البحث والقياس، وتقوم بحذفها عند طباعة المجلة.
- (12) أن يُراعى في منهج توثيق المصادر والمراجع داخل النص نظام (APA)، وهو نظام يعتمد ذكر الاسم والتاريخ (name/year) داخل المتن، ولا يقبل نظام ترقيم المراجع داخل النص مع وضع الحاشية أسفل الصفحة، وتوضع المصادر والمراجع داخل المتن بين قوسين حسب الأمثلة الآتية: يذكر اسم عائلة المؤلف متبوعاً بفاصلة، فسنة النشر، مثلاً: (مجاهد، 1988م). وفي حالة الاقتباس المباشر يضاف رقم الصفحة مباشرة بعد تاريخ النشر مثلاً: (خيري، 1985م، ص:33). أما إذا كان للمصدر مؤلفان فيذكران مع اتباع الخطوات السابقة مثلاً: (الفالح وعياش، 1424هـ). وفي حالة وجود أكثر من مؤلفين فتذكر أسماء عوائلهم أول مرة، مثلاً: (مجاهد والعودات والشيخ، 1408هـ)، وإذا تكرر الاقتباس من المصدر نفسه فيشار إلى اسم عائلة المؤلف الأول فقط، ويكتب بعده وآخرون مثل: (مجاهد وآخرون، 1408هـ)، على أن تكتب معلومات النشر كاملة في قائمة المصادر والمراجع.
- (13) تخرج الأحاديث والآثار على النحو الآتي:
(صحيح البخاري، ج:1، ص:5، رقم الحديث:511).
- (14) توضع قائمة المصادر والمراجع في نهاية البحث مرتبة ترتيباً هجائياً حسب اسم العائلة، ووفق نظام جمعية علم النفس الأمريكية (APA) الإصدار السادس، وبحجم (12) للعربي و(9) للإنجليزي، وترتب البيانات البليوغرافية على النحو الآتي:

• الاقتباس من كتاب لمؤلف واحد:

الخوجلي، أحمد. (2004م). *مبادئ فيزياء الجوامد*. الخرطوم، السودان: عزة للنشر والتوزيع.

- **الاقتباس من كتاب لأكثر من مؤلف:**
نيوباي، تيموثي؛ ستيبتش، دونالد؛ راس، جيمس. (1434هـ/2013م). *التقنية التعليمية للتعليم والتعلم*. الرياض، المملكة العربية السعودية: دار جامعة الملك سعود للنشر.
- **الاقتباس من دورية:**
النافع، عبداللطيف حمود. (1427هـ). أثر قيادة السيارات خارج الطرق المعبدة في الغطاء النباتي بالمنزهات البرية: دراسة في حماية البيئة، في وسط المملكة العربية السعودية. *المجلة السعودية في علوم الحياة*، 14 (1)، 53-72.
- **الاقتباس من رسالة ماجستير أو دكتوراه:**
القاضي، إيمان عبدالله. (1429هـ). *النباتات الطبيعية للبيئة الساحلية بين رأسي تنورة والملوح بالمنطقة الشرقية: دراسة في الجغرافيا النباتية وحماية البيئة*. رسالة دكتوراه غير منشورة، كلية الآداب للبنات، الدمام؛ المملكة العربية السعودية: جامعة الملك فيصل.
- **الاقتباس من الشبكة العنكبوتية (الإنترنت):**
- **الاقتباس من كتاب:**
المزروع—ي، م.ر. و المدني، م.ف. (2010م). *تقييم الأداء في مؤسسات التعليم العالي*. المعرف الرقمي (DOI:10.xxxx/xxxx-xxxxxxx-x)، أو برتوكول نقل النصوص التشعبي (<http://www...>)، أو الرقم المعياري الدولي للكتاب (ISBN : 000-0- 00 - 000000-0)
- **الاقتباس من مقالة في دورية:**
المدني، م.ف. (2014). مفهوم الحوار في تقريب وجهات النظر. *المجلة البريطانية لتكنولوجيا التعليم*، 11 (6)، 260-225. المعرف الرقمي (DOI:10.xxxx/xxxx-xxxxxxx-x) أو برتوكول نقل النصوص التشعبي (<http://www...>) (ISSN: 1467 - المجلة - الدولي للرقم المعياري التسلسلي الدولي للمجلة - 8535)
- 15) يلتزم الباحث بترجمة (أو رومنة) أسماء المصادر والمراجع العربية إلى اللغة الإنجليزية في قائمة المصادر والمراجع. وعلى سبيل المثال:
الجبر، سليمان. (1991م). تقويم طرق تدريس الجغرافيا ومدى اختلافها باختلاف خبرات المدرسين وجنسياتهم وتخصصاتهم في المرحلة المتوسطة بالمملكة العربية السعودية. *مجلة جامعة الملك سعود- العلوم التربوية*، 3 (1)، 170-143.
- Al-Gabr, S. (1991). The Evaluation of Geography Instruction and the Variety of its Teaching Concerning the Experience, Nationality, and the Field of Study in Intermediate Schools in Saudi Arabia (*in Arabic*). *Journal of King Saud University- Educational Sciences*, 3(1), 143-170.
- 16) تستخدم الأرقام العربية الأصلية (0، 1، 2، 3، ...) في البحث.
- 17) تؤول جميع حقوق النشر للمجلة في حال إرسال البحث للتحكيم وقبوله للنشر.

ثانياً: المرفقات المطلوب إرسالها للمجلة:

- 1) نسخة إلكترونية من البحث بصيغتي (WORD) و (PDF)، وترسلان على البريد الإلكتروني الآتي:
s.journal@nbu.edu.sa & s.journal.nbu@gmail.com
- 2) السيرة الذاتية للباحث، متضمنة اسمه باللغتين العربية والإنجليزية، وعنوان البريد الإلكتروني الحالي، ورتبته العلمية.
- 3) تعبئة النماذج الآتية:
 - أ - نموذج طلب نشر بحث في المجلة.
 - ب - نموذج تعهد بأن البحث غير منشور أو مقدم للنشر في مكان آخر.

ثالثاً: تنبيهات عامة

- 1) أصول البحث التي تصل إلى المجلة لا تردّ سواء نُشِرت أم لم تنشر.
- 2) الآراء الواردة في البحوث المنشورة تعبر عن وجهة نظر أصحابها.

المحتويات

الأبحاث الإنجليزية

- تأثير التركيب المعدني على إشعاعية صخور الجرانيت الحديث والبيجماتيت لمنطقة جبل الدُّب، شمالي الصحراء الشرقية، مصر
دعاء انور مصطفى، محمود هاني شلبي، إبراهيم عبد الناجي سالم، سمير محمد علي وأنس مالك الشريف 82
- دراسة للمقارنة بين معياري ضغط الفيديو: H.264 وترميز الفيديو عالي الكفاءة
محمد عبدالمنان بار 100
- السلوك الديناميكي لمعوض القدرة التفاعلية الثابت على رد الفعل أثناء أعطال الشبكة بما في ذلك محطة طاقة الرياح
عزالدين التوتي 116
- علاقة مؤشر كتلة الجسم والعمر والجنس مع كثافة المعادن بالعظام عند مرضى بمستشفى الملك فهد الجامعي
أسامة عبدالله مبروك خيرالله، علي عبدالكريم الغامدي، عرفات محمد غوجا، عادل عثمان بخيت، وسيد محمد سادات 132
- الحالة التغذوية للسيدات المصابات بسرطان الثدي
إكرام رجب سليمان، إيزيس عازر نوار، هبة جابر الشريدي، ومريم علي جنيحة 142

- License*. 1 (1). ISSN 2377-732X.
- Key, T.J., Schatzkin, A., Willett, W.C., Allen, N.E., Spencer, E.A. & Travis, R.C. (2004). Diet, nutrition and the prevention of cancer. *Public Health Nutr.*, 7(1), 187-200.
- Năsui, B., & Ciuciuc N (2013). Dairy products and red meat intake and the risk of breast cancer - a case-control study in females from Transylvania. *Palestrica of the Third Millennium Civilization & Sport*, 14(3), 171-174.
- Neuhouser, M.L., Aragaki, A.K., Prentice, R.L., Manson, J.E., Chlebowski, R. & Carty, C.L. (2015). Overweight, Obesity and Postmenopausal Invasive Breast Cancer Risk. *JAMA Oncol.*, 1(5), 611–621.
- Sulaiman, S., Shahril, M.R., Wafa, S.W., Shahrudin, S.H., & Hussin, S.N. (2014). Dietary carbohydrate, fiber, sugar, and risk of breast cancer according to menopausal status in Malaysia. *Asian Pac J Cancer Prev.*, 15(14), 5959-64.
- WHO. (2013). Breast Cancer, 91, 626–627.
- Szafranski, M. (2012). Weight Loss during Chemo. American Cancer Society, Retrieved from: <http://blogs.cancer.org/expertvoices/2012/01/24/weight-loss-during-chemo>
- Wallace, D.R. (2016). Natural Products as a Source of Anti-Cancer Lead Compounds: Ginger and Breast Cancer. USA. *J of Pharmacol & Clin Res.*, 1(3).
- Wu AH, Yu, M.C., Tseng, C.C., Hankin, J., & Pike, M.C. (2003). Green tea and risk of breast cancer in Asian Americans. *Int J Cancer*, 106 (4), 574-9.

4. CONCLUSIONS

From the results of the current study, it can be concluded that:

most of the patients drank a little of water, consumed lots of sugar, did not eat breakfast daily, did not eat vegetables and fruits daily, ate high-fat meat, chicken, and dairy products, and they rarely used healthy oil in cooking. From the results of this study, we can conclude that chemotherapy negatively affects the health status of the patients because it decreased their muscle mass and body weight and increased the liver enzymes, while hormone therapy caused the body weight gain of the patients.

5. RECOMMENDATION

From the results of the current study, it can be recommended that:

nutrition should be taken into consideration the prevention and treatment of cancer cases generally and breast cancer especially. Treatment of cancer patients should aim to maintain good nutrition and health status of the patients.

REFERENCES

- Al Hazah, H. M. (2010). Human Anthro Pometric (*In Arabic*), *In Nutrition Cyclopedia. Mosaiker, A. A. Studies and Researches Center* (EDs). Manama, Al Bahrain: International Academy.
- Amaral, P., Miguel, R., Mehdad, A., Cruz, C., Monteiro, G.I., Camilo, M., & Ravasco, P. (2010). Body fat and poor diet in breast cancer women. *Nutr Hosp.*, 25(3), 456-461.
- American Cancer Society. (2014). Breast Cancer. Retrieved from: <http://www.cancer.org/acs/groups/cid/documents/webcontent/003090-pdf.pdf>
- Bissonauth, V., Shatenstein, B., & Ghadirian, P. (2008). Nutrition and breast cancer among sporadic cases and gene mutation carriers: *An overview. Cancer Detection and Prevention*, 32(1), 52–64.
- Breastcancer, Org. (2018). Two New Genetic Mutations Linked to Higher Risk of Breast Cancer. Retrieved from: <http://www.breastcancer.org/research-news/two-new-genetic-mutations-linked-to-bc>.
- Ceccatto, Z., De Liz, S., Cardoso, A.L., Sabel, C., Gonzalez, D.A., da Silva, E.L., Galvan, D., & Di Pietro, P.F. (2015). Nutrition education may help prevent breast cancer reoccurrence, *Brazil- Journal of Nutrition*, 47(1).
- Chauhan, P., Yadav, R., Kaushal, V., & Beniwal, P. (2016). Evaluation of serum biochemical profile of breast cancer patients. *International Journal of Medical Research & Health Sciences*, 5(7), 1-7.
- Clinical Pharmacy Guide. (2015). Chemotherapy Assessment and Review (4th ed.). Hematology and Associated Laboratory Tests. *BC Cancer Agency*. 1-6.
- David, Y.B., Gesundheit, B., Urkin, J., & Kapelushnik, J. (2004). Water intake and cancer prevention. *J Clin Oncol*, 22(2), 383-5.
- Do, M.H., Lee, S.S, Jung, P.J., & Lee, M.H. (2007). Intake of Fruits, Vegetables, and Soy Foods in Relation to Breast Cancer Risk in Korean Women: A Case-Control Study. *Lawrence Erlbaum Associates, Inc.*, 57(1), 20–27.
- Egeberg, R., Olsen, A., Loft, S., Christensen, J., Johnsen, N.F., Overvad K., & Tjønneland, A. (2009). Intake of whole grain products and risk of breast cancer by hormone receptor status and histology among postmenopausal women. *Int J Cancer*, 124(3), 745-50.
- Erica, K. (2014). Global Cancer Fact Sheet. Retrieved from: <http://komensandiego.org/wp-content/uploads/2014/04/2014-Breast-Cancer-Fact-Sheet-6-10-14-FINAL.pdf>.
- Falasca M., Casari, I., & Maffucci, T. (2014). Cancer Chemoprevention with Nuts. *JNCI J Natl Cancer Inst.*, 106(9), 1 – 10.
- Ibrahim, A.S., Khaled, H.M., Mikhail, N.N., Baraka, H. & Kamel, H. (2014). Cancer Incidence in Egypt: Results of the National Population-Based Cancer Registry Program, Cairo, Egypt. *Journal of Cancer Epidemiology*, 7(1), 18.
- Jiang Y, Pan Y, Rhea, P.R, Tan, L., Gagea, M., Cohen, L., Fischer, S.M., & Yang, P. (2016). A Sucrose-Enriched Diet Promotes Tumorigenesis in Mammary Gland in Part through the 12-Lipoxygenase Pathway. *Cancer Res.*, 76, 24-29.
- Karim, S.A., Ghalib, H.H., Fattah, F.H., Gubari, M.I., & Majeed A.B. (2015). Height, weight, and body mass index association with breast cancer risk in Iraqi Kurdish women. *Creative Commons Attribution 3.0*

with hormonal therapy at the beginning was 3.84(10^6 cell/ml), and one month later it increased to 3.91, the differences were significant at $p \leq (0.05)$. and the average of PLT of patients who were treated with chemotherapy at the beginning of taking results was 309.3(billion/L) and one month later it decreased to 280.9(billion/L) the differences were not significant. While the average of PLT of patients who were treated with hormonal therapy at the beginning of taking results was 307.2(billion/L) and one month later it increased to 323.7(billion/L) the differences were not significant. The Hb average of patients who were treated with chemotherapy at the beginning of taking results was 11.5(g/dl) and one month later it decreased to 11.2, g/dl) the differences were not significant. While the average of Hb of patients who were treated with hormonal therapy at the beginning of taking

results was 11.4 g/dl) and one month later it increased to 11.6 the differences were significant at $p \leq (0.05)$. Haematologic toxicity is a major dose-limiting side effect of cytotoxic chemotherapy drug administration. Since bone marrow cells proliferate continuously and a majority of chemotherapy drugs have their greatest effect on rapidly growing cells, suppression of bone marrow activity (myelosuppression) is prevalent. Myelosuppression is the most common cause of treatment delays and dose reductions in cancer patients receiving chemotherapy. Myeloid stem cells are the precursors to neutrophils, monocytes, platelets, and red blood cells; therefore, myelosuppression leads to a reduction in the number of white blood cells (WBCs), platelets, and red blood cells (RBCs) (Clinical Pharmacy Guide,2015).

Table 7: Percentage distribution of the patients according to Mean and SD of AST, ALT, Urea, Creatinine and Blood Picture during chemotherapy treatment

Items	Chemotherapy				Normal
	The beginning $\bar{X} \pm SD$	After month $\bar{X} \pm SD$	difference	T	
AST	36.6 ± 43.1	47.3 ± 58.6	10.7	2.1*	< 35 IU/L
ALT	30.5 ± 18.8	40.0 ± 25.9	9.5	2.045*	< 35 IU/L
Urea	29.1 ± 12.9	27.1 ± 11.4	-2	1.146	20-40 mg/dL
Creatinine	.98 ± .38	0.83 ± .16	-15	1.336	0.5 - 1.4 mg/dL
WBC	4.9 ± 1.5	4.2 ± 2.4	-.7	1.333	4,500 -10,500 (cells/ml)
RBC	3.89±.55	3.63±.63	-.26	2.66**	4.0 - 4.9 (x 10^6 /ml)
PLT	309.3 ± 128.9	280.9 ± 118.4	-28.4	0.681	100-450 billion/L
Hb	11.5 ± 1.6	11.2 ± 2.0	-.3	1.2	12.0 - 15.0 (g/dl)

* Significant at the 0.05 level
 ** Significant at the 0.01 level

Table 8: Percentage distribution of the patients according to Mean and SD of AST, ALT, Urea, Creatinine and Blood Picture during hormonal therapy treatment

Items	Hormonal therapy				Normal
	The beginning $\bar{X} \pm SD$	After month $\bar{X} \pm SD$	difference	T	
AST	20.7 ± 6.3	18.4 ± 3.9	-2.3	2.1*	< 35 IU/L
ALT	18.1 ± 13.2	17.0 ± 13.1	-1.1	1.136	< 35 IU/L
Urea	24.1 ± 7.0	22.0 ± 7.2	-2.1	2.4*	20-40 mg/dL
Creatinine	.90 ± .17	.87 ± .19	-0.3	1.29	0.5 - 1.4 mg/dL
WBC	5.07 ± 1.7	5.0 ± 1.3	-0.07	0.48	4,500 -10,500 (cells/ml)
RBC	3.84 ± .43	3.91± .42	0.07	2.55*	4.0 - 4.9 (x 10^6 /ml)
PLT	307.2 ± 72.4	323.7 ± 70.6	1.5	1.52	100-450 billion/L
Hb	11.4 ± 1.1	11.6 ± 1.0	.2	2.0*	12.0 - 15.0 (g/dl)

* Significant at the 0.05 level

Women who were overweight and obese had increased invasive breast cancer risk vs. normal-weight women. The risk was greatest for obesity grades 2+3 (BMI>35.0 kg/m²). BMI \geq 35.0 kg/m² was strongly associated with risk for ER+/PR+ breast cancers. Obesity grade 2+3 was also associated with advanced disease including larger tumor size, positive lymph nodes, and deaths after breast cancer. Women with baseline BMI<25.0 kg/m² who gained >5% of body weight over the follow-up period had an increased breast cancer risk, but among women already overweight or obese we found no association of weight change (gain or loss) with breast cancer during follow-up. There was no effect modification of the BMI-breast cancer relationship by postmenopausal hormone therapy (HT) and the direction of association across BMI categories was similar for never, past, and current HT use (Neuhouser, Aragaki, Prentice, Manson, Chlebowski, Carty, et al 2015).

A review of published studies, concentrating on recent systematic reviews, meta-analyses, and large prospective studies showed that Overweight/obesity increases the risk for cancers of the esophagus (adenocarcinoma), colorectum, breast (postmenopausal), endometrium, and kidney; body weight should be maintained in the body mass index range of 18.5-25 kg/m², and weight gain in adulthood should be avoided (Key, Aragaki, Prentice, Manson, Chlebowski, Carty, 2004).

3.4 Hematological and Biochemical Measurements

The Tables (7) and (8) refer to the distribution of the study sample according to laboratory tests. The results show the mean and SD of AST, ALT, Urea, Creatinine, and Blood Picture during treatment.

The data in Tables (7) and (8) show that the average AST (IU/ L) of patients who were treated with chemotherapy at the beginning of the study was 36.6, and one month later increased to 47.3, the differences were significant at $p \leq (0.05)$. While, the average AST of patients who treated with hormonal therapy at the beginning was 20.7, and one month later decreased to 18.4, the differences were significant at $p \leq (0.05)$.

The data in Tables (7) and (8) show that the average of ALT of patients who treated with chemotherapy at the

beginning was 30.5, and one month later it increased to 42.0 the differences were significant at $p \leq (0.05)$. While, the average ALT of patients who treated with hormonal therapy at the beginning was 18.1, and one month later it decreased to 17, the differences were non-significant.

The data in tables (7) and (8) show that the average of serum urea for the patients who were treated with chemotherapy was 29.1, and 27.1 (mg/ dl) at the beginning and one month later respectively the differences were non-significant. While, the average of urea of patients who treated with hormonal therapy at the beginning was 24.1, and one month later it decreased to 22 the differences were significant at $p \leq (0.05)$.

The data in Tables (7) and (8) show that the average serum creatinine of patients who treated with chemotherapy was 0.98(mg/ dl) and 0.83 (mg/ dl) at the beginning and one month later respectively the differences were no significant. While, the average creatinine of patients who treated with hormonal therapy was 0.90 (mg/dl), and one month later it decreased to 0.87(mg/ dl), the differences were not significant.

These results are in agreement with some researchers who found a decreasing pattern of blood urea nitrogen level was noted during chemotherapy treatment as a non-significant value. No specific alterations were observed in the creatinine level during the different courses of chemotherapy. However, Aspartate aminotransferase (AST or SGOT) level increases as the courses of chemotherapy further proceeds and increased alanine aminotransferase (ALT or SGPT) level indicate the improper liver function (Chauhan, Yadav, Kaushal, and Beniwal, 2016).

Also, this study indicates the average WBC of patients who were treated with chemotherapy at the beginning was 4.9(cell/ ml), and one month later it decreased to 4.2(cell/ ml), the differences were not significant. While, the average WBC of patients who were treated with hormonal therapy at the beginning was 5.07, and one month later it decreased to 5, the differences were not significant. Also, the average RBC of patients who were treated with chemotherapy at the beginning was 3.89(10^6 /ml) and one month later it decreased to 3.63(10^6 /ml) the differences were significant at (0.01). While, the average RBC of patients who were treated

increased risk of breast cancer. There was a positive association between BMI and breast cancer risk for both pre- and postmenopausal women, but the

association was stronger among postmenopausal women (Karim, Ghalib, Fattah, Gubari, and Majeed 2015).

Table 5: Percentage distribution of the patients according to height, weight, BMI, arm circumference, and triceps during chemotherapy treatment

Items	Chemotherapy (n =30)				Normal
	The beginning $\bar{X} \pm SD$	After month $\bar{X} \pm SD$	difference	T	
Height (cm)	160.7 ± 6.1				163 cm
Weight (kg)	80.13 ± 10.9	76.5 ± 11.7	- 3.63	3.2**	57 kg
BMI	31.1 ± 4.7	27.42± 5.0	- 3.68		21.5
Arm (cm)	35.8 ± 4.1	34.20± 4.1	- 1.6	1.6	
Triceps (mm)	27.3 ± 5.0	25.30± 5.6	- 2	1.084	

* Significant at the 0.05 level

** Significant at the 0.01 level

Table 6: Percentage distribution of the patients according to height, weight, BMI, arm circumference, and triceps during hormonal therapy treatment

Items	Hormonal therapy (n=30)				Normal
	The beginning $\bar{X} \pm SD$	After month $\bar{X} \pm SD$	difference	T	
Height (cm)	159.5 ± 6.8				163 cm
Weight (kg)	83.7 ± 16.2	84.9 ± 16.5	1.2	3.413**	57 kg
BMI	33.0 ± 6.0	33.43 ± 6.0	0.43	2.595*	21.5
Arm (cm)	36.6 ± 5.0	37.8 ± 5.0	1.2	3.077**	
Triceps (mm)	31.3 ± 7.9	32.7 ± 8.2	1.2	1.418	

* Significant at the 0.05 level

** Significant at the 0.01 level

Concerning the average of arm circumference of patients who treated with chemotherapy at the beginning was 35.8, and one month later it decreased to 34.20, the differences were no significant, and the average of arm circumference of patients who treated with hormonal therapy at the beginning was 36.6, and one month later it increased to 37.8, the differences were significant at (0.01).

Concerning the average of arm Triceps of patients who treated with chemotherapy at the beginning was 27.3, and one month later it decreased to 25.3, the differences were not significant, and the average of Triceps of patients who treated with hormonal therapy at the beginning was 31.3, and one month later it increased to 32.7 the differences were not significant.

Continued table 4: Percentage distribution of the patients according to food frequency

Statement	Options	Daily		Weekly		Monthly		Never		Total	
		N	%	N	%	N	%	N	%	N	%
Dairy products	Skimmed milk	2	1.7					118	98.3	2	1.7
	Full-fat milk	98	81.7	4	3.3			18	15	102	85
	Yogurt	12	10	40	33.3	8	6.7	60	50	60	50
	Ice cream			22	18.3	30	25	68	56.7	52	43.3
	Low-fat cheese	2	1.7	34	28.3	34	28.3	50	41.7	70	58.3
	Medium-fat cheese	34	28.3	68	56.7	4	3.3	14	11.7	106	88.3
	High-fat cheese	40	33.3	66	55	2	1.7	12	10	108	90
Fats and oil group	olive oil	2	1.7					118	97.3	2	1.7
	Mix oil*	86	71.7					34	28.3	86	71.7
	Flaxseed oil							120	100		
	Corn, Sunflower oil	36	30					84	70	36	30
	Animal fats	32	26.7	2	1.7			86	71.7	34	28.3
	Margarine	82	68.3					38	31.7	82	68.3

Mix oil* (Blended edible refined oil from sunflower and soybean oil)..

The Table (4) shows that most of the patients (81.7%) were drinking full-fat milk daily, but (98.3%) never drink skimmed milk, (33.3%) were eating yogurt weekly, but (50%) never eat yogurt, and (56.7%) were eating medium-fat cheese weekly, and (55%) were eating high-fat cheese weekly.

The most of patients (71.7%) cooked with mix oil, and (68.3%) cooked with margarine but (97.3%) never used olive oil, and (100%) never used flaxseed oil. The results indicated that most of the patients ate high-fat dairy products and they rarely used healthy oil in cooking.

Food intake may have a role in preventing breast cancer. Evidence suggests that fruits and vegetables, low-fat dairy products, fish, monounsaturated and polyunsaturated fatty acids, vitamin D, calcium, and phytoestrogens may reduce the risk of breast cancer. However, a high intake of meat, poultry, total energy, total fat, and saturated fatty acids may play a causative role in this disease (Bissonauth, *et al.*, 2008).

3.3 Nutritional Assessment

The data in Tables (5) and (6) show that the average patient's weight who treated with chemotherapy was 80.1 kg at the beginning, and one month later it decreased to 76.5 kg, the differences were significant at (0.01). Weight loss is one of the most common side effects of chemotherapy. Nausea and vomiting caused by many of the drugs dampen a patient's appetite (Szafranski,2012). While, the average weight of patients who treated with hormonal therapy at the beginning was 83.7 kg, and one month later it increased to 84.9 kg, the differences were significant at (0.01).

Also, the average BMI of patients who were treated with chemotherapy at the beginning was 31.10, and one month later it decreased to 27.42, the differences were significant at (0.01). While the average BMI of patients who were treated with hormonal therapy at the beginning was 33 and one month later was 33.43, the differences were significant at $p \leq (0.05)$. Height, weight, and BMI were associated with an

3.2.3 Food Frequency

Table (4) shows that all of the patients (100%) were eating balady bread daily, (78.3%) were eating rice weekly, (76.7%) were eating pasta weekly, (73.7%) ate boiled potatoes weekly, (95%) ate French fries weekly, but (93.3%) never eat cornflakes. These results indicate that balady bread is the main source of carbohydrate. In conclusion, intake of whole-grain products was not associated with the risk of breast cancer in a cohort of Danish postmenopausal women (Egeberg, Olsen, Loft, Christensen, Johnsen, Overvad, and Tjønneland 2009). The results indicate that half of the patients (50%) were eating leafy vegetables weekly, (61.7%) were eating tuberous vegetables weekly, (86.7%) were eating fresh vegetables weekly, (75%) were eating

salad weekly, and (56.7%) ate fresh fruit weekly. The results indicate that most patients didn't eat vegetables and fruits daily. The evidence suggested that high consumption of grapes, tomatoes, and soybeans could have a significant protective effect against breast cancer in Korean women (Do, Lee, Jung, and Lee 2007). The data shows that almost all of the patients (96.7%) weren't eating low-fat meat, but (45%) were eating high-fat meat weekly. The study of (Nāsui and Ciuciuc, 2013) highlights the importance of decreasing the consumption of dietary high-fat animal products to prevent breast cancer risk.

(46.7%) ate chickens with skin weekly, (93.3%) ate fish weekly, (63.3%) ate legumes weekly, and (55%) ate kidney and liver weekly. The results indicated that most of the patients ate high-fat meat and chicken.

Table 4: Percentage distribution of the patients according to food frequency

Groups N= 120	Options	Daily		Weekly		Monthly		Never		Total	
		N	%	N	%	N	%	N	%	N	%
Bread and cereals	Balady bread	120	100							120	100
	Rice	18	15	94	78			8	6.7	112	93.3
	Pasta			92	77	18	15	10	8.3	110	91.7
	Baking products	12	10	36	30	28	23	20	16.7	100	83.3
	Peas			66	55	25	42	4	3.3	116	96.7
	Boiled potatoes			88	74	24	20	8	6.7	112	93.3
	French fries			114	95	6	5			120	100
	Cornflakes			2	1.7	6	5	112	93.3	8	6.7
Vegetables and fruit	Leafy Vegetables	34	28.3	60	50	14	12	12	10	108	90
	Tuberous vegetables			74	62	34	28	12	10	108	90
	Fresh vegetables	10	8.3	104	87	6	5			120	100
	Frozen Vegetables			24	20	4	3.3	92	76.7	28	23.3
	Salad	20	16.7	90	75	4	3.3	6	5	114	95
	Fresh fruits	34	28.3	68	57	18	15			120	100
	Kiwi	2	1.7	26	22	4	3.3	88	73.3	32	26.7
	Pomegranate			58	48	18	15	44	36.7	76	63.3
	Grapes	2	1.7	80	67	20	17	18	15	102	85
Meat, legumes, and chickens	Low-fat meat			4	3.3			116	96.7	4	3.3
	medium-fat meat			6	27	16	13	72	60	48	40
	high-fat meat			54	45	14	12	52	43.3	68	56.7
	chickens with skin			56	47	4	3.3	60	50	60	50
	Skinless chickens			54	45	4	3.3	58	48.3	62	51.7
	Fish			112	93	2	1.7	6	5	114	95
	Salmon and tuna			32	27	40	33	72	60	48	40
	Crustaceans			4	6.7	24	40	32	53.3	28	46.7
	Eggs	54	45	58	48	6	5	2	1.7	118	98.3
	Legumes	18	15	76	63	16	13	10	8.3	110	91.7
	liver and kidneys			66	55	22	18	32	26.7	88	73.3

diagnosed histologically confirmed breast cancer (n = 44) with controls (n = 55) with non-neoplastic conditions and no history of malignancies in the same hospital for their dietary food and beverage consumption. In logistic regression analysis, water drinking appeared strongly inversely, and significantly associated with breast cancer risk. The unadjusted OR for water drinking was 0.31 (95% CI, 0.13 to 0.72), which remained unaltered after age adjustment. This risk estimate represented a 4.7-fold difference in the odds of exposure between cases and controls. The authors stated that water intake may play a role in limiting carcinogenesis via water requirement-related mechanisms. They hypothesized that subclinical or “chronic” dehydration may compromise intracellular water, alter cellular concentrations, affect the activity of enzymes in metabolic regulation, and inhibit cellular carcinogen removal (David et al., 2004).

3.2.2 Beverages

Table (3) shows that (31.6%) didn't drink canned juices, (26.7%) rarely did that, while (16.7%) always did that. While more than half of the patients (61.7%) always drank natural juices, (20%) sometimes did that, while (5%) didn't do that. Most of the patients (71.7%) didn't drink

ginger, (10%) always or sometimes did that, while (8.3%) rarely did that. Wallace, (2016) conducted that biologically active components of ginger consist of gingerols, zingerones, shogaols, and zerumbone which demonstrate anti-cancer effects in a variety of cancer cell lines. Also, most of the patients (73.4%) didn't drink cinnamon, while (10%) only did that. About (36.7%) always drank herbal beverages, but (26.6%) of the patients didn't do that, while (16.7%) rarely did that. Also, most of the patients (81.6%) didn't drink green tea, but only (5%) always did that. Most of the patients (75%) always drank black tea, while (3%) rarely did that. The risk of breast cancer was not related to black tea consumption. In contrast, green tea drinkers showed a significantly reduced risk of breast cancer (Wu,2003). Data in Table (3) indicates that (43.3%) of the patients always drank Nescafe, (31.7%) didn't do that, while (6.7%) rarely they did. Besides, more than half of the patients (60%) didn't drink coffee, but only (10%) sometimes or rarely did that. Also, half of the patients (50%) didn't drink cocoa, (25%) sometimes, while (10%) rarely did that. About more than half the patients (60%) always drink soft drink, (18.3%) sometimes did that, while (10%) didn't drink soft drinks. Most of the patients drink unhealthy drinks such as (soft drinks, Nescafe).

Table 3: Percentage distribution of the patients according to Favourite drinks

Statement	Always		Sometimes		Rarely		Never		Total	
	N	%	N	%	N	%	N	%	N	%
Favorite drinks										
Canned juices	20	16.7	30	25	32	26.7	38	31.6	120	100
Fresh juices	74	61.7	24	20	16	13.3	6	5	120	100
Ginger	12	10	12	10	10	8.3	86	71.7	120	100
Cinnamon	12	10	10	8.3	10	8.3	88	73.4	120	100
Herbal beverages	44	36.7	24	20	20	16.7	32	26.6	120	100
Green tea	6	5	8	6.7	8	6.7	98	81.6	120	100
Black tea	90	75	8	6.7	6	5	16	13.3	120	100
Nescafe	52	43.3	22	18.3	8	6.7	38	31.7	120	100
Coffee	24	20	12	10	12	10	72	60	120	100
Cocoa	18	15	30	25	12	10	60	50	120	100
Soft drinks	72	60	22	18.3	14	11.7	12	10	120	100

Type of Snacks	Always	14	11.6
Nuts	Sometimes	38	31.7
	Rarely	38	31.7
	Never	30	25
	Total	120	100
Vegetables and Fruits	Always	74	61.7
	Sometimes	44	36.6
	Rarely	2	1.7
	Never	0	0
	Total	120	100
Snacks food (chips, biscuits,	Always	32	26.7
	Sometimes	32	26.7
	Rarely	14	11.7
	Never	42	35
	Total	120	100
Sweets	Always	54	45
	Sometimes	42	35
	Rarely	14	11.7
	Never	10	8.3
	Total	120	100
Amount of drinking water	little (less than 6 cups)	80	66.7
	Medium (6-8 cups)	16	13.3
	a lot (more than 8)	24	20
	Total	120	100
Sugar (tablespoon)	1	4	3.3
	2	10	8.3
	3	18	15
	4	20	16.7
	more than 4	68	56.7
	Total	120	100

The population-based case-control study was conducted in Malaysia with 382 breast cancer patients and 382 controls. The food intake pattern was assessed via an interviewer-administered food frequency questionnaire. A significant two-fold increased risk of breast cancer among premenopausal and postmenopausal women was observed in the highest quartile of sugar. A higher intake of dietary fiber was associated with a significantly lower breast cancer risk among both

premenopausal and postmenopausal women. The results show that sugar and dietary fiber intake were independently related to pre- and postmenopausal breast cancer risk. However, no association was observed for dietary carbohydrate intake (Sulaiman, Shahril, Wafa, Shahrudin, & Hussin, 2014). David et al. (2004) conducted that a hospital-based case-control study to investigate the hypothesis that water drinking protects against breast cancer. They compared a group of women with newly

3.2 Food Habits

3.2.1 Food

The data in Table (2) indicates that the majority of the patients (75%) were eating three meals every day, while only (25%) of the patients were eating two meals only every day. Most of the patients (88.3%) said that the most important meal was lunch, (6.7%) was dinner, and (5%) was breakfast.

The results show that (16.7%) of patients didn't eat snacks between meals, more half (58.3%) ate two snacks between meals daily, while (5%) ate three snacks between meals daily.

Concerning the data of the type of snacks in the table (2) show that (31.7%) of the patients ate nuts sometimes or rarely, (25%) didn't eat nuts, while (11.6%) always eat it. Some studies have suggested that nut consumption is associated with reduced cancer mortality (Falasca, Casari, and Maffucci, 2014).

About (61.7) always ate vegetables and fruits, while (1.7%) did that rarely. Also, it is found that (35%) of them didn't eat a snack such as chips, biscuits, and other junk food, (53.4%) always and sometimes eat these foods, while (11.7%) rarely eat it. About (45%) of patients always eat sweets between meals, (35%) did that sometimes, but only (11.8%) didn't eat any

sweets between meals, and (8.3%) never eat it.

Also, the data in Table (2) indicates that (66.7%) of the patients drunk a little water (less than 6 cups), while (20%) drank a lot of water (more than 8 cups). David, Gesundheit, Urkin, & Kapelushnik, (2004) stated that water intake may play a role in limiting carcinogenesis. They hypothesized that subclinical or "chronic" dehydration may compromise intracellular water, alter cellular concentrations, affect the activity of enzymes in metabolic regulation, and inhibit cellular carcinogen removal. Also, (56%) of the patients consumed a lot of sugar (more than 4 spoons) daily, while (3.3%) consumed one spoon of sugar daily. The high amounts of dietary sugar in the typical Western diet may increase the risk of breast cancer and metastasis to the lungs, according to a study at The University of Texas MD Anderson Cancer Center (Jiang, Pan, Rhea, Tan, Gagea, Cohen, Fischer, and Yang, 2016).

Throughout 2006, 71 consecutive women with breast cancer in University Hospital Santa Maria, Portugal, mean age was 60 ± 12 (36-90) years. Food frequency analysis showed a low intake of vegetables and wholegrain cereals rich in complex carbohydrates (sources of fiber and phytochemicals), of fatty fish & nuts, primary sources of n-3 PUFA's and a high intake of saturated fat (Amaral, Miguel, Mehdad, Cruz, Monteiro, Camilo & Ravasco, 2010)

Table 2: Percentage distribution of the patients according to food habits

Statement	Options	N	%
Number of meals	Two meals	30	25
	Three meals	90	75
	Total	120	100
The most important meal	Dinner	8	6.7
	Lunch	106	88.3
	Breakfast	6	5
	Total	120	100
Number of Snacks	no snacks	20	16.7
	One	24	20
	Two	70	58.3
	Three	6	5
	Total	120	100

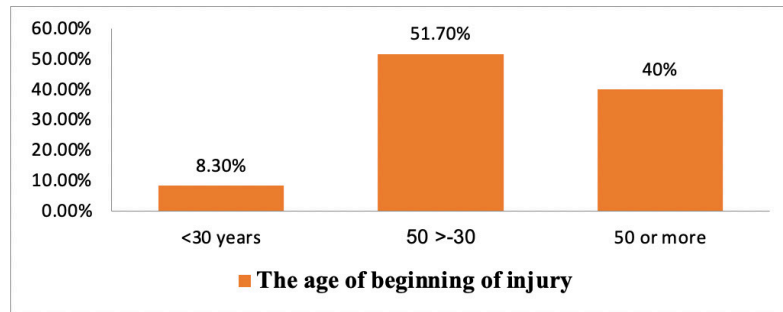


Figure 1: Percentage distributions of patients according to the age of beginning of the injury

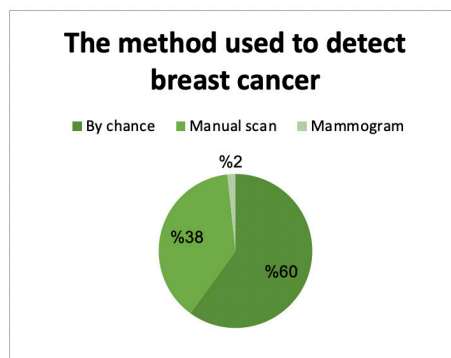


Figure 2: Percentage distributions of patients according to the method used to detect breast cancer

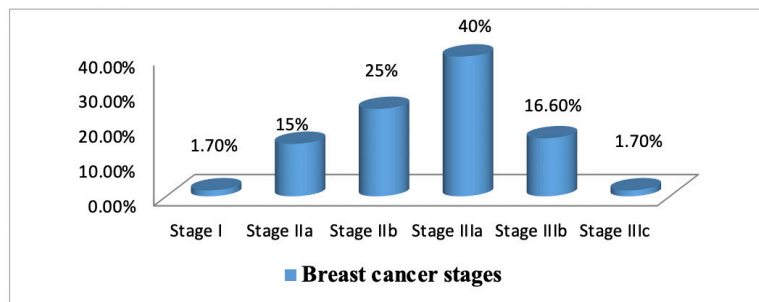


Figure 3: Percentage distributions of patients according to breast cancer stages

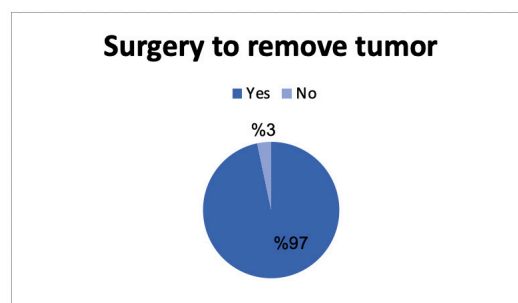


Figure 4: Percentage distributions of patients according to surgery to remove the tumor

while (16.7%) worked. Half (50%) of employed patients were laborers, (30%) were working in government, and only (20%) were working in private sectors. Most of the patients (95%) were living in cities, and about two-thirds of them (65%) were living in low neighborhoods. The results in Table (1) indicate that more than half of the patients their family size was (3-

5) person and only (13.3%) was less than 3, while (26.7%) had 4 or more children and only (8.3%) had no children. The half of patients in this study (50%) their monthly income was less than 1000, (40%) was 1000(EGP Pound)to less than 2000, and only (1.7%) was 3000 to less than 4000. The mean ranged from 728.5 – 1332.

Continued Table 1: Percentage distribution of the patients according to some demographic characteristics

Demographic Characteristics	Options	N	%
Family Size	less than 3	16	13.3
	5—3	76	63.3
	6 – 8	28	23.4
	Total	120	100
Number Of Children	1	18	15
	2	30	25
	3	30	25
	4 or more	32	26.7
	No	10	8.3
	Total	120	100
Monthly Income (EGP)	< 1,000 pounds	60	50
	1000 - < 2000	48	40
	2000 -< 3000	10	8.3
	3000 - < 4000	2	1.7
	Total	120	100
	(\bar{X}) \pm SD	1332 \pm 728.5	

The data in (Fig. 1) indicates that more than half of the patients (51.7%) their age at the beginning of injury ranged from 30 years to less than 50, (40%) were 50 years old or more, and only (8.3%) were less than 30 years. Figure (2) show that more than half of the patients (60%) discovered cancer by chance, (38.3%) by manual scan, and only (1.7%) by the mammogram. Concerning the breast cancer stages, the data in Figures (3, and 4) indicates (40%) of the patients were in stage IIIa, (25%) were in stage IIb, and (1.7%) only

were in stage I or in stage IIIc.

Cancer staging is based on the size of cancer, whether the cancer is invasive or non-invasive, whether lymph nodes are involved, and whether cancer has spread to other places beyond the breast as described by (Breastcancer.org.,2018).

The data indicates that half of the patients (50%) treated by chemotherapy and (50%) treated by hormone therapy. Most patients (97%) removed the tumor.

Table 1: Percentage distribution of the patients according to some demographic characteristics

Demographic Characteristics	Statement	N	%
Age (yrs.)	25-35 years	18	15
	36-45	24	20
	46-55	42	35
	56-65	26	21.7
	66 or more	10	8.3
	Total	120	100
	$\bar{X} \pm SD$	49.4 \pm 11.4	
Marital Status	Single	2	1.7
	Married	106	88.3
	Divorced	4	3.3
	Widow	8	6.7
	Total	120	100
Education Level	Illiterate	50	41.7
	read and write	46	38.3
	Mediate	16	13.3
	University	8	6.7
	Total	120	100
Occupation	Work	20	16.7
	Does not work	100	83.3
	Total	120	100
Type of Job	Laborers	10	50
	Gov. Employee	6	30
	Private Employee	4	20
	Total	20	100
Residence	City	114	95
	Village	6	5
	Total	120	100
Neighborhood	Low	78	65
	Mediate	40	33.3
	High	2	1.7
	Total	120	100

play a causative role in this disease (Bissonauth, Shatenstein & Ghadirian, 2008).

In a relatively new study, researchers from the Federal University of Santa Catarina provided eighteen Brazilian breast cancer patients with nutrition education for 12 months as compared with a 75-patient control group. The main goals of the nutrition education were to reduce the patients' consumption of red and processed meat which harm cancer patients and increase fruit and vegetable intake which have antioxidant effects that have been shown to reduce the aggravating effects of chemotherapy treatment and, consequently, may reduce the risk of breast cancer recurrence. The results showed that significant reductions in red and processed meat as well as increased fruit and vegetable intake among the experimental group concerning their peers in the comparison group, who had two times greater body weight increase during the study and three times BMI (Ceccatto., De Liz, Cardoso, Sabel, Gonzalez, da Silva, Galvan & Di Pietro, 2015).

Aim of the study

This study aimed to study the nutritional and health status of breast cancer female patients.

2. MATERIAL AND METHODS

2.1. Materials

An intended sample comprising 120 breast cancer female patients, chosen from (Cancer management and research department - Medical Research Institute, Alexandria University). The information of 60 patients was collected during the hormonal therapy and another 60 cases their information was collected during chemotherapy. The anthropometric and biochemical measurements were carried in 30 patients before the start of chemotherapy and in another 30 patients before the start of hormonal treatment. The measurements were repeated after one month from the start of chemotherapy and hormonal treatment. Metastatic cases and patients with advanced breast cancer at presentation

were excluded from the study. The relevant data were collected from using designed a special questionnaire by interview.

2.2 Type of Treatment Received by Patients

1. Chemotherapy (anthracyclines- based treatment) for 6 cycles every 21 days.
2. Hormonal treatment for patients with hormonal receptors (either tamoxifen or aromatase inhibitors) in the form of daily tablets.

2.3 Nutritional Status

Included food frequency and nutritional assessment height (cm), weight (kg), body mass index (BMI), Mid-upper arm circumference (MUAC)cm, and subcutaneous fat thickness (Triceps)mm. according to (Al Hazah, 2010).

2.4 Biochemical Measurements

These measurements were done by specialists in the hospital. It included ALT, AST, Urea and Creatinine, and Hb, WBC, RBC, and Platelets.

2.5 Statistical Analysis

The data were tabulated and statistically analyzed using descriptive analysis, percentage, mean and Standard deviation as well as t-test between variables using the (SPSS version 14.0).

3. RESULTS AND DISCUSSION

3.1 Demographic Characteristics of Patients

The data in (Table 1) indicates that (70%) of the sample their ages were less than 56 years, while (30%) their ages were 56 years or more.

The results of education level indicate that (41.75%) of the patients were illiterate, and (38.3%) of them could read and write, but the patients with medium educations were (13.3%), while (6.7%) of them were university graduates.

Most of the patients (83.3%) were unemployed,

1. INTRODUCTION

There has been great interest in cancer in general and breast cancer in particular since the last few decades of the twentieth century. Nearly 40 years ago, the former first lady of the United States of America (USA), Betty Ford, announced to the world that she had been diagnosed with breast cancer and would undergo a radical mastectomy to remove the tumor. Ford's brave decision to make her diagnosis public broke the silence around the disease and prompted millions of women to go for screening. And, as they did, detection rates in the USA rose sharply. Researchers called it the "Betty Ford blip" (WHO, 2013).

Breast cancer is a malignant tumor that starts in the cells of the breast. A malignant tumor is a group of cancer cells that can grow into (invade) surrounding tissues or spread (metastasize) to distant areas of the body. The disease occurs almost entirely in women, but men can get it, too (American Cancer Society, 2014).

Around 5% to 10% of breast cancer cases are thought to be hereditary, caused by abnormal genes passed from parent to child. Most inherited cases of breast cancer are associated with two abnormal genes: *BRCA1* (Breast cancer gene one) and *BRCA2* (Breast cancer gene two), (Breastcancer.org, 2018).

Breast cancer is the most common cancer among women and the 2nd most common cancer overall. It is estimated that nearly 1.7 million new cases of breast cancer were diagnosed around the world in 2012 representing 25 percent of all cancers. Since 2008, breast cancer incidence around the world has increased by more than 20 percent, while the mortality rate has increased by 14 percent. Every 19 seconds, somewhere in the world, a case of breast cancer is diagnosed in a woman. The number of breast cancer cases are increasing worldwide, with the number of cases in some countries increasing much faster than the global trend. The number of women with breast cancer in Malaysia, for example, grew from 1,529 to 8,429, an annual increase of 5.7 percent between 1980 and 2010. Over the same period, breast cancer cases in the United States

went from 127,425 cases to 241,249 cases with an annual increase of 2.1 percent. The regions with the most growth in breast cancer incidence are North Africa and the Middle East, Oceania, Southeast Asia, Western sub-Saharan Africa, and Central Latin America. In developing countries, breast cancer cases are diagnosed commonly in younger women making 44.1 percent of the overall number of cancer cases. In 2010, women at reproductive age (ages 15-49) in developing countries made up 23 percent of the total global of breast cancer cases. This means that the incidence of breast cancer in women under 50 in the developing countries is twice than of developed countries. Worldwide, breast cancer is the fourth most common cancer in women, and the seventh overall, with an estimated 528,000 new cases in 2012 (Erica, 2014). National Cancer Registry Program (NCRP) stratified Egypt into 3 geographical strata: lower, middle, and upper. Abstractors collected data from medical records of cancer centers, national tertiary care institutions, Health Insurance Organization, Government-Subsidized Treatment Program, and death records. Incidence rates were calculated at a regional and national level. Future projection up to 2050 was also calculated. Results indicated that age-standardized incidence rates per 100,000 were 166.6 (both sexes), 175.9 (males), and 157.0 (females). Commonest sites were liver (23.8%), breast (15.4%), and bladder (6.9%) in both sexes. Liver (33.6%) and bladder (10.7%) are common among men, Breast (32.0%) and liver (13.5%) are common among women. By 2050, a 3-fold increase in incident cancer relative to 2013. These data are considered the only available cancer registry at the national and regional levels of Egypt. Studying the rates of individual cancer sites might help in giving clues for preventive programs (Ibrahim, Khaled, Mikhail, Baraka, & Kamel, 2014).

Food intake may have a role in preventing breast cancer. Evidence suggests that fruits and vegetables, low-fat dairy products, fish, monounsaturated and polyunsaturated fatty acids, vitamin D, calcium, and phytoestrogens may reduce the risk of breast cancer. However, a high intake of meat, poultry, total energy, total fat, and saturated fatty acids may



المملكة العربية السعودية
جامعة الحدود الشمالية (NBU)

مجلة الشمال للعلوم الأساسية والتطبيقية (JNBAS)

طباعة - ردمد: 1658-7022 / الكتروني - ردمد: 1658-7014

www.nbu.edu.sa
http://jnbas.nbu.edu.sa

مجلة الشمال
للعلوم
الأساسية والتطبيقية
دورية علمية محكمة

جامعة الحدود الشمالية

1658-7022
1658-7014



الحالة التغذوية للسيدات المصابات بسرطان الثدي

إكرام رجب سليمان*¹، إيزيس عازر نوار¹، هبة جابر الشريدي²، مريم علي جنيبة³

1. أستاذ الغذاء وتغذية الإنسان - قسم الاقتصاد المنزلي - كلية الزراعة - جامعة الإسكندرية.
2. أستاذ مساعد علاج الأورام - قسم علاج وأبحاث الأورام معهد البحوث الطبية - جامعة الإسكندرية.
3. قسم الاقتصاد المنزلي - كلية الزراعة - جامعة الإسكندرية.

(قدم للنشر في 1441/04/04 هـ ؛ وقبل للنشر في 1442/01/15 هـ)

ملخص البحث: أجريت هذه الدراسة لتقييم الحالة التغذوية للمصابات بسرطان الثدي، حيث تم جمع البيانات الميدانية باستخدام استمارة استبيان (60 مريضة أثناء العلاج الكيميائي و60 مريضة أثناء العلاج الهرموني). وقد تم تقييم الحالة التغذوية وتقييم العادات الغذائية واستخدام بعض المقاييس الجسمية والتحليل المعملية، وتم إجراء تلك المقاييس والاختبارات على 30 سيدة قبل العلاج الكيماوي و30 قبل العلاج الهرموني وبعد شهر من أخذ العلاج أيضا. أوضحت النتائج أن (75%) من أفراد العينة يأكلون 3 وجبات يوميا. و(66.7%) يشربن كمية قليلة من الماء. ووجد أن (56%) من أفراد العينة يتناولون الكثير من السكر. أكثر المشروبات التي تتناولها المريضات يوميا العصائر الطبيعية والمشروبات الطبيعية وأن الخبز البلدي هو المصدر الرئيسي للكربوهيدرات. كما لوحظ أن المريضات يتناولن الخضروات والفواكه الطازجة يوميا، وكذلك الألبان ومنتجاتها كاملة الدسم أسبوعيا، وأنهن نادرا ما يتناولن الزيوت الصحية. أظهرت النتائج بعد شهر من اخذ العلاج الكيماوي انخفاض كلا من متوسط الوزن، ومتوسط كتلة الجسم (BMI)، ومتوسط محيط الذراع، ومتوسط الدهون تحت الجلد (العضلة ثلاثية الرؤوس). نستخلص من هذه النتائج أن العلاج الكيماوي يؤثر على الحالة الصحية للمريضات. وأظهرت النتائج أن العلاج الهرموني أدى لزيادة كلا من متوسط الوزن، ومتوسط كتلة الجسم (BMI)، ومتوسط محيط الذراع ومتوسط الدهون تحت الجلد (العضلة ثلاثية الرؤوس). وأدى العلاج الكيماوي لارتفاع في مستوى انزيمات الكبد. مع انخفاض كلا من متوسط نسبة اليوريا والكرياتينين وعدد كرات الدم البيضاء، وعدد كرات الدم الحمراء، ومعدل هييموجلوبين الدم وعدد الصفائح الدموية (WBCs&RBCs&Hb&PLT). بينما أدى العلاج الهرموني إلى انخفاض معدل أنزيمات الكبد واليوريا والكرياتينين.

كلمات مفتاحية: سرطان الثدي، الحالة التغذوية، الطعام، العلاج الكيماوي، العلاج الهرموني، انزيمات الكبد.

JNBAS ©1658-7022 . (1441هـ/2020م) نشر بواسطة جامعة الحدود الشمالية. جميع الحقوق محفوظة.

* للمراسلة:

أستاذ ، قسم الاقتصاد المنزلي ، كلية - الزراعة الشاطبي، جامعة الاسكندرية، الاسكندرية، جمهورية مصر العربية.

e-mail:solimanekram@Gmail.com



jnbas.nbu.edu.sa

DOI: 10.12816/0056079



KINGDOM OF SAUDI ARABIA
Northern Border University (NBU)
Journal of the North for Basic and Applied Sciences
(JNBAS)

p- ISSN: 1658 - 7022 / e- ISSN: 1658 - 7014

www.nbu.edu.sa
<http://jnbas.nbu.edu.sa>

J
N
B
A
S

Journal of the North
for Basic and
Applied Sciences

Peer-Reviewed Scientific Journal

Northern Border University
www.nbu.edu.sa

Nutritional Status of Breast Cancer Female Patients

Ekram R. Soliman^{*1}, Isis A. Nawar¹, Heba G. Elsheredy², Mariam A. Ginena³

1. Professor of Food and Human Nutrition, Department of Home Economics, Faculty of Agriculture, Alexandria University.
2. Assistant Professor of Oncology, Cancer Management, and Research Department, Medical Research Institute, Alexandria University.
3. Department of Home, Economics, Faculty of Agriculture, Alexandria University.

(Received 02 /12/2019; Accepted 03 /09 /2020)

Abstract: The major aim of this study was to assess the nutritional status of Breast cancer Female Patients. One questionnaire was designed and data were collected from one research sample comprising (60 patients treated with hormonal therapy and 60 patients treated with chemotherapy). The anthropometric and biochemical measurements were carried in 30 patients before the start of chemotherapy and another 30 patients before the start of hormonal treatment. The measurements were repeated after one month from the start of chemotherapy and hormonal treatment. The data indicated that (75%) were eating three meals every day, (66.7%) drunk a little water, and (56%) consumed a lot of sugar daily. The patients always drink fresh juices, and herbal beverages. Balady bread is the main source of carbohydrates. The patients were eating fresh vegetables and fruits. Most of them were eating fish weekly. From the results, we can conclude that chemotherapy affects the health status of patients because it decreases muscle mass and weight of patients. Also, these results show that hormonal treatment may increase weight if it would be used for a long period. The results show chemotherapy increases the average of liver enzymes and decreases the average of "Urea, Creatinine, WBC, RBC, Hb, and PLT. However, the hormonal treatment decreases the average of liver enzymes and decreases an average of Urea and Creatinine.

Keywords: Breast cancer, nutritional status, food, chemotherapy, hormonal, liver enzymes.

1658-7022© JNBAS. (1441 H/2020). Published by Northern Border University (NBU). All Rights Reserved.



jnbas.nbu.edu.sa

*** Corresponding Author:**

Professor, Dept. of Home Economics, Faculty of Agriculture, Alexandria University, Alexandria, Egypt.

DOI: 10.12816/0056079

- Lee, E., Kim, D., Kim, K., Kim, K., Choi, S.H. (2012). Age-Related Bone Mineral Density Patterns in Koreans (KNHANES IV). *The Journal of Clinical Endocrinology & Metabolism*, 97(9), 3310–3318. <https://doi.org/10.1210/jc.2012-1488>
- Lee, S., Park, Y., Park, S., Kim, T., Choi, H., Lee, S., Kim, S., et al. (2012). Increased frequency of osteoporosis and BMD below the expected range for age among South Korean females with rheumatoid arthritis. *International Journal of Rheumatic Diseases*, 15(3), 289–296. doi: 10.1111/j.1756-185X.2012.01729.x.
- Loudm, K.J., Gordon, C.M., Micheli, L.J., Field, A.E. (2005). Correlates of stress fractures among preadolescent and adolescent girls. *Pediatrics*, 115(4), 399–406.
- Marshall, L., Lang, T., Lambert, L., Zmuda, J., Ensrud, K., (2009). Dimensions and Volumetric BMD of the Proximal Femur and Their Relation to Age Among Older U.S. Men. *J Bone Miner Res.*, (21), 1197–1206. doi: 10.1359/JBMR.060506.
- Mazocco, L., & Chagas, P. (2017). Association between body mass index and osteoporosis in women from northwestern RioGrande do Sul. *Rev Bras Reumatol*, 57(4), 299–350.
- Mobley, S., Ha, E., Landoll, J., Badenop-Sevens, N.E., Clairmont, A., Goel, P., Matkovic, V. (2005). Children with bone fragility fractures have reduced bone mineral areal density at the forearm and hip and higher percent body fat. *J Bone Miner Res* 20, S34.
- Nandi, A., Sinha, N., Ong, E., Sonmez, H., and Poretsky, L. (2016). Is there a role for vitamin D in human reproduction?. *Hormone Molecular Biology and Clinical Investigation*, *online+, 25(1), 15-28.
- National Institute of Health (NIH, 2015). Osteoporosis Overview. [online], Available at: URL <https://www.bones.nih.gov/health-info/bone/osteoporosis/overview> [Accessed 10April. 2018].
- Oommen, A. and Al-Zahrani, I. (2014), Prevalence of Osteoporosis and Factors Associated with Osteoporosis in Females above 40 years in the Northern Part of Saudi Arabia, *Int J Res Med Sci.*, 2(1), 274-278.
- Paniagua, M.A., Malphurs, J.E., Samos, L.F. (2006). BMI and low bone mass in an elderly male nursing home population. *Clin Interv Aging.*, 1(3), 283-287.
- Prabha V., and Stanly, A.M. (2015). Effect of body mass index on bone mineral density. *Int J Community Med Public Health*, 2(4), 380-383
- Ravn, P., Cizza, G., Bjarnason, N. H., Thompson, D., Daley, M., Wasnich, R. D. et al. (1999). Low body mass index in early postmenopausal females. Early Postmenopausal Intervention Cohort (EPIC) study group. *Journal of Bone and Mineral Research*, (14), 1622–1627.
- Sadat-Ali M. and AlElq A., (2006). Osteoporosis among male Saudi Arabs: a pilot study. *Ann Saudi Med.*, 26(6), 450–454.
- Salamat, M. R., Salamat, A. H., Abedi, I., and Janghorbani, M. (2013). Relationship between Weight, Body Mass Index and Bone Mineral Density in Men Referred for Dual-Energy X-Ray Absorptiometry Scan in Isfahan, Iran. ID 205963 <https://doi.org/10.1155/2013/205963>
- Sözen, T., Özışık, L. & Başaran, N. C. (2017). An overview and management of osteoporosis. *Eur J Rheumatol*, (4), 46-56.
- Stagi, S., Cavalli, L., Iurato, C., Seminara, S., Brandi, M.L., deMartino, M. (2013). Bone metabolism in children and adolescents: main characteristics of the determinants of peak bone mass. *Clin Cases Miner Bone Metab*, (10), 1729.
- Wee, J., Sng, BY., Shen, L., Lim, CT., Singh, G., Das, S. (2013). The relationship between body mass index and physical activity levels in relation to bone mineral density in premenopausal and postmenopausal females. *Arch Osteoporos.* 8(1-2), 162. doi: 10.1007/s11657-013-0162-z.
- WHO. (2004). scientific group on the assessment of osteoporosis at primary health care level Summary Meeting Report Brussels, Belgium, 5-7 May 2004, World Health Organization. <https://www.who.int/chp/topics/Osteoporosis.pdf>.
- Zhang, X., Hua, T., Zhu, J., Peng, K., Yang, J., Kang, S. (2019). Body compositions differently contribute to BMD in different age and gender: a pilot study by QCT. *Archives of Osteoporosis*, 14(1), 31. DOI: 10.1007/s11657-019-0574-5.

5. CONCLUSION

In conclusion, based on this study, there is a positive association between BMI, age, and osteoporosis. Increased BMI is positively linked with increased BMD and reduced risk of osteoporosis. Age above 45 years, is a contributing factor in the increased risk of low bone mineral density in adults.

REFERENCES

- Akhlaque, U., Ayaz, S., Akhtar, N., Ahmad, N. (2017). Association of bone mineral density and body mass index in a cohort of Pakistanis: Relation to gender, menopause, and ethnicity. *The Egyptian Rheumatologist*, (39), 39–43.
- Alyami, S., Alqahtani, M., Alsadah, M., Altumaysi, N., Abu-zaid, O., Goja, A. (2019). Association between dietary intake and bone density among female Students at Imam Abdulrahman Bin Faisal University, Saudi Arabia. *Int J Community Med Public Health*, 6(11), 4699–4705. DOI /10.18203/2394-6040.
- Bierhals, I.O., dos Santos Vaz, J., Bielemann, R.M., de Mola, C. L., Barrosm F. C., Goncalves, H. (2019). Associations between body mass index, body composition, and bone density in young adults: findings from a southern Brazilian cohort. *BMC Musculoskelet Disord* 20. <https://doi.org/10.1186/s12891-019-2656-3>.
- CDC, (Center for Disease Control and Prevention), URL: <https://www.cdc.gov/healthyweight/assessing/index.html>
- Chan, K.M., Anderson, M., Lau, E. (2003). Exercise interventions: defusing the world's osteoporosis time bomb. *Bulletin of the World Health Organization*, 81(11),827-30.
- De Laet, C., Kanis, J., Oden, A., Johanson, H., Johnell, O., Delmas, P.(2005). Body mass index as a predictor of fracture risk: A meta-analysis. *Osteoporos Int* 16:1330–1338.
- El Hage, R., Jacob, C., Moussa, E., Benhamou, C.L., Jaffre, C. (2009). Total body, lumbar spine and hip bone mineral density in overweight adolescent girls: decreased or increased?. *J Bone Miner Metab.* 27(5), 629–33.
- Elwakil, W. A., Mohasseb, D., Elkaffash, D., Elshereef, S., Elshafey, M. (2016). Serum Leptin and osteoporosis in Postmenopausal Females with Primary Knee Osteoarthritis. *Egypt Rheumatol*, 38 (3), 209-215. <https://doi.org/10.1016/j.ejr.2016.02.002>.
- Fawzy, T., Muttappallymyalil, J., Sreedharan, J., Ahmed, A., Alshamsi, S. O. S., Saif, M., Humaid, S., Al Ali, M.S.S.H.B., Al Balsooshi, K. A. (2011). Association between Body Mass Index and Bone Mineral Density in Patients Referred for Dual-Energy X-Ray Absorptiometry Scan in Ajman. UAE. *J.Osteoporos.*, 2011; 2011: 876309.
- Galvard, H., Elmsta, S., Elmsta, B., Robertson, E., (1996). Differences in body composition between female geriatric hip fracture patients and healthy controls: body fat is more important as an explanatory factor for the fracture than body weight and lean body mass. *Aging (Milano)*, (8), 282–286.
- Genant, H. K., Cooper, C., Poor, G., Reid, I., Ehrlich, G., Kanis, J.,(1999). Interim Report and Recommendations of the World Health Organization Task-Force for Osteoporosis. *Osteoporosis International*, 10 (4), 259–264.
- Hoxha, R., Islami, H., Qorraj-Bytyqi, H., Thaçi, S., and Bahtiri, E. (2014). Relationship of Weight and Body Mass Index with Bone Mineral Density in Adult Men from Kosovo. *Mater Sociomed*, 26(5), 306–308. doi: 10.5455/msm.2014.26.306-308
- Hsu, Y., Venners, S., Terwedow, H., Feng, Y., Niu, T., Li, Z., Laird, N., et al., (2006). Relation of body composition, fat mass, and serum lipids to osteoporotic fractures and bone mineral density in Chinese men and females. *Am J Clin Nutr* 83:146–154.
- Ibrahim, S.E., Elshishtawy, H.F., Helmy, A., (2011). Serum Leptin Concentration, Bone Mineral Density, and Bone Biochemical Markers in a Sample of Egyptian Females: A Possible Relationship. *Egypt Rheumatol*, 33(4), 171-7.
- Janicka, A., Wren, T.A., Sanchez, M.M., Dorey, F., Kim, P.S., Mittelman, S.D., Gilsanz, V. (2007). Fat mass is not beneficial to bone in adolescents and young adults. *J Clin Endocrinol Meta*, (92),143–147.
- Langsetmo, L.; Hitchcock, C.L.; Kingwell, E.J.; Davison, K.S.; Berger, C.; Forsmo, S.; Zhou, W.; Kreiger, N.; and Prior, J.C. (2012). Physical activity, body mass index, and bone mineral density—associations in a prospective population-based cohort of females and men: The Canadian Multicentre Osteoporosis Study (CaMos). *Bone*, (50), 401–408.

due to age-related bone density lowering. Due to that, during the aging, the bones become thin or osteoporotic, and increasing age is a contributing factor in the increased risk for incident fractures in adults (Lee, Kim, Kim, Kim & Choi, 2012), but it is most common in females than males, especially after menopause due to the reduction in estrogen hormone levels (Nandi, Sinha, Ong, Sonmez, & Poretsky, 2016). As a result, decreased levels of bone minerals such as calcium will lead to the lightweight of bones, reduced density, and increased bone fragility (Oommen & AlZahrani, 2013). This finding is in line with another study done in Pakistan at a tertiary medical care center for rehabilitation. The authors of this study reported that the majority of the study population in the age group below 50 years had a normal BMD while the BMD of those in the age group above 50 years is in the osteopenic range (Akhlaque, Ayaz, Akhtar & Ahmad, 2017). Another study reported that a significant reduction of BMD was found for the age group between 40 and 59 years among patients with rheumatoid arthritis mainly in the spine, femoral neck, and total hip (Lee, Park, Park, Kim, Choi, Lee, & Kim, 2012), and there was substantial diversity of femoral morphology and volumetric BMD among older men (Marshall, Lang, Lambert, Zmuda, & Ensrud, 2009).

In a recent study conducted in China on 394 participants, including 122 male (representing 31%) and 272 females (representing 69%), authors observed that there was a slow decrease of BMD with male aging, while there was a gradual increase of BMD among female before 30–49 years and then it got decreased rapidly (Zhang, et al., 2019).

According to BMD measurement, it has been observed in this study that the osteoporotic rate is reduced when the BMI increased. The relation between BMD and BMI was illustrated in figures (4 and 5). Hip and lumbar rates of osteoporosis were found higher (77.8 and 66.7%) in study groups with low BMI (underweight groups) then the osteoporotic rate was reduced (67.1 and 25.6%) with increases in BMI in normal groups and obese groups (39.7 and 9.9%), respectively. On the other hand, with increased BMI, the BMD has increased

thus the rate of low BMD was reduced. It has been noticed that BMD of overweight and obese subjects was in the normal range leading to decreased risk for osteoporosis. This is because bony eminences are cushioned by body fats leading to the decreased effect of the direct impact of potential falls (Galvard, Elmsta, Elmsta, & Robertson, 1996).

In contrast to the findings in the above studies, some studies excluded that increased level of fat mass does not protect the bone against osteoporosis (De Laet, Kanis, Oden, Johanson, Johnell, & Delmas, 2005; Mobley, Landoll, Badenop-Sevens, Clairmont, Goel, & Matkovic, 2005; Hsu, Venners, Terwedow, Feng, Niu, & Laird, 2006; Janicka, Wren, Sanchez, Dorey, Kim, Mittelman, & Gilsanz, 2007).

The result of this study showed that all patients (males and females) with low BMI were more subjected to low BMD. Similar study by Prabha and Stanley, reported that there is a consistent association between low BMI and low BMD (Prabha and Stanley, 2015). Thus, a high BMI is a factor that lowers the rate of osteoporosis among obese individuals. Many types of research had reached similar conclusions that females with high BMI are protected from osteoporosis (Salamat, et al., 2013).

Other studies showed that higher BMI levels are associated with higher BMD score in males and females (Akhlaque, et al., 2017; Salamat, et al., 2013; De Laet, et al., 2005). A cross-sectional study conducted by Salamat, et al., reported that increased BMI level and body weight were associated with high BMD score, and obesity significantly decreased the level of osteoporosis fracture risk especially among males (Salamat, et al., 2013). Analysis of age-adjusted linear regression done by other cross-sectional studies found that BMI weight is positively associated with BMD scores (Mobley, et al., 2005). In a study made by El Hage, Jacob, Moussa, Benhamou, & Jaffre, (2009), reported that increased obesity is usually associated with a higher level of BMD, this is mainly due to improved bone mass among males and females as a result of converting androgen to estrogen especially within the adipose tissue (Janicka, et al., 2007).

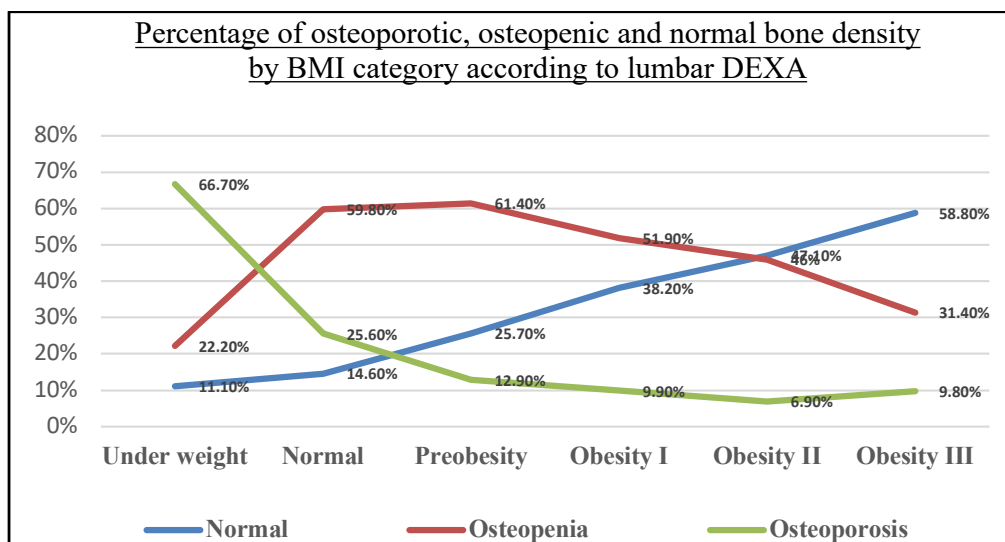


Figure 5: Percentage of osteoporotic, osteopenic, and normal bone density by BMI category according to lumbar DEXA

Discussion: It is well known that obesity and osteoporosis are considered as major health problems that threaten people all over the world. In this study, analysis has been done to find the relationship between BMI and age with the BMD among Saudi males and females referred to as King Fahad University Hospital (KFUH).

It has been found that low BMD is a major risk factor that may predispose to osteoporosis, and it can lead to increased bone fragility and fractures risk in the elderly population. It affects about (66.4 and 77.4%) of females and males aged between 50 and 70 years, respectively, and (94.4 and 100%) of those aged >70 years and older, respectively (Data (figure) not shown)

The incidence of fragile bone and fractures were increased during the last years among the Saudi population. In our study, it has been found that the prevalence of osteoporosis in the hip and lumbar region among our study sample were 34% and 46%, respectively. This might be due to many predisposing factors leading to low BMD and increased probability of osteoporotic fractures, for example, hormonal status, age, smoking, diet, BMI, physical activity, etc. However, up to 80% of BMD is genetically determined, leaving 20% to be

influenced by environmental factors (Stagi, Cavalli, Iurato, Seminara, Brandi & deMartino, 2013). Low protective dietary intake which is poor in calcium, magnesium and phosphorous directly affects the bone mineral content on the body. A similar study was conducted among elderly males by Paniagua, et al, it noticed that 35.6% were osteopenic and 27.1% were osteoporotic (Paniagua, Malphurs & Samos, 2006).

It has been observed that most of the studies emphasized the importance of exercise in increasing BMD. A cohort prospective study was conducted among the Canadian population by Langsetmo et al reported that physical activity (PA) is very important for increasing BMD. They also stated that increased PA is usually associated with increased BMD and decreased BMI (Langsetmo, Hitchcock, Kingwell, Davison, Berger, Forsmo, Zhou, Kreiger, & Prior, 2012). Other studies from different regions have also indicated that regular exercise at a younger age will maximize BMD and reduce fracture risk (Chan, Anderson & Lau, 2003; Loudm, Gordon, Micheli & Field, 2005).

Another finding of this study was that bone mass growth began to decline after 45 years of age, and bone loss increases with age. This is mainly

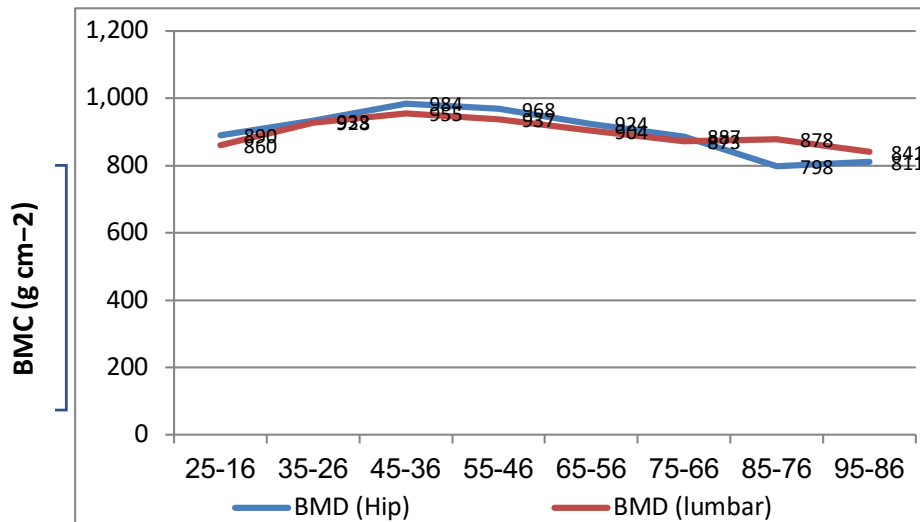


Figure 3: BMD against age groups according to hip area and lumbar region DEXA (15 years interval)

Association of BMI and BMD: The results in Figures (4 and 5) show the prevalence of osteoporosis was high (77.8, and 66.7%) in hip and lumbar, respectively among patients with underweight compared to (39.7, 9.9%), and (29.9, 6.9%) in an obese 1, and obese11,

respectively. It is noted that with the increase in BMI, BMD is increased, and the frequency of osteoporosis is reduced. Also, we noted that the risk of low BMD among underweight individuals is more compared to normal and obese individuals.

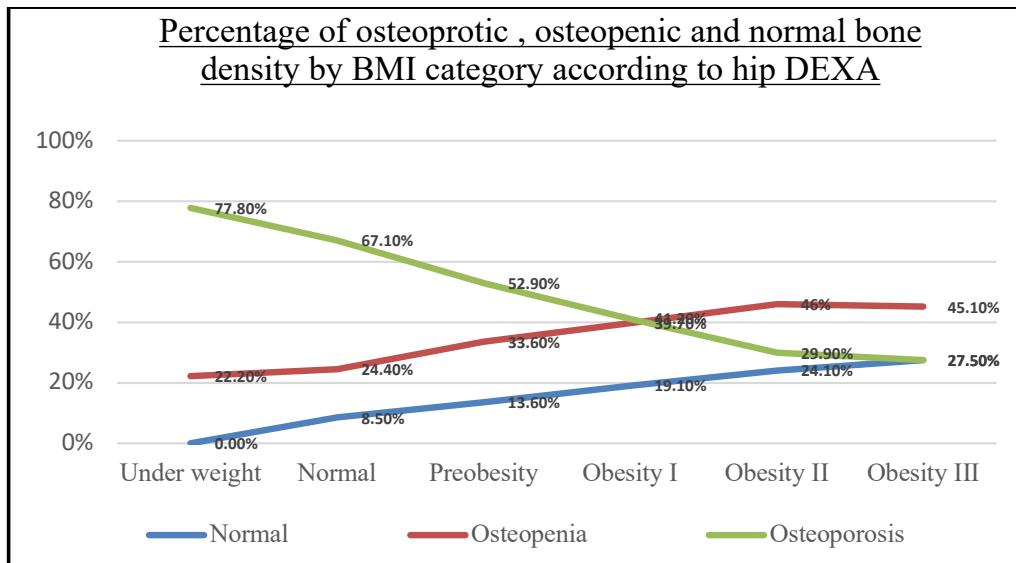


Figure 4: Percentage of osteoporotic, osteopenic, and normal bone density by BMI category according to hip DEXA

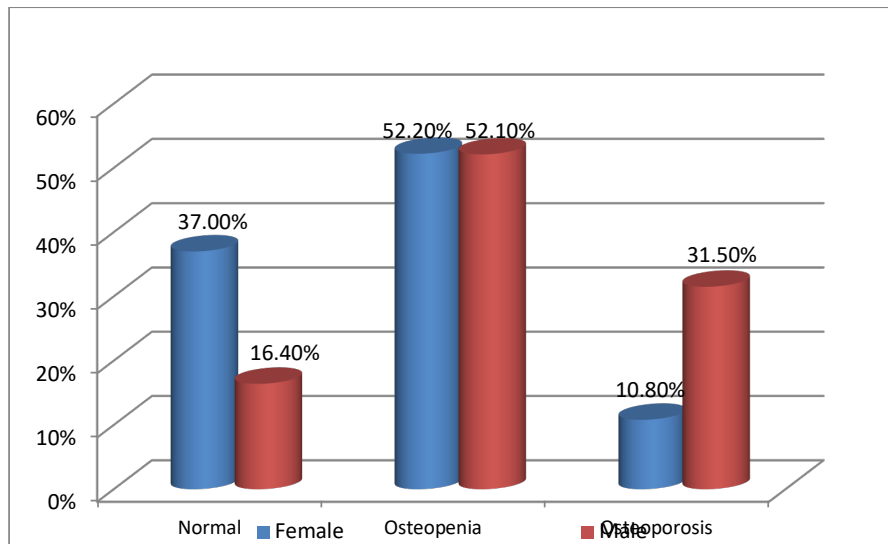


Figure 1: Percentage of osteoporotic, osteopenic, and normal cases, distributed by gender according to hip DEXA:

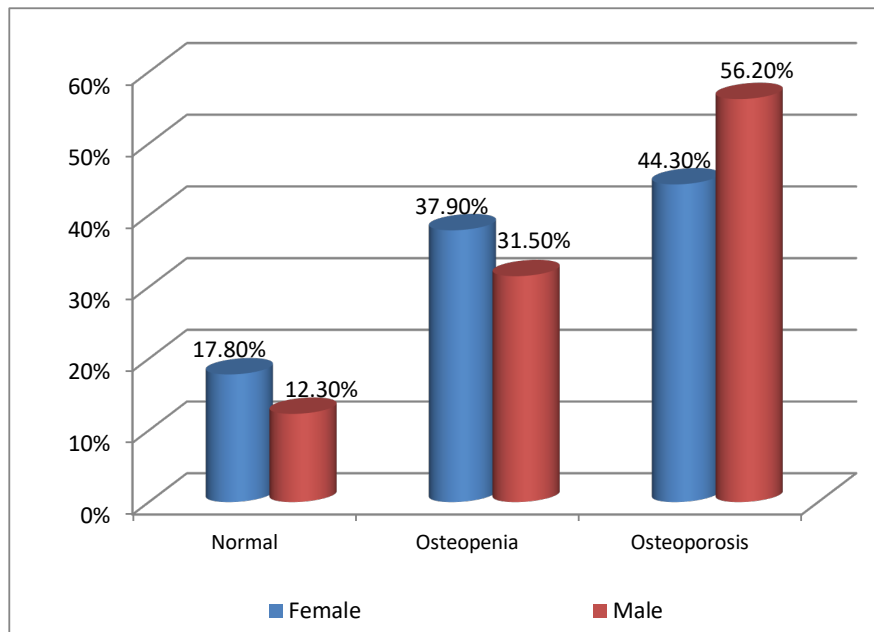


Figure 2: Percentage of osteoporotic, osteopenic, and normal cases, distributed by gender according to lumbar DEXA:

BMD level according to Patients age: In this study, age is considered as the main factor for bone health and development. The linkage of BMD and age were illustrated in figure 3. The data showed that

the bone density increases during the life till age year 45, then started to decline gradually and more losses were recorded in the hip region in patients above 80 years.

were performed by a qualified bone densitometer technologist using Hologic - Delphi QCR series Model 4500A. The procedure followed was as described by the manufacturer's manual. Based on the formula; weight (kg)/height square (m²), BMI was calculated and according to the standard classification of BMI by CDC (normal weight is between 18.5 and 24.9, underweight is below 18.5, overweight is between 25.0 and 29.9, while obese is above 30.0 (CDC, Center for Disease Control and Prevention))

3. DATA ANALYSIS

Data was collected and analyzed using version 23 of IBM-SPSS. Descriptive analysis, frequencies, and correlations were performed. Results were presented in tables, bar charts, and line charts.

4. FINDINGS AND DISCUSSION

Demographic factors and BMD of the patients: 500 cases were selected for the study, 427

(85.4%) were females, and 73 (14.6%) males. Table 1 gives the general characteristics of our study population. The mean BMI is (31.0 (± 7.7)), BMD at the hip area and lumbar region are 929.6 (± 223.3) and 929.6 (± 223.3) (mg/cm²), respectively. T-Score was ranged from osteoporosis to normal in the hip with (-4) to (18) and from (-11.00) to (11.00) for lumbar, respectively.

Prevalence of Low Bone Density: Figures 1 & 2 showed the frequency of normal BMD, osteopenic, and osteoporotic patients' measures at the hip and lumbar regions respectively. For females (17.8%) and (37%) normal, (37.9%) and (52.2%) osteopenia, and (44.30%) and (10.8%) osteoporosis was recorded in hip and lumbar, respectively, while (12.3%) and (16.4%) for males had normal, (31.5%) and (52.1%) osteopenia, and (56.2) and (13.5%) osteoporosis for hip and lumbar, respectively. The overall percentage of osteoporosis for hip and lumbar among both genders was 34% and 46%, respectively which is considered a higher prevalence rate.

Table1. General characteristics of the patients:

	Minimum	Maximum	Mean (SD)	95% Confidence Interval	
				Lower	Upper
Height (m)	1.26	1.82	1.56 (± 0.09)	1.56	1.57
Weight (Kg)	35.0	165.0	76.8 (± 18.7)	75.167	78.395
Body mass index	16.00	99.0	31.0 (± 7.7)	30.4	31.7
Age (yrs.)	18.00	90	56.03 (± 12.7)	54.9	57.1
BMD at hip area (mg/cm ²)	425	3886	929.6 (± 223.3)	910.60	950.1
T-score at hip area	-4.00-	18.00	-.78 (± 1.5)	-.89	-.63
Z-score at hip area	-3.00-	19.00	-.122 (± 1.5)	-.24	.02
BMD at lumbar region (mg/cm ²)	68	2373	911.90(± 192.9)	893.85	928.11
T-score at lumbar region	-11.00-	11.00	-2.22 (± 1.8)	-2.40	-2.07
Z-score at lumbar region	-7.00-	12.00	-0.97- (± 1.8)	-1.16	-.82

1. INTRODUCTION

Osteoporosis is a metabolic disease in which bone mass, quality, and microarchitecture decline leading to increased bone fragility (NIH, 2015). It is considered a serious health problem because it is associated with different types of life-threatening fractures such as vertebral, hip, and forearm fractures. BMD is a clinical indicator of bone wellbeing and health. It is referred to as the amount of minerals such as calcium and phosphorus per volume of the bone mass unit. DEXA represents the “gold standard” for diagnosis and treatment of osteoporosis and fractures risk prediction as recommended by WHO (WHO, 2004). T-score is the standard deviation (SD) of BMD of a specific bone compared to that of a healthy 30 years old individual of the same gender. A T-score value of more than -1.0 is considered normal, T-score value in the range between -1.0 up to -2.5 is considered as osteopenia and a T-score value more than -2.5 is considered as osteoporosis (Genant, Cooper, Poor, Reid, Ehrlich & Kanis 1999). There are many factors may affect BMD and osteoporosis, including gender and age (Sözen, Özışık & Başaran, 2017), BMI (Zhang, Hua, Zhu, Peng, Yang, & Kang, 2019), reduced dietary calcium and vitamin D intake (Alyami, Alqahtani, Alsadah, Altumaysi, Abuzaid & Goja, 2019) and lack of exercise (Wee, Sng, Shen, Lim, Singh & Das, 2013).

This study was conducted among patients referred to DEXA at King Fahad University Hospital (KFUH) to identify the association of BMD with age and gender and BMI.

Recently, many researchers stated that BMI and BMD are positively related. Such researches stated that the most important risk factor for the occurrence of low BMD is low BMI (Bierhals, dos Santos Vaz, Bielemann, de Mola, Barros, Goncalves, 2019); Mazocco & Chagas, 2017), which can be used as a strong predictor for bone strength and osteoporosis (Prabha & Stanly, 2015). A prospective study was done by Ravn, Cizza, Bjarnason, Thompson, Daley & Wasnich, (1999) and stated that the risk of bone loss in females with low BMI in early postmenopausal was higher compared to those

with higher BMI. A study was done in Ajman (UAE) highlighted BMI as a good indicator for measurements of BMD (Fawzy, Muttappallymyalil, Sreedharan, Alshamsi & Al Balsooshi, 2011). Thus, low BMI is considered as a risk factor for low BMD, while overweight decreases the risk for osteoporosis (Salamat, Salamat, Abedi, & Janghorbani, 2013). Other studies also indicated the negative relationship between age and femoral neck BMD may be considered as good guidance for the initiation of early assessment as well as prevention of osteoporosis and fracture risk among the elderly population (Hoxha, Islami, Qorraj-Bytyqi, Thaçi, & Bahtiri, 2014).

It has been reported that fat mass has a role in bone metabolism (Ibrahim, Elshishtawy, & Helmy, 2011) and osteoarthritis does not prevent the occurrence of osteoporosis in postmenopausal females (Elwakil, Mohasseb, Elkaffash, Elshereef, & Elshafey, 2016). Previous studies in Saudi Arabia stated that the prevalence of osteoporosis is increased among both genders including pre and post-menopausal females as well as males (Sadat-Ali, & AlElq, 2006; Oommen & AlZahrani, 2013).

2. BODY

Study design: with the approval of King Fahad University Hospital (KFUH) this retrospective study was conducted on 578 cases referred to DEXA in KFUH during the period between December 2016 and December 2018. DEXA reports were collected by datasheet and analyzed (appendix 1).

Inclusive criteria: No missing variable in the DEXA report, all cases were only recruited from KFUH in good physical and mental conditions.

Exclusive criteria: Cases that did not satisfy any of the inclusion criteria were excluded. 78 patients were excluded for chronic diseases related to hormonal disturbances.

Data Collection: Data Collection was done using a datasheet that includes little demographic data (gender, height, weight, and age). It also includes a DEXA report for both the hip area and the lumbar region (BMD, T-score, Z-score, WHO classification, and fracture risk). DEXA scans



المملكة العربية السعودية
جامعة الحدود الشمالية (NBU)

مجلة الشمال للعلوم الأساسية والتطبيقية (JNBAS)

طباعة - ردمد: 1658-7022 / الكتروني - ردمد: 1658-7014

www.nbu.edu.sa
http://jnbas.nbu.edu.sa

مجلة الشمال
للعلوم
الأساسية والتطبيقية
دورية علمية محكمة

جامعة الحدود الشمالية

1658-7022
1658-7014



علاقة مؤشر كتلة الجسم والعمر والجنس مع كثافة المعادن بالعظام عند مرضى بمستشفى جامعة الملك فهد

أسامة عبدالله مبروك خيرالله، علي عبدالكريم الغامدي، عرفات محمد غوجا، عادل عثمان بخيت، سيد محمد سادات

(قدم للنشر في 1441/03/27 هـ ؛ وقبل للنشر في 1442/01/15 هـ)

ملخص: تعتبر الكثافة المعدنية للعظام (BMD) مؤشر مهم لاحتمال الإصابة بهشاشة العظام وخطر الإصابة بالكسر. هنالك العديد من عوامل الخطورة التي تؤدي الى انخفاض كثافة المعادن في العظام، حيث إن حوالي 80 % منها يتم تحديدها وراثياً واما نسبة 20 % المتبقية ناتجة بتأثير لعوامل البيئية بما في ذلك مؤشر كتلة الجسم (BMI)، العمر، نمط الحياة والتغذية. أجريت هذه الدراسة بأثر رجعي لتقييم عدد 500 تقرير (DXA) جمعت من مستشفى الملك فهد الجامعي بالخبر (KFUH). تشمل اهم البيانات التي تم جمعها وهي: بيانات ديموغرافية للمريض، العمر، الطول والوزن، قياس الكثافة المعدنية للعظام لمنطقة الورك ومنطقة الفقرات القطنية أسفل الظهر، T-score، Z-score، تم تحليل البيانات باستخدام الحزمة الإحصائية للعلوم الاجتماعية (SPSS) الإصدار 23. أظهرت النتائج أن النسبة المئوية الإجمالية لمرضى هشاشة العظام كانت 34 % في منطقة الورك و 46% في منطقة الفقرات القطنية أسفل الظهر وفقاً لمعايير منظمة الصحة العالمية. تزداد الكثافة المعدنية للعظام مع زيادة العمر حتى عمر 45 عاماً ثم تبدأ تنخفض تدريجياً للمرضى التي تتراوح اعمارهم ما بين 45 و 75 عاماً مع حدوث فقدان كمية كبيرة للكثافة المعدنية للعظام للأعمار فوق 75 عاماً. أيضاً أظهرت النتائج ان معدل انتشار مرض هشاشة العظام أعلى بين المرضى الذين يعانون من نقص الوزن ($25-BMI = 18$) مقارنة بمرضى السمنة ($40-BMI = 30$) (77.8 %، 29.9% في منطقة الورك و 66.7 %، 6.9% في منطقة أسفل الظهر على التوالي. خلصت الدراسة إلى أنه هناك ارتباط إيجابي بين مؤشر كتلة الجسم والجنس والعمر وهشاشة العظام. حيث ترتبط زيادة مؤشر كتلة الجسم بشكل إيجابي بزيادة كثافة المعادن بالعظام وانخفاض خطر الإصابة بهشاشة العظام، كما ان تعدد الزيادة في العمر، خاصة بعد 45 عاماً، عاملاً مساهماً في زيادة خطر انخفاض كثافة المعادن في العظام لدى البالغين.

كلمات مفتاحية: هشاشة العظام، الكثافة المعدنية للعظام (BMD)، مؤشر كتلة الجسم (BMI)، الطاقة المزدوجة لقياس امتصاص الأشعة السينية (DXA).

JNBAS ©1658-7022 . (1441هـ/2020م) نشر بواسطة جامعة الحدود الشمالية. جميع الحقوق محفوظة.

* للمراسلة:

أستاذ مساعد، قسم العلوم الإشعاعية، كلية العلوم الطبية التطبيقية، جامعة الامام عبدالرحمن بن فيصل، ص ب: 1982، رمز بريدي: 34221، المدينة الدمام، المملكة العربية السعودية.

e-mail: oakheiralla@iau.edu.



jnbas.nbu.edu.sa

DOI: 10.12816/0056077



KINGDOM OF SAUDI ARABIA
Northern Border University (NBU)
Journal of the North for Basic and Applied Sciences
(JNBAS)

p- ISSN: 1658 - 7022 / e- ISSN: 1658 - 7014

www.nbu.edu.sa
http://jnbas.nbu.edu.sa



Journal of the North
for Basic and
Applied Sciences

Peer-Reviewed Scientific Journal

Northern Border University
www.nbu.edu.sa

Volume 5
Issue 2
2020

Association of Body Mass Index, Age, and Gender with Bone Mineral Density in Patients Referred to King Fahad University Hospital

Osama A M Kheiralla^{*1}, Arafat M Goja², Adel O Bakheet¹, Ali Al-Ghamdi¹, Syed M Sadath¹

(Received 25/11/2019; Accepted 03 /09 /2020)

Abstract: Bone mineral density (BMD) is an important indicator of the possibility of osteoporosis and the risk of bone fracture. Multiple risk factors may lead to low BMD, up to 80% of these risk factors are genetically determined and the remaining 20% are influenced by environmental factors including body mass index (BMI), age, lifestyle, and nutrition. This study aims to assess whether age, gender, and BMI can be used as an indicator or risk factor for low BMD.

A retrospective study was conducted on 500 DXA reports collected from KFUH. The collected data include patient demographic factors: age, height and weight, DXA report give BMD measurement for hip area and lumbar region, T-score, and Z-score. Data were analyzed using SPSS version 23. The results demonstrated that the overall percentage of osteoporosis was 34% in the hip area and 46% in the lumbar region according to WHO criteria. BMD increases as age increases till the age of 45yrs. BMD starts to declines gradually among patients aged between 45 and 75 yrs., with gross losses occurs for ages > 75 yrs. Also the prevalence of osteoporosis shows a higher among under-weighted patients (BMI = 18-25) than among obese patients (BMI = 30-40) 77.8%, 29.9% in hip area and 66.7%, 6.9% in lumbar region respectively. There is a positive association between BMI, gender, age, and osteoporosis. Increased BMI is positively linked with increased BMD and reduced risk of osteoporosis. An increase in age, especially after 45 years, is a contributing factor in the increased risk of low BMD in adults.

Keywords: Osteoporosis, Bone mineral density (BMD), body mass index (BMI), Dual-energy X-ray absorptiometry (DXA),

1658-7022© JNBAS. (1441 H/2020). Published by Northern Border University (NBU). All Rights Reserved.



jnbas.nbu.edu.sa

DOI: 10.12816/0056077

* Corresponding Author:

1. Department of Radiological Sciences, College of Applied Medical Sciences, Imam Abdulrahman Bin Faisal University, P.O. Box 1982, Dammam, Saudi Arabia.
2. Department of Clinical Nutrition, College of Applied Medical Sciences, Imam Abdulrahman Bin Faisal University, P.O. Box 1982, Dammam, Saudi Arabia.

e-mail: oakheiralla@iau.edu.

- <https://doi.org/10.13189/aep.2015.030204>.
- Jiashen, T., Ching-Ming L., Yu-Huei C. (2018). Improving the Penetration of Wind Power with Dynamic Thermal Rating System, Static VAR Compensator and Multi-Objective Genetic Algorithm. *Energies*, 11(4), 815-830. <https://doi:10.3390/en11040815>.
- Kang T., Choi S., Morsy A. S., and Enjeti P. N. (2017). Series voltage regulator for a distribution transformer to compensate voltage sag/swell. *IEEE Transactions on Industrial Electronics*, 64(6), 4501–4510. <https://doi.org/10.1109/tie.2017.2668982>.
- Mohammad, M. K., & Akbar, I. (2017). Implementation of SVC based on grey theory and fuzzy logic to improve LVRT capability of wind distributed generations. *Turkish Journal of Electrical Engineering & Computer Sciences*, 25(1), 422-433. <http://dx.doi.org/10.3906/elk-1410-153>.
- Nitin, K. S., & Ashwani, K. (2016). Reactive Power Control in Decentralized Hybrid Power System with STATCOM using GA, ANN and ANFIS Methods. *International Journal of Electrical Power & Energy Systems*. 83, 175-187. <https://doi.org/10.1016/j.ijepes.2016.04.009>.
- Olusayo, A. A., Josiah L. M. and Yskandar H. (2019). Optimal Allocation of Renewable Energy Hybrid Distributed Generations for Small-Signal Stability Enhancement. *Energies*, 12, 4777, 1-31; <https://doi:10.3390/en12244777>.
- Oyekanmi, W. A., Radman, G., Babalola, A. A. & Uzochi, L. O. (2013). Effect of Static VAR Compensator positioning on a grid-connected wind turbine-driven Squirrel Cage Induction Generator. *2013 IEEE International Conference on Emerging & Sustainable Technologies for Power & ICT in a Developing Society (NIGERCON)*, Owerri, 247-252. <https://doi.org/10.1109/nigercon.2013.6715663>.
- Pathak, A. K., Sharma, M. P., & Gupta, M. (2016). Static VAR Compensator Rating Finalization and Review of High Wind Penetration Effect in Western Rajasthan. *2016 IEEE 1st International Conference on Power Electronics, Intelligent Control and Energy Systems (ICPEICES)*, Delhi, 1-6. <https://doi.org/10.1109/icpeices.2016.7853091>.
- Pan, Y., Liu, F., Chen, L., Wang, J., Qiu, F., Shen, C., Mei, S. (2018). Towards the Robust Small-Signal Stability Region of Power Systems under Perturbations Such as Uncertain and Volatile Wind Generation. *IEEE Trans. Power Syst.*, 33(2), 1790–1799. <https://doi.org/10.1109/tpwrs.2017.2714759>.
- Raju, S.K., & Pillai, G.N. (2016). Design and Real Time Implementation of Type-2 Fuzzy Vector Control for DFIG Based Wind Generators. *Renewable Energy*, 88, 40-50. <https://doi.org/10.1016/j.renene.2015.11.006>.
- Stalin, A. S., Shiva B. M., Revanth, R., Velbharathi, A., & Durai, R. D. (2015). Design and Implementation of Accurate Reactive Power Compensator for Renewable Grid Connected Transmission System. *2015 International Conference on Industrial Instrumentation and Control (ICIC)*, Pune, 1392-1397. <https://doi.org/10.1109/iic.2015.7150966>.
- Srinivasa, R., Srinivasa, R. V. (2015). A Generalized Approach for Determination of Optimal Location and Performance Analysis of FACTS Devices. *International Journal of Electrical Power & Energy Systems*. 73,711-724. <http://dx.doi.org/10.1016/j.ijepes.2015.06.004>.
- Tamer, F., & Mohamed. S. Z. (2017). New approach to Design SVC-based Stabilizer using Genetic Algorithm and Rough Set Theory. *IET Generation, Transmission and Distribution*, 11(2), 372-382, <https://doi.org/10.1049/iet-gtd.2016.0701>.
- Vanishree, J. & Ramesh, V. (2018). Optimization of size and cost of Static VAR Compensator using Dragonfly algorithm for voltage profile improvement in power transmission systems. *International Journal of Renewable Energy Research*, 8(1). Online ISSN: 1309-0127.
- Ye, W., Vera S., & Miguel, L-B-Z. (2016). Impact of high penetration of variable renewable generation on frequency dynamics in the continental Europe interconnected system. *IET Renew. Power Generation*, 10(1), 10–16. <https://doi.org/10.1049/iet-rpg.2015.0141>.

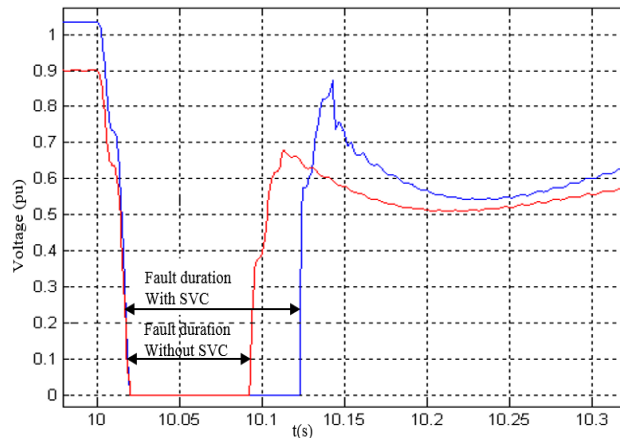


Figure 20. Zoom of Figure 19

The curves in Figures 19 and 20 prove that the stability of the wind power plant can be maintained for a period of 115 milliseconds when the SVC is coupled. But, if the latter is ignored, the wind farm loses its stability after a short circuit duration of 83 milliseconds.

6. CONCLUSION

A static VAR compensator was developed in this paper in order to obtain an improvement in the voltage quality by studying some operating regimes. In another section of this work, the dynamic behavior of the wind power plant was studied. This behavior was analyzed during short-circuit faults and voltage sags with and without SVC. These faults can cause situations of instability in the generation system and thus cause significant power oscillations or even their sudden losses. The simulation results showed that in the presence of the static VAR compensator, the variation of the voltage across the terminals of the power plant can be kept in the $\pm 10\%$ range for different operating cases. The grid upstream of the wind power plant was relieved of the transit of the reactive power great part. This study showed that the presence of the SVC can maintain the stability of the wind farm for longer periods of time in the event of occurring faults.

ACKNOWLEDGEMENTS

The author gratefully acknowledges the approval

and the support of this research study by the grant No. 7527-ENG-2018-1-8-F from the Deanship of Scientific Research at Northern Border University, Arar, KSA.

REFERENCES

- Altıntaş, O. Okten, B. Karsu, Ö. Kocaman, A.S. (2018). Bi-objective optimization of a grid-connected decentralized energy system. *International Journal Energy Research*, 42(2),447–465. <https://doi.org/10.1002/er.3813>.
- Deng, Y.Y., Kornelis B., & Kees V. D. L. (2012). Transition to a fully sustainable global energy system. *Energy Strategy Reviews*, 1(2), 109-121. <http://dx.doi.org/10.1016/j.esr.2012.07.003>.
- Ezzeddine, T. (2019). Reactive power analysis and frequency control of autonomous wind induction generator using particle swarm optimization and fuzzy logic. *Energy Exploration & Exploitation*, 0(0) 1–28, [http://doi: 10.1177/0144598719886373](http://doi:10.1177/0144598719886373).
- Hemeida M. G., Rezk Hegazy, Hamada Mohamed M. (2018). A Comprehensive Comparison of STATCOM versus SVC-based Fuzzy Controller for Stability Improvement of Wind Farm Connected to Multi-Machine Power System. *Electrical Engineering*, 100(2), 935-951, <https://doi.org/10.1007/s00202-017-0559-6>.
- Hemeida, M. G., Hussien, Hegazy R., & Abdel Wahab, M. A. (2015). Stabilization of a Wind Farm Using Static VAR Compensators (SVC) Based Fuzzy Logic Controller. *Advances in Energy and Power*, 3(2), 61-74.

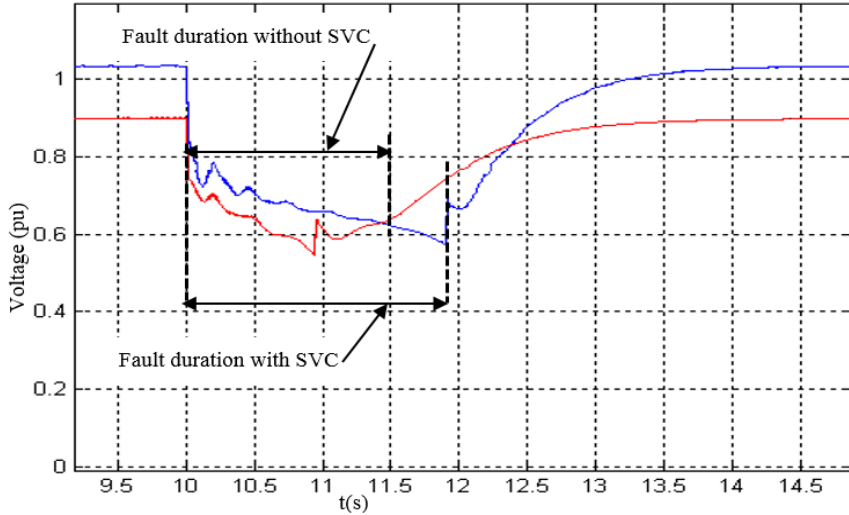


Figure 18: Voltage at node 5 for a 30% depth dip and $K_u= 0.3$

5.1.2. Three-phase Short-circuit

The design of an electrical installation and the materials to be implemented, as well as the determination of the protections require the calculation of the short-circuit currents at any point of the grid. Before installing any decentralized production unit, such as wind power plants, in the distribution grid, it is imperative to check the protections selectivity even adjust them, since the wind turbine contributes

to short-circuit current in the grid (Pan, Liu, CHen, Wang, Qiu, SHen, & Mei, 2018). This contribution can reach from 4 to 8 times the machine rated current. For this reason, one must take into account all these constraints when designing our SVC as well as its location. The short circuit simulated in this part is a balanced three-phase short circuit. Figures 19 and 20, show the simulation results after application of a three-phase short-circuit at time $t = 10s$ at node 6 as given in Figure 2.

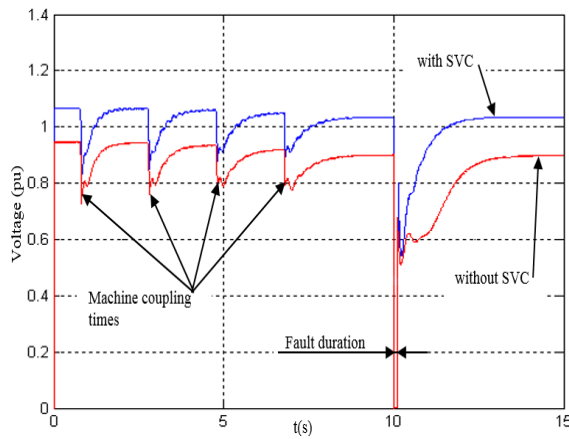


Figure 19: Voltage evolution at node 5 during a three phase short circuit

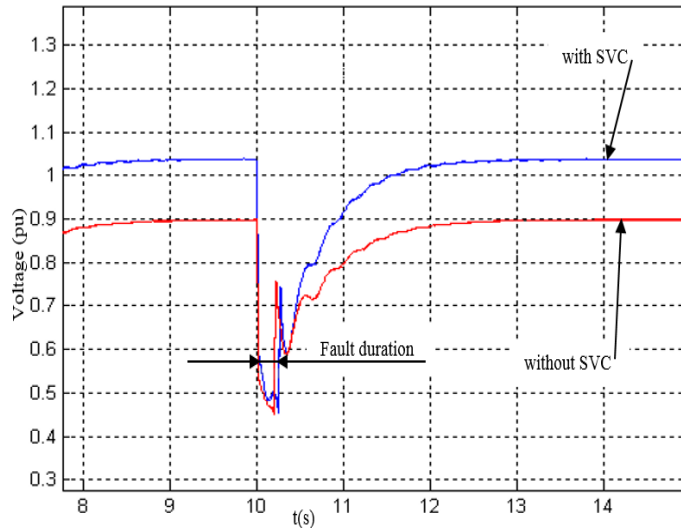


Figure 16: Voltage at node 5 for a 50% depth dip and $K_u=0.3$

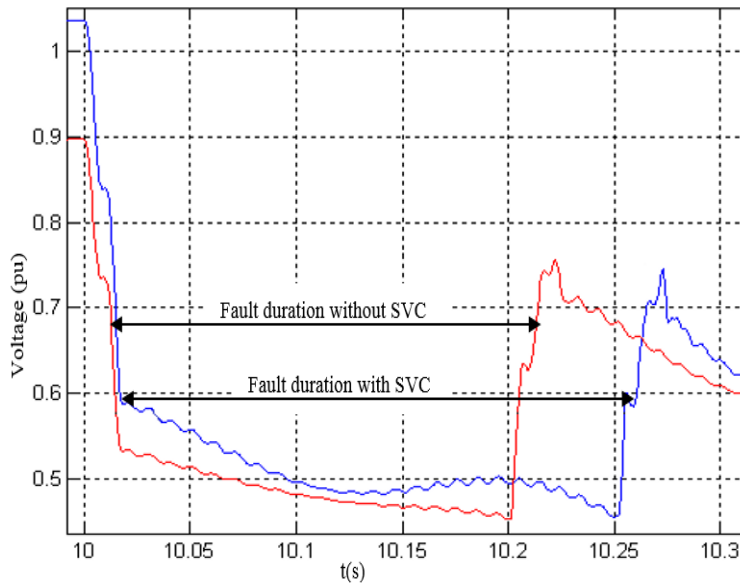


Figure 17: Zoom of Figure 16

Also, in the same way for a voltage dip of 30%, which is represented by figure 18, one was able to maintain the stable state of the wind farm for a du-

ration of 1.9s by the use of SVC. But, when the static VAR compensator is ignored, only during 0.935 seconds the power plant keeps its stability.

Figures 14 and 15 show the evolution of active and reactive power, at the distribution grid at the wind farm coupling node. Consequently, the wind

farm loses its stability when it can recover its normal operation when the Static VAR Compensator is placed.

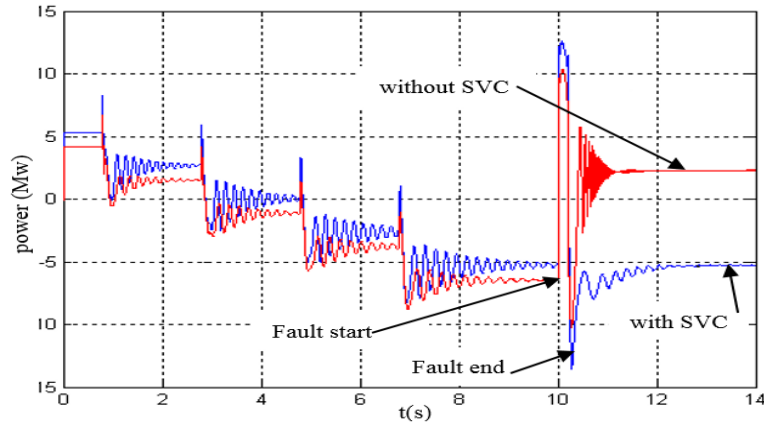


Figure 14: Active power at equivalent Thevenin's generator outputs (Node 5) for 60% dip depth

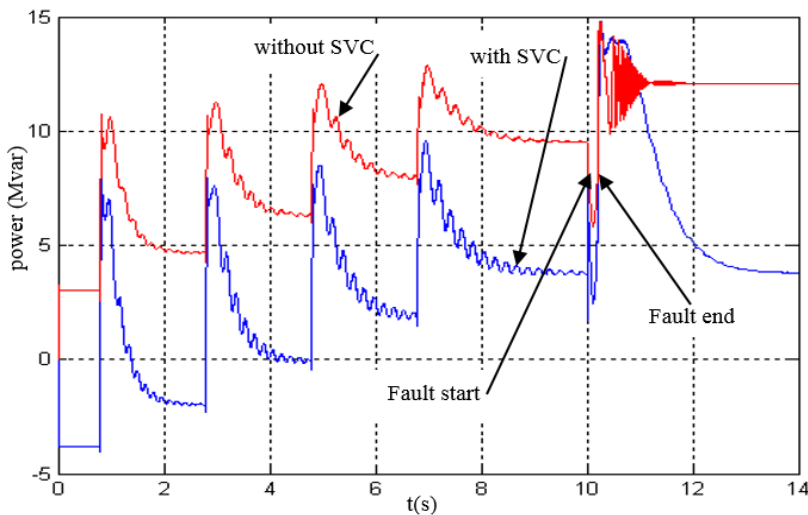


Figure 15: Reactive power at equivalent Thevenin's generator outputs (Node 5) for 60% dip depth

Figures 16 and 17 represent the voltage evolution at node n° 5 for a depth of the sag of 50%, with and without SVC. The wind farm was able to restore its normal operating condition after a longer period (250 milliseconds) in the

presence of the SVC which can be done in 200 ms in the absence of the SVC. It is clear that the compensator was able to extend the time interval during which the wind farm keeps its stability.

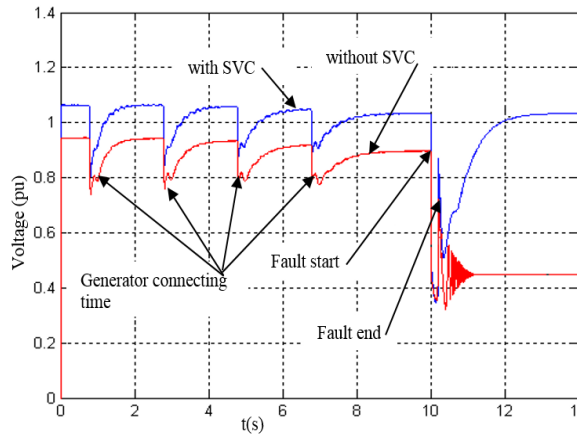


Figure 11: Zoom of figure 10

Figures 12 and 13 show the active and reactive powers at the wind power plant output. It can be noted that at the fault time, the wind farm deliv-

ers reactive power to the grid and that it no longer supplies active power once it has lost synchronism (figure.12).

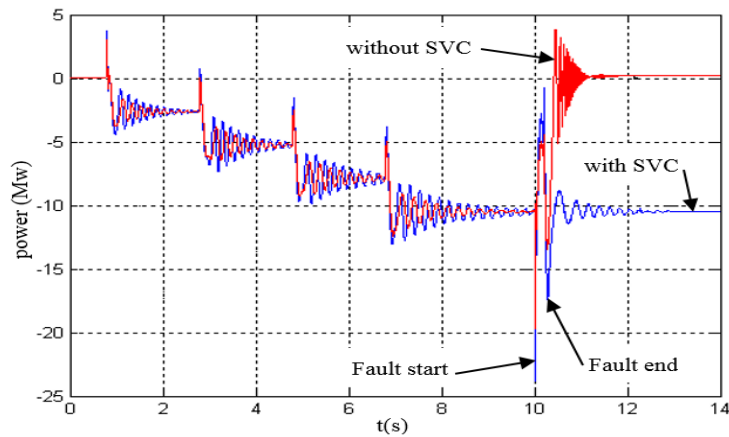


Figure 12: Active power supplied by power plant for a 60% depth dip

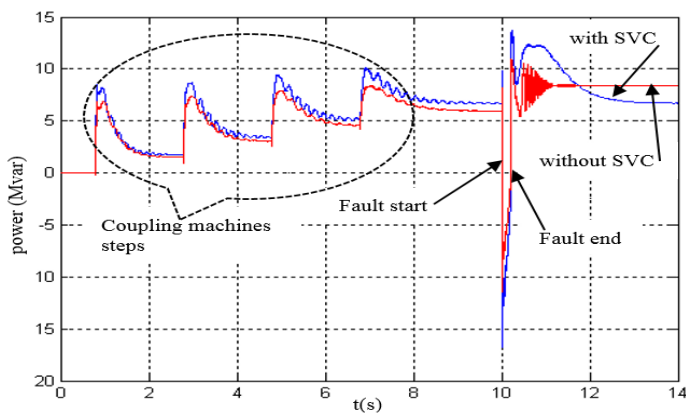


Figure 13: Reactive power supplied by the power plant for a 60% depth dip

It is remarked that the generators request a strong starting current at the machine coupling time which explains the significant consumption of reactive power. In practice, this transient is attenuated by the coupling dimmer whose role is the soft starting

5. DYNAMIC BEHAVIOR OF SVC DURING GRID FAULTS

5.1. Characteristics of Grid Faults

In this section, the ability of wind farms is examined. This is to maintain their stability face to the faults that may arise in a network using the static reactive power compensator. Indeed, their integration into the electrical energy transmission and distribution grid posed problems related to the grid stability and the injected power quality. In addition, wind farms are generally located at the sending end of the line where the grid is characterized by a low short-circuit power and therefore they can suffer the consequences of its weakness and can lead to poor quality of the power supply. The quality of the voltage is linked on the one hand, to the voltage value and its frequency between pre-defined limits and on the other hand, to the absence of disturbances. The disturbances that can affect the voltage are:

- brief overvoltage, likely to damage the devices,
- three-phase voltage imbalances,
- quick variations in voltage, voltage sags,
- distorted waveforms: flicker, harmonics.

5.1.1. Voltage Sags (dips)

A voltage sag is a sudden drop in the supply voltage, at a node on an electrical power grid, ranging from 90% to 1% (IEC 61000-2-1) or between 90% and 10% (IEEE 1159). Voltage dips (sags) are characterized by their amplitude and their duration. The duration of the voltage dip can range from 10 milliseconds to 3 minutes. Phenomena whose duration is less than 10 milliseconds are considered as transient phenomena. The voltage dips are mainly caused by phenomena leading to high currents which cause a large voltage drop across the impedances of the grid elements. Other random phenomena, namely atmospheric conditions and strikes with foreign bodies (car percussion, earthworks, etc.) can be the cause of voltage sags. Voltage sags are likely to disturb the operation of certain industrial installations as well as many devices connected to the grid (Kang, Choi, Morsy & Enjeti 2017). They are the most common cause of energy quality problems. Indeed, this fault type can cause degraded functioning of the electrical equipment as well as their destruction. For each type of voltage sag, the appropriate Z_F load must be coupled to determine the desired depth (Figure 2). In Figure 10, one shows the voltage evolution at node 5 with and without SVC for a wind torque equal to the rated torque. The 32 asynchronous generators are coupled by group of eight wind turbines. The fault was created at time $t_0 = 10$ s. Figures 10 and 11 show that the wind farm is capable to restore its normal operating state after a 192 milliseconds dip duration and a depth of 60% when the SVC is coupled but the wind farm loses its stability in the absence of SVC.

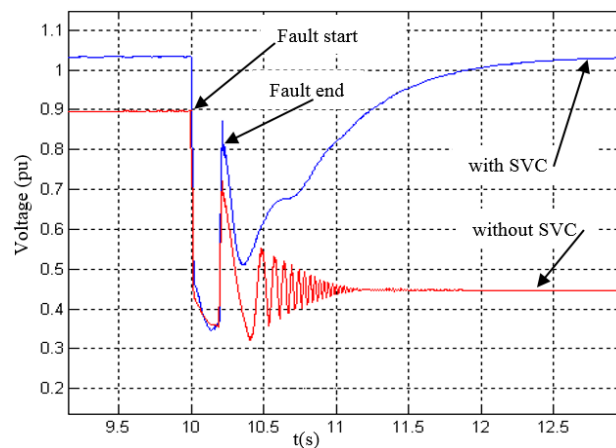


Figure 10: voltage at Node 5 with 60% depth dip

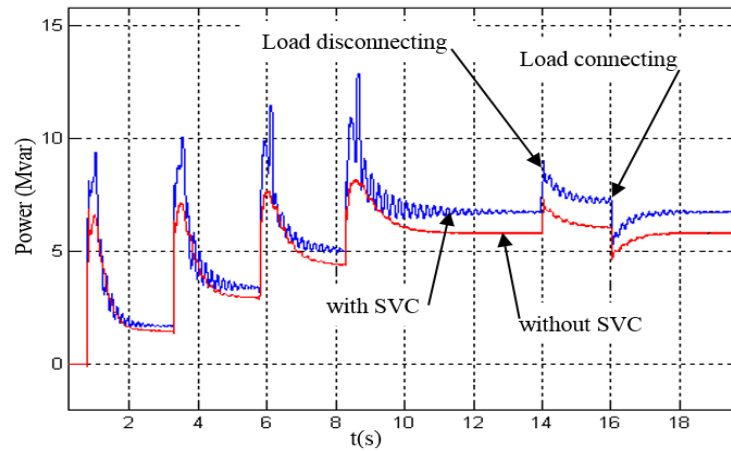


Figure 7: reactive power absorbed by 32 wind generator

Figures 8 and 9 show the active and reactive power at the output of the Thevenin's equivalent generator (supplied by the grid) with and without SVC. These two characteristics show the improvement

introduced by the use of SVC by reducing the reactive power transmitted by the grid upstream of node 5 which minimizes losses in the transmission and distribution lines.

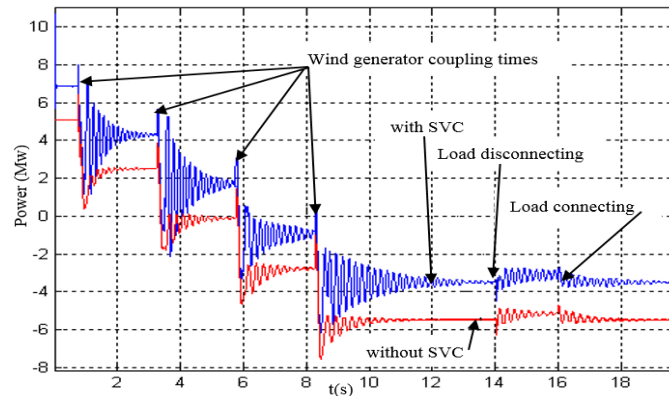


Figure 8: Active power at the output of Thevenin's equivalent generator

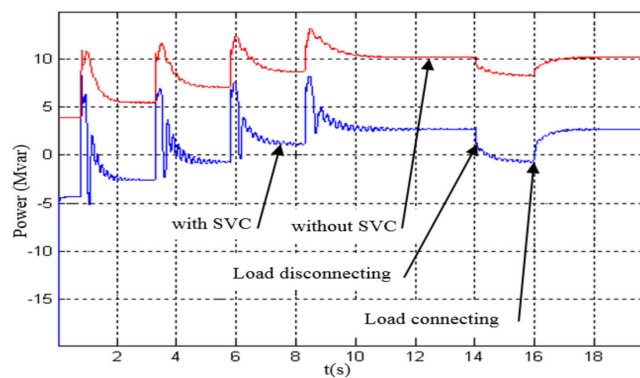


Figure 9: Active power at the output of Thevenin's equivalent generator

2.1.2. Design Controller

Ziegler and Nichols determined by simulation for various types of processes the parameters of the PI controller. The settings indicated in Table 1 correspond to the values approaching the opti-

mum of the criterion and generally give a relatively satisfactory behavior in regulation. The choice was fixed on a PI type controller given its essential role for the cancellation of the position static error without altering the initial performance of the system.

Table 1: Parameter of PI controller

Controller	Step response method	Sustained oscillation method
$Kp(1+1/\tau_i s)$	$Kp=0.9/(a*Tr)$ $\tau_i=3.3* Tr$	$Kp=0.5*K_0$ $\tau_i=0.83*T_0$

3. Operating Regime Analysis

Let us consider the case where the wind torque has the same value of the rated torque. For this regime, the simulation was carried out for load factor $ku = 0.5$ which means that the grid is heavily loaded. Figure 6 shows the voltage evolution at the node 5 with and without the use of SVC. The

32 induction generators are attached to the grid by groups of eight wind turbines, given the impossibility of coupling them together because the wind torque is very high and one can only connect 11 machines simultaneously. Figure 6 shows that the voltage drop at node 5 can exceed 10% without using the SVC, which justifies the need for compensation.

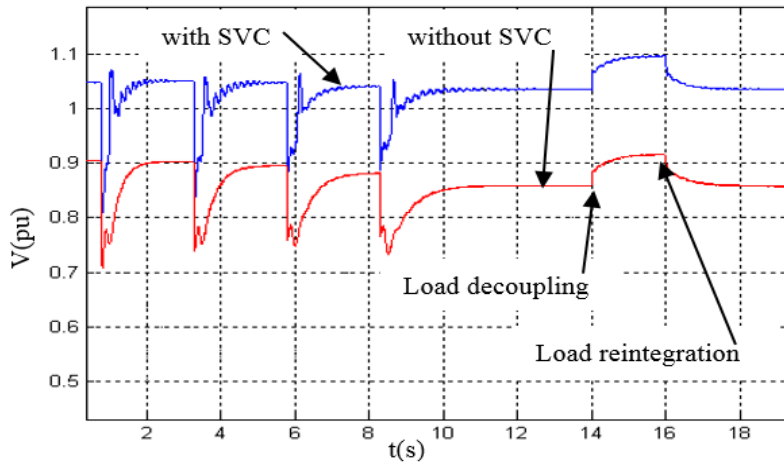


Figure 6: voltage evolution at node 5 of the grid

Figures 7 shows the impact of the sudden variation of the load on the quality of the reactive power absorbed by the wind turbines. This load variation is materialized by disconnecting the load and their connecting. It is noted that the consumption of

the reactive power is reduced at the time of their connecting. The loads disconnection generates an overvoltage at the coupling node of the wind farm. Consequently, a greater consumption of the reactive power is attained.

2.1. Voltage Regulation

This strategy is based on a successive comparison of the grid voltage across the terminals of the power plant to the reference voltage. The result of this

comparison can be processed by the regulator. The latter, in turn, determines the firing angle of the thyristors α according to the chosen control law. The block diagram of the control loop is given in Figure 5.

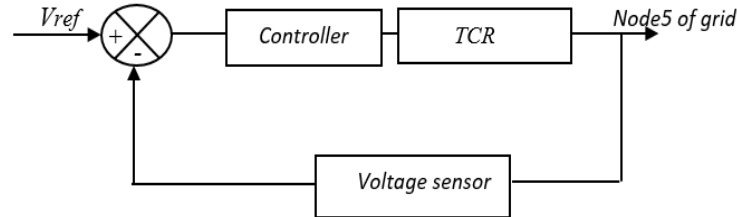


Figure 4: Block diagram of the control loop

However, the synthesis of the controller requires knowledge of the transfer function of the absorber in order to be able to deduce the appropriate parameters. This step requires the identification of the process.

2.1.1. Identification

In this work, to model the TCR, one proceed-

ed by a step response analysis in order to determine the parameters of the selected model. This method consists in stimulating the process (TCR) by a step in alpha (firing angle of thyristor) and analyzing the behavior of the system response. The shape of the TCR response can be approximated by Figure 5.

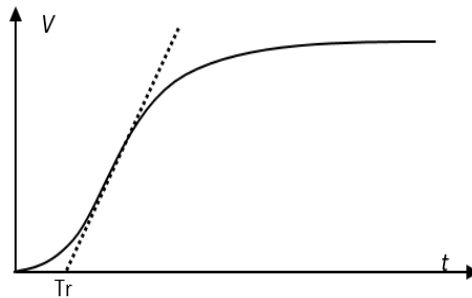


Figure 5: step response shape of the TCR

Using the Ziegler-Nichols approximation, it is possible to determine the parameters of the proportional integral (PI) or proportional integral derivative (PID) type controller associated with an aperiodic response process without having to carry out the exact identification. The simplified model adopted for the process is then written as follow:

$$H(s) = \left(\frac{a}{s}\right)e^{-Trs} \tag{5}$$

where S is a complex number frequency parameter. This model therefore corresponds to an integrator with a gain and Tr delay.

2.3.Active And Reactive Power in Wind Generating

The consumption of reactive power of the wind power plant depends on the active power supplied, which itself depends on the mechanical power received from the wind. The actually solution used for reactive power compensation is based on the use of capacitor

banks or steps for each wind turbine. This approach consists in replacing the local compensation of each wind turbine with a global compensation of the entire power plant as well as the loads which are in the vicinity of the coupling node of the wind turbine to the electrical grid. The dynamic compensation is assured by the developed SVC which is shown in Figure 3.

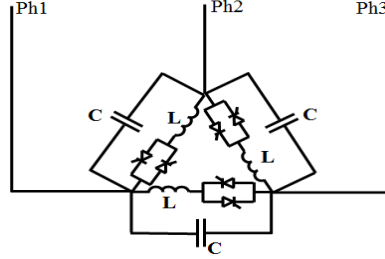


Figure 3: Three phase scheme of the studied SVC

2. Compensator Design

The compensator studied makes it possible to maintain a voltage level at the coupling node of the wind turbine. The allowed voltage drop ΔV must not exceed 10% ($\Delta V \leq 10\%$). The elements that constitute the static reactive power compensator are calculated in such a way that the latter can compensate the wind turbines as well as the neighboring loads. The maximum reactive power absorbed by the wind

turbine is around 6.44 MVAR. The reactive power required is around 4.65 MVAR for a load coefficient $ku = 0.5$ which means that the grid is heavily loaded. The fixed capacitor is designed to provide a fixed maximum reactive power Q_{cond} equal to the sum of these two reactive powers. Let us assume that L absorbs a part of reactive power which is provided by the total maximum capacitor C and that this inductance involves an internal resistance R_L . The removed capacitor $C(\psi)$ can be expressed as:

$$C(\psi) = \frac{1}{\omega\pi^2 \sqrt{R_L^2 + (L\omega)^2}} \left(\frac{1}{2} - \frac{1}{2} \cos 2(\psi - \beta) + (\beta - \psi)^2 + (\beta - \psi)(\sin 2\psi - \sin 2\beta) \right) \sin \phi_1 \quad (2)$$

So, the variation of the R load is accompanied by a change of a final equivalent capacitor $C_{eq}(\psi)$ through changing the firing angle ψ . In this case, the equivalent reactive power available is defined by:

$$Q_{eq} = U^2 \omega C_{eq}(\psi) \quad (3)$$

The coil, placed in series with a dimmer, serves to absorb the excess reactive power supplied by the capacitor banks. If this coil is considered purely inductive, the reactive power absorbed by the coil, in each arm, is given by the following relation:

$$Q_L = \frac{V^2}{\pi L \omega} (2\pi - 2\alpha + \sin 2\alpha) \quad (4)$$

where α is the firing angle of the thyristors. The absorber's reactive power consumption is maximum for a control angle $\alpha = \pi / 2$. This will allow us to deduce the value of the inductance L of the coil in each arm of the three phase dimmer.

2.2. Wind Generator Modelling

The Doubly-Fed Induction Generator (DFIG) is the dominant technology for variable-speed wind power generation. Indeed, the accessibility to the stator and the rotor offers the opportunity to have several degrees of freedom to properly control the transfer of power and the power factor with all the possibilities of recovery or the injection of energy into the windings of the machine.

However, a disadvantage of the DFIG is its vulnerability to grid disturbances because the stator windings are connected directly to the grid. Therefore, the maintenance requirements and potential failure of brushes and slip rings are a significant disadvantage of DFIG. In addition, this type of the machine has complex control schemes. Also, it

has limited fault ride through capability and needs protection schemes.

On the other hand, the induction generator is simple, reliable, and requires very little maintenance which makes it competitive and that can explain their increasing in the electrical energy production.

For these reasons, the choice of using squirrel cage machine is the result of a compromise which favors the structure's robustness relative to the regulation facilities.

The squirrel cage induction generator model is developed using an analytical model. This model is implemented in Matlab/Simulink. The latter is based on Park two-phase frame to study the steady state and it is given by the following equations system.

$$\begin{cases} \frac{di_{\mu d}}{dt} = -\frac{R_s}{L_s} i_{sd} + \frac{1}{L_s} V_{sd} \\ \frac{di_{\mu q}}{dt} = -\frac{R_s}{L_s} i_{sq} + \frac{1}{L_s} V_{sq} \\ \frac{di_{sd}}{dt} = \frac{R_r}{\sigma L_r} i_{\mu d} + \frac{1}{\sigma} \omega_r i_{\mu q} - \left(\frac{R_s}{\sigma L_s} + \frac{R_r}{\sigma L_r} \right) i_{sd} - \omega_r i_{sq} + \frac{1}{\sigma L_s} V_{sd} \\ \frac{di_{sq}}{dt} = -\frac{1}{\sigma} \omega_r i_{\mu d} + \frac{R_r}{\sigma L_r} i_{sq} + \omega_r i_{sd} - \left(\frac{R_s}{\sigma L_s} + \frac{R_r}{\sigma L_r} \right) i_{sq} + \frac{1}{\sigma L_s} V_{sq} \\ \frac{d\omega_r}{dt} = \frac{p}{J} [pL_s(i_{\mu d}i_{sq} - i_{\mu q}i_{sd}) - C_v] = C_{em} - C_v \end{cases} \quad (1)$$

Where

$$\sigma = 1 - \frac{M_{sr}^2}{L_s L_r} : \text{coefficient of dispersion}$$

C_v : The wind torque related to the rotor of the machine,

C_{em} : The developed electromagnetic torque.

The parameters of the induction generator are given by: Rotor resistance: $R_r = 0.00396 \Omega$; Stator resistance: $R_s = 0.0058 \Omega$; Stator inductance: $L_s = 0.00986 \text{ H}$; Rotor inductance: $L_r = 0.00986 \text{ H}$; Mutual inductance: $M_{sr} = 0.00954 \text{ H}$.

using the static VAR compensator. Subsequently, one investigates in the role of the SVC in improving the stability of the wind power plant during grid faults such as sags and short-circuits.

2. DYNAMIC REACTIVE POWER COMPENSATION

2.1. Grid Modeling

The wind turbines are installed at the end of the grid of Houaria, from the high-voltage substation in Korba. The latter is a Mediterranean town located at the east of the governorate of Nabeul (Cap Bon). The city of Korba province has 34,807 inhabitants (2004 census) and the average altitude is 316 m. The outgoing line substation in Korba is characterized by an operating voltage fixed by the voltage

regulator at 32 kV. The overall grid consists of 32 wind generators with a unit power of 330 kW, with a rated voltage of 400V/ 690V. Let us consider 17 nodes given by Figure 1. The single-phase single-line diagram of the grid can be represented by a Thevenin model seen from node n°5 while keeping the two start of loads 7-9 and 10-15 as shown in Figure 2 (load 1, 2). The load n°1 represents the total of the loads of nodes 7, 8 and 9 and the load n°2 groups together the load of nodes 10, 11, 12, 13, 14, and 15. These loads can be disconnected by acting on the switch K. The E_{th} and Z_{th} parameters depend on the state of the grid, i.e. the load coefficient defined by the ratio of the effective power by the power installed in each feeder. The load coefficient K_u is considered the same for all loads. The consumption of electrical energy is highly variable in the Sidi-Daoud region, especially since the significant load in this region are seasonal.

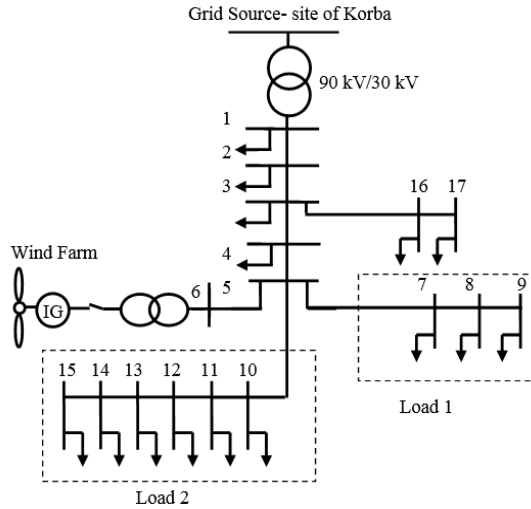


Figure 1: Simplified single-line diagram

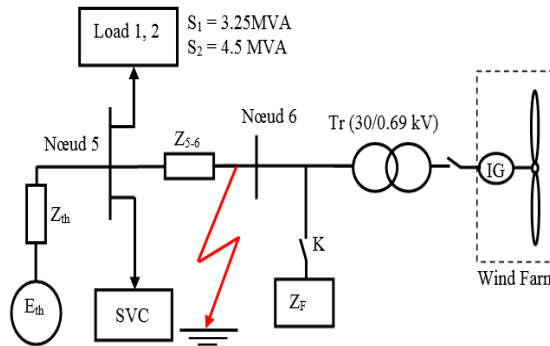


Figure 2: Thevenin's model of the grid and the wind farm of the grid

1. INTRODUCTION

The energy is at the heart of the operating of all industrial societies. An accessibility of energy, at reasonable prices and without limits, appeared as a necessary condition for economic developments and individual comfort. However, the increasing use of non-renewable energies by industrialists leads to increased depletion of fossil and fissile resources (Ye, Vera & Miguel, 2016). This causes the progressive degradation of the environment and threatens the health of human beings. Major and rapid climate change, due to an increase in the greenhouse effect, requires a reasonable and harmless use of energy as part of a sustainable development model. There is thus a correlation between the problems of energy, environment, and development.

Today, wind power is considered one of the most promising renewable energies for the planet's energy future. The development of this technology continues to assert itself around the world given its clean and inexhaustible. As a result, wind energy is an alternative solution to meet the needs of today's society. The proliferation of wind turbines has pushed researchers to invest in this area to increase the efficiency of electromechanical conversion and improve the quality of energy that can be distributed to different types of receivers (Deng, Kornelis & Kees, 2012, Altınta, Okten, Karsu & Kocaman, 2018, Olusayo, Josiah & Yskandar, 2019). Three-phase induction machines based on wind turbines is relatively widespread as energy generating devices. These induction machines are widely used to provide electrical energy for the individual as well as for technical sites (Vanishree & Ramesh 2018, Hemeida, Hussien & Abdel Wahab 2015). In addition, wind power plants are generally located at the end of the line where the network is characterized by a low short-circuit power. Consequently, these wind turbines suffer the consequences of the weakness of the line and may possibly aggravate the phenomenon of voltage fluctuations. This can lead to poor quality of the power supply. As a studied special case, the Sidi-Daoud wind power plant (first unit) is equipped with asynchronous squirrel-cage machines with a unit power of 330 kW, with a nominal voltage of 400/690 Volts. Each group of 4 machines is connected to the grid through a step-up transformer

(0.69kV / 30kV) of 1.6 MVA. These wind turbines are located at the end of the distribution grid (30 kV) in the North region of Cap Bon. The other end of this local distribution grid is supplied by the step down transformer (90 kV / 30 kV) from Korba, whose short-circuit power is 577 MVA. The main load for the region is made up of housing, pumping stations, and the seasonal food industry. The compensation of each wind generator is done by four stages of batteries (50 kVAR, 50 kVAR, 30 kVAR and 30 kVAR). However, this technique has the disadvantage of providing a reactive power generally higher or lower than the requested power. This reactive power fluctuation alters the quality of the voltage at the coupling node of the wind turbine to the power grid. One must also take into account the harmful effects of mechanical switching which can cause transients of large currents and that this switching is not so fast to be able to follow the instantaneous power variations. Consequently, dynamic compensation of reactive power seems to be good alternative at the connection nodes of wind turbines both to provide the reactive power required by these wind turbines in a unified manner and for the maintenance of voltage on the grid.

The focus of this work consists on the study of system based on power electronics components called SVC. The latter makes it possible to design a control strategy for the voltages and the reactive power flows crossing through the grid (Mohammad & Akbar, 2017, Jiashen, Ching-Ming & Yu-Huei, 2018, Oyekanmi, Radman, Babalola & Uzoechi, 2013, Pathak, Sharma & Gupta, 2016, Raju & Pillai, 2016). Static reactive power compensators are shunt generating or absorbing the reactive power. They can be used to regulate the voltage, at the nodes of grid connection by feeding an active or reactive current (Nitin & Ashwani, 2016, Srinivasa & Srinivasa, 2015, Stalin, Shiva, Revanth, Velbharathi & Durai, 2015, Tamer & Mohamed, 2017, Hemeida, Rezk & Hamada, 2018). Consequently, it can be identified as a variable impedance that can be sometimes inductive or capacitive. SVCs consist of thyristor-controlled reactors and/or capacitors and are used to improve the dynamic performance of electrical systems (Ezzeddine, 2019). Through this study one start by identifying the various SVC components, which allow us to synthesize the controller which must be placed in the feedback control system. The voltage quality improvement is, thereafter, studied



المملكة العربية السعودية
جامعة الحدود الشمالية (NBU)

مجلة الشمال للعلوم الأساسية والتطبيقية (JNBAS)

طباعة - ردمد: 1658-7022 / الكتروني - ردمد: 1658-7014

www.nbu.edu.sa
http://jnbas.nbu.edu.sa

مجلة الشمال
للعلوم
الأساسية والتطبيقية
دورية علمية محكمة

جامعة الحدود الشمالية

1658-7022
1658-7014



السلوك الديناميكي لمعوض القدرة التفاعلية الثابت على رد الفعل أثناء أعطال الشبكة بما في ذلك محطة طاقة الرياح

عزالدين التوتي 201

1. قسم الهندسة الكهربائية بكلية الهندسة- جامعة الحدود الشمالية- عرعر- المملكة العربية السعودية
2. قسم الهندسة الكهربائية بالمدرسة الوطنية العليا للمهندسين بتونس -جامعة تونس - تونس

(قدم للنشر في 1441/07/01هـ؛ وقبل للنشر في 1442/01/15هـ)

ملخص: تستخدم الآلات الحثية على نطاق واسع كمولدات في طاقة الرياح بسبب متانتها وموثوقيتها وتكلفتها المنخفضة وصيانتها. ومع ذلك، نظرًا للطلب الملح على الطاقة التفاعلية من النظام الذي تتصل به، فإن استخدام هذا النوع من المولدات ينطوي على مشكلات جديدة تتعلق بجودة الطاقة ذات الصلة بالاندماج، والتي تتكون عمومًا من تعديل الجهد وتعويض القدرة التفاعلية. هذه المشاكل قد تسبب انخفاض الجهد وعدم الاستقرار الديناميكي المحتمل.

في هذه الورقة البحثية، نحن مهتمون بتطوير معوض ثابت لتثبيت الجهد عبر توربينات الرياح إلى جانب الشبكة عن طريق تعويض ديناميكي للقوة التفاعلية. يستخدم المعوض، بالإضافة إلى المكثفات الثابتة المركبة بالتوازي ملفًا متغيرًا بواسطة الثايرستور لضمان استجابة ديناميكية للقدرة التفاعلية المتغيرة لمحطة توليد الطاقة التي تحتوي على توربينات الرياح والمزودة بمولدات غير متزامنة وكذلك الأحمال المجاورة.

يعرض هذا العمل أيضًا السلوك الديناميكي لـ SVC أثناء بعض الأخطاء التي قد تحدث في الشبكة التي تضم محطة طاقة الرياح. ثم يتم اختبار أداء SVC لأنظمة التشغيل المختلفة. أظهرت هذه الدراسة انخفاض مستوى تذبذب الجهد، وبالتالي توحيد جودة الجهد في نقطة الاقتران. أيضًا، أظهر هذا التحليل تحسن استقرار محطة الطاقة أمام العيوب المدروسة.

كلمات مفتاحية: محطة طاقة الرياح، SVC، TCR، جودة الجهد، أخطاء الشبكة.

JNBAS ©1658-7022 . (1441هـ/2020م) نشر بواسطة جامعة الحدود الشمالية. جميع الحقوق محفوظة.

* للمراسلة:

أستاذ مساعد، قسم الهندسة الكهربائية، كلية الهندسة، جامعة الحدود الشمالية، ص ب: 1321، رمز بريدي: 91431، عرعر، المملكة العربية السعودية.

e-mail: touti.these09@gmail.com



jnbas.nbu.edu.sa

DOI: 10.12816/0056078



KINGDOM OF SAUDI ARABIA
Northern Border University (NBU)
Journal of the North for Basic and Applied Sciences
(JNBAS)
p- ISSN: 1658 - 7022 / e- ISSN: 1658 - 7014
www.nbu.edu.sa
http://jnbas.nbu.edu.sa



Journal of the North
for Basic and
Applied Sciences

Peer-Reviewed Scientific Journal

Northern Border University
www.nbu.edu.sa

Volume 5
Issue 2
2020

Dynamic Behavior of Static VAR Compensator during Faults of Grid Including Wind Power Plant

E. Touti^{1,2}

1. Department of Electrical Engineering, Northern Border University, Arar, 1321, Saudi Arabia
2. Department of Electrical Engineering, LISIER, University of Tunis, Tunisia

(Received 25/02/2020; Accepted 03 /09 /2020)

Abstract: Induction machines are widely used as generators in wind power generations because of their robustness, reliability, low cost, and maintenance. Nevertheless, due to their reactive power demand from the system to which they are connected, the use of this type of generators carries new related power quality problems, which generally consist of voltage regulation and reactive power compensation.

To stabilize the voltage across a wind turbine coupled to the grid, a Static VAR Compensator (SVC) is developed in this paper. The compensator, based on a Fixed Capacitor Thyristor Controlled Reactor (FC-TCR) type uses a capacitor bank mounted in parallel with a thyristor-controlled coil to ensure a dynamic response to the variable reactive power of a power plant which contains wind turbine equipped with induction generators. This work presents the dynamic behavior of the SVC during faults that may occur in the grid. Then, the SVC performance is tested for different operating regimes. This study showed the reduction of the voltage fluctuation level and subsequently a consolidation of the voltage quality at the coupling node. Also, this analysis showed the improvement of the stability of the power plant in front of the studied faults.

Keywords: Wind farm, SVC, TCR, voltage quality, grid faults.

1658-7022© JNBAS. (1441 H/2020). Published by Northern Border University (NBU). All Rights Reserved.



jnbas.nbu.edu.sa

DOI: 10.12816/0056078

* **Corresponding Author:**

Assistant Professor, Dept. Electrical Engineering, Faculty Engineering - Northern Border - University, P.O. Box: 1321, Postal Code: 91431, Arar, Kingdom of Saudi Arabia.

e-mail:touti.these09@gmail.com

- Shi, Y. Q., & Sun, H. (2008). *Image and video compression for multimedia engineering: Fundamentals, algorithms, and standards*. CRC press.
- Statista Research Department, (2019). *Mobile phone video viewers in the United States 2014-2020*. Retrieved from: <https://www.statista.com/statistics/209348/mobile-video-viewers-in-the-united-states/>
- Sullivan, G. J., Ohm, J. R., Han, W. J., & Wiegand, T. (2012). Overview of the high efficiency video coding (HEVC) standard. *IEEE Transactions on circuits and systems for video technology*, 22(12), 1649-1668.
- Sze, V., Budagavi, M., & Sullivan, G. J. (2014). High efficiency video coding (HEVC). *Integrated Circuit and Systems, Algorithms and Architectures. Springer*, 39, 40.
- Tan, H. L., Ko, C. C., & Rahardja, S. (2016). Fast coding quad-tree decisions using prediction residuals statistics for high efficiency video coding (HEVC). *IEEE Transactions on Broadcasting*, 62(1), 128-133.
- Tech, G., Chen, Y., Müller, K., Ohm, J. R., Vetro, A., & Wang, Y. K. (2016). Overview of the multiview and 3D extensions of high efficiency video coding. *IEEE Transactions on Circuits and Systems for Video Technology*, 26(1), 35-49.
- Verna, P. (2019). *Global Digital Video 2019*. Retrieved from: <https://www.emarketer.com/content/digital-video-2019>.
- Vetro, A., Wiegand, T., & Sullivan, G. J. (2011). Overview of the stereo and multiview video coding extensions of the H. 264/MPEG-4 AVC standard. *Proceedings of the IEEE*, 99(4), 626-642.
- Wiegand, T., Sullivan, G. J., Bjontegaard, G., & Luthra, A. (2003). Overview of the H. 264/AVC video coding standard. *IEEE Transactions on circuits and systems for video technology*, 13(7), 560-576.
- Xu, J., Joshi, R., & Cohen, R. A. (2016). Overview of the emerging HEVC screen content coding extension. *IEEE Transactions on Circuits and Systems for Video Technology*, 26(1), 50-62.
- Yan, C., Zhang, Y., Dai, F., & Li, L. (2013, March). Highly parallel framework for HEVC motion estimation on many-core platform. In *2013 Data Compression Conference* (pp. 6372-).
- Yang, C. L., Po, L. M., & Lam, W. H. (2004, October). A fast H. 264 intra prediction algorithm using macroblock properties. In *Image Processing, 2004. ICIP'04. 2004 International Conference on* (Vol. 1, pp. 461464-).
- Yeh, C. H., Fan, K. J., Chen, M. J., & Li, G. L. (2010). Fast mode decision algorithm for scalable video coding using Bayesian theorem detection and Markov process. *IEEE Transactions on Circuits and Systems for Video Technology*, 20(4), 563-574.
- Yin, P., Tourapis, H. Y., Tourapis, A. M., & Boyce, J. (2003, September). Fast mode decision and motion estimation for JVT/H. 264. In *Image Processing, 2003. ICIP 2003. Proceedings. 2003 International Conference on* (Vol. 3, pp. III-853).
- Zhang, Q., Yang, Y., Chang, H., Zhang, W., & Gan, Y. (2017). Fast intra mode decision for depth coding in 3D-HEVC. *Multidimensional Systems and Signal Processing*, 28(4), 1203-1226.
- Zhang, T., & Mao, S. (2019). An overview of emerging video coding standards. *GetMobile: Mobile Computing and Communications*, 22(4), 13-20.

- Baltimore, MD, 2017, pp. 1-4.
- Jou, S. Y., Chang, S. J., & Chang, T. S. (2015). Fast motion estimation algorithm and design for real time QFHD high efficiency video coding. *IEEE Transactions on Circuits and Systems for Video Technology*, 25(9), 1533-1544.
- Jung, S. W., Baek, S. J., Park, C. S., & Ko, S. J. (2010). Fast mode decision using all-zero block detection for fidelity and spatial scalable video coding. *IEEE Transactions on Circuits and Systems for Video Technology*, 20(2), 201-206.
- Khan, S. N., & Khattak, S. (2017, November). Early decision of CU splitting, using base view information, for low complexity MV-HEVC. In *Multi-topic Conference (INMIC), 2017 International* (pp. 16-). IEEE.
- Khattak, S. (2013, June). Framework for low-complexity multiview video coding. In *Proc. 14th annual post graduate symposium on the convergence of Telecommunications, Networking, and Broadcasting (PGNet2013), Liverpool, UK*.
- Khattak, S. (2014). *Low complexity multiview video coding* (Doctoral dissertation). De Montfort University, Leicester, UK.
- Kim, C., Shih, H. H., & Kuo, C. C. J. (2006). Fast H. 264 intra-prediction mode selection using joint spatial and transform domain features. *Journal of Visual Communication and Image Representation*, 17(2), 291-310.
- Koumaras, H., Kourtis, M. A., & Martakos, D. (2012). Benchmarking the encoding efficiency of h. 265/hevc and h. 264/avc. In *2012 Future Network & Mobile Summit (FutureNetw)* (pp. 17-).
- Kuo, C. M., Chung, S. C., & Shih, P. Y. (2006). Kalman filtering based rate-constrained motion estimation for very low bit rate video coding. *IEEE transactions on circuits and systems for video technology*, 16(1), 3-18.
- Lee, J. H., Jang, K. S., Kim, B. G., Jeong, S., & Choi, J. S. (2015, January). Fast intra mode decision algorithm based on local binary patterns in High Efficiency Video Coding (HEVC). In *Consumer Electronics (ICCE), 2015 IEEE International Conference on* (pp. 270272-).
- Liu, S. (2019). *Online video codecs and containers share worldwide 2016-2018*. Retrieved from: <https://www.statista.com/statistics/710673/worldwide-video-codecs-containers-share-online/>
- Lu, X., & Martin, G. R. (2013). Fast mode decision algorithm for the H. 264/AVC scalable video coding extension. *IEEE Transactions on Circuits and Systems for Video Technology*, 23(5), 846-855.
- Lv, H., Wang, R., Xie, X., Jia, H., & Gao, W. (2012, November). A comparison of fractional-pel interpolation filters in HEVC and H. 264/AVC. In *2012 Visual Communications and Image Processing* (pp. 16-).
- Nguyen, T., & Marpe, D. (2012, May). Performance analysis of HEVC-based intra coding for still image compression. In *2012 Picture Coding Symposium* (pp. 233236-).
- Ozer, J. (2019). *A video codec licensing update*. Retrieved from: <https://www.streamingmedia.com/Articles/ReadArticle.aspx?ArticleID=129386>
- Pan, F., Lin, X., Rahardja, S., Lim, K. P., Li, Z. G., Wu, D., & Wu, S. (2005). Fast mode decision algorithm for intraprediction in H. 264/AVC video coding. *IEEE Transactions on Circuits and Systems for Video Technology*, 15(7), 813-822.
- Pourazad, M. T., Doutre, C., Azimi, M., & Nasiopoulos, P. (2012). HEVC: The new gold standard for video compression: How does HEVC compare with H. 264/AVC? *IEEE consumer electronics magazine*, 1(3), 36-46.
- Rayburn, D. (2015). *HEVC Advance Patent Pool Creates Confusion, Lacks Transparency*. Retrieved from: <https://www.streamingmedia.com/Articles/Editorial/Featured-Articles/HEVC-Advance-Patent-Pool-Creates-Confusion-Lacks-Transparency-105235.aspx>
- Richardson, I. E. (2010). *The H. 264 advanced video compression standard*. John Wiley & Sons.
- Roesler, P. (2019). *Internet video to account for 80% of global traffic by 2019*. Retrieved from: <https://www.webmarketingpros.com/internet-video-to-account-for-80-of-global-traffic-by-2019/>.
- Rutz, G (2016). *The Cost of Codecs: Royalty-Bearing Video Compression Standards and the Road that Lies Ahead*. Retrieved from: <https://www.cablelabs.com/the-cost-of-codecs-royalty-bearing-video-compression-standards-and-the-road-that-lies-ahead>
- Segall, A., Baroncini, V., Boyce, J., Chen, J., & Suzuki, T. (2017). Joint Call for Proposals on Video Compression with Capability beyond HEVC. *Joint Video Exploration Team (JVET) of ITU-T SG, 16*.
- Segall, C. A., Katsaggelos, A. K., Molina, R., & Mateos, J. (2004). Bayesian resolution enhancement of compressed video. *IEEE Transactions on image processing*, 13(7), 898-911.
- Shen, L., An, P., Zhang, Z., Hu, Q., & Chen, Z. (2015). A 3D-HEVC fast mode decision algorithm for real-time applications. *ACM Transactions on Multimedia Computing, Communications, and Applications (TOMM)*, 11(3), 34.

HEVC. This feature is more useful for higher resolution videos. It also allows HEVC to achieve much better lossy compression performance compared to H.264. However, the flexibility of HEVC comes at the cost of higher computational complexity. Despite this, in terms of market penetration, H.264 has been a more successful codec compared to HEVC, largely due to its simple licensing structure. From the comparison of H.264 and HEVC, it can be learned that the popularity of a video compression standard depends on both its compression performance as well as its simple licensing structure. It is expected that while developing future video coding standards, both these aspects will be considered.

REFERENCES

- Belghith, F., Kibeya, H., Loukil, H., Ayed, M. A. B., & Masmoudi, N. (2016). A new fast motion estimation algorithm using fast mode decision for high-efficiency video coding standard. *Journal of Real-Time Image Processing, 11*(4), 675-691.
- Bhaskaran, V., & Konstantinides, K. (1997). *Image and video compression standards: algorithms and architectures* (Vol. 408). Springer Science & Business Media.
- Cai, Q., Song, L., Li, G., & Ling, N. (2012, December). Lossy and lossless intra coding performance evaluation: HEVC, H. 264/AVC, JPEG 2000 and JPEG LS. In *Proceedings of The 2012 Asia Pacific Signal and Information Processing Association Annual Summit and Conference* (pp. 19-).
- Chiang, J. C., Peng, K. K., Wu, C. C., Deng, C. Y., & Lie, W. N. (2019). Fast intra mode decision and fast CU size decision for depth video coding in 3D-HEVC. *Signal Processing: Image Communication, 71*, 13-23.
- De-Luxán-Hernández, S., Schwarz H., Marpe, D. and Wiegand, T. (2018). Line-Based Intra Prediction for Next-Generation Video Coding. *2018 25th IEEE International Conference on Image Processing (ICIP)*, Athens, 2018, pp. 221-225.
- Diehl, S., & Karmasin, M. (Eds.). (2013). *Media and convergence management*. Berlin: Springer.
- Digital Rebellion. (2019). *Video space calculator*. Retrieved from: <https://www.digitalrebellion.com/webapps/vidocalc>.
- Dominguez, H., Villegas, O., Sanchez, V., Casas, E., & Rao, K. (2014). The H.264 Video Coding Standard. *IEEE Potentials*, vol. 33, no. 2, pp. 32-38, March-April 2014.
- Fu, C. H., Zhang, H. B., Su, W. M., Tsang, S. H., & Chan, Y. L. (2015, July). Fast wedgelet pattern decision for DMM in 3D-HEVC. In *Digital Signal Processing (DSP), 2015 IEEE International Conference on* (pp. 477481-).
- Garcia, R., & Kalva, H. (2014). Subjective evaluation of HEVC and AVC/H. 264 in mobile environments. *IEEE Transactions on Consumer Electronics, 60*(1), 116-123.
- Grois, D., Marpe, D., Mulyoff, A., Itzhaky, B., & Hadar, O. (2013, December). Performance comparison of h. 265/mpeg-hevc, vp9, and h. 264/mpeg-avc encoders. In *2013 Picture Coding Symposium (PCS)* (pp. 394-397).
- Grois, D., Nguyen, T., & Marpe, D. (2016, December). Coding efficiency comparison of AV1/VP9, H. 265/MPEG-HEVC, and H. 264/MPEG-AVC encoders. In *PCS* (pp. 15-).
- Gul, A., & Khattak, S. (2018). Bayesian early mode decision technique for multiview video coding. *Journal of Graphics, Vision and Image Processing, 18*(1), 15-24.
- Gupta, R., Khanna, M. T., & Chaudhury, S. (2013). Visual saliency guided video compression algorithm. *Signal Processing: Image Communication, 28*(9), 1006-1022.
- H.264/AVC Reference Software (JM 18.3). (2019). Retrieved from: <http://iphome.hhi.de/suehring/tml/download/>
- Hannuksela, M. M., Yan, Y., Huang, X., & Li, H. (2015, September). Overview of the multiview high efficiency video coding (MV-HEVC) standard. In *Image Processing (ICIP), 2015 IEEE International Conference on* (pp. 21542158-). IEEE.
- HEVC Reference Software (HM 7.0). (2019). Retrieved from: <http://hevc.kw.bbc.co.uk/git/w/jetvc-hm.git>
- Ho, Y. S., & Oh, K. J. (2007, June). Overview of multiview video coding. In *Systems, Signals and Image Processing, 2007 and 6th EURASIP Conference focused on Speech and Image Processing, Multimedia Communications and Services. 14th International Workshop on* (pp. 512-).
- Hruska, J. (2013). H.265 standard finalized, could finally replace MPEG-2 and usher in UHD TV. Retrieved from: <https://www.extremetech.com/extreme/147000-h-265-standard-finalized-could-finally-replace-mpeg-2-and-usher-in-uhdtv>
- Jiang, C. and Nooshabadi, S. (2017). H.265/HEVC encoder optimization with parallel-efficient algorithm and QP-based early termination. *2017 IEEE International Symposium on Circuits and Systems (ISCAS)*,

Table 2: Royalty structure of H.264 and HEVC (Rutz, 2016; Ozer, 2019)

Codec	Licensing Organization	Per device royalties	
		Royalty (per unit)	Yearly Cap (Millions)
H.264/AVC	MPEG-LA	\$0.1-\$0.2 depending on volume. No royalties for volumes less than 100,000 units	\$9.75
HEVC	MPEG-LA	\$0.20	\$25
	HEVC Advance	\$0.866	\$25
	Velos Media	\$1.00-2.50	None
	Others	+	+

From Table 2, it can be seen that H.264’s license is owned by a single organization (Rutz, 2016). On the other hand, HEVC’s license is owned by at least three patent pools. These include MPEG-LA, HEVC Advance, and Velos Media. Each of these organizations have a different royalty structure which makes it difficult to understand the royalty structure of HEVC (Rayburn, 2015). What complicates the HEVC royalty structure even further is that apart from these three licensing organizations, there may be individual patent holders who can claim royalties for using HEVC based products. Hence, unlike H.264, where the cost of deployment can be estimated in advance, with HEVC, it is difficult to estimate the total cost of deployment of HEVC due to its complex royalty structure (Rayburn, 2015).

3.5 Beyond H.264 and HEVC

As discussed in the previous sections, while HEVC is technologically superior to H.264, due to its complicated licensing strategy, it has not been as popular as H.264. Hence, there is a need for a video compression standard which combines the strengths of both H.264 (i.e., simple licensing structure) and HEVC (i.e., efficient compression performance). In this regard, currently, there are many video coding standardization activities taking place. This section presents an overview of the recent advances and expected future developments in the field of video compression research.

In terms of standardization work, MPEG and VCEG

are currently working on developing a new video compression standard. This activity is called video compression with capability beyond HEVC (Segall, Baroncini, Boyce, Chen, & Suzuki, 2017). The new activity is expected to result in the development of a new video compression standard which has better compression efficiency compared to HEVC. The standard is expected to be finalized by the end of 2020. Hence, a lot of the video coding research in future is expected to be based on this new standard. The Alliance of Open Media (AOM) is a consortium of industries including Facebook, Google, Microsoft, Apple, IBM, Intel, and Netflix, etc. The alliance has recently combined efforts to develop a royalty-free video compression standard. Their new standard is called the AOM Audio Video 1 (AOM AV1) (Grois, Nguyen, & Marpe, 2016). AOM AV1 achieves around 30% better compression efficiency compared to HEVC. However, the current version of the encoder is very slow. Research is currently being performed to speed up the AOM AV1 encoder.

4. CONCLUSIONS

In this paper, the two most recent video compression standards of H.264 and HEVC were reviewed. It can be concluded from the review that both the standards are based on the well-known principle of hybrid video coding. Moreover, HEVC employs more efficient techniques such as allowing more flexible and finer partitioning of blocks compared to

3.3 Market Adoption

In terms of market penetration, HEVC has not yet

gained as much success as H.264. As can be seen in Figure 9 (Liu, 2019).

**

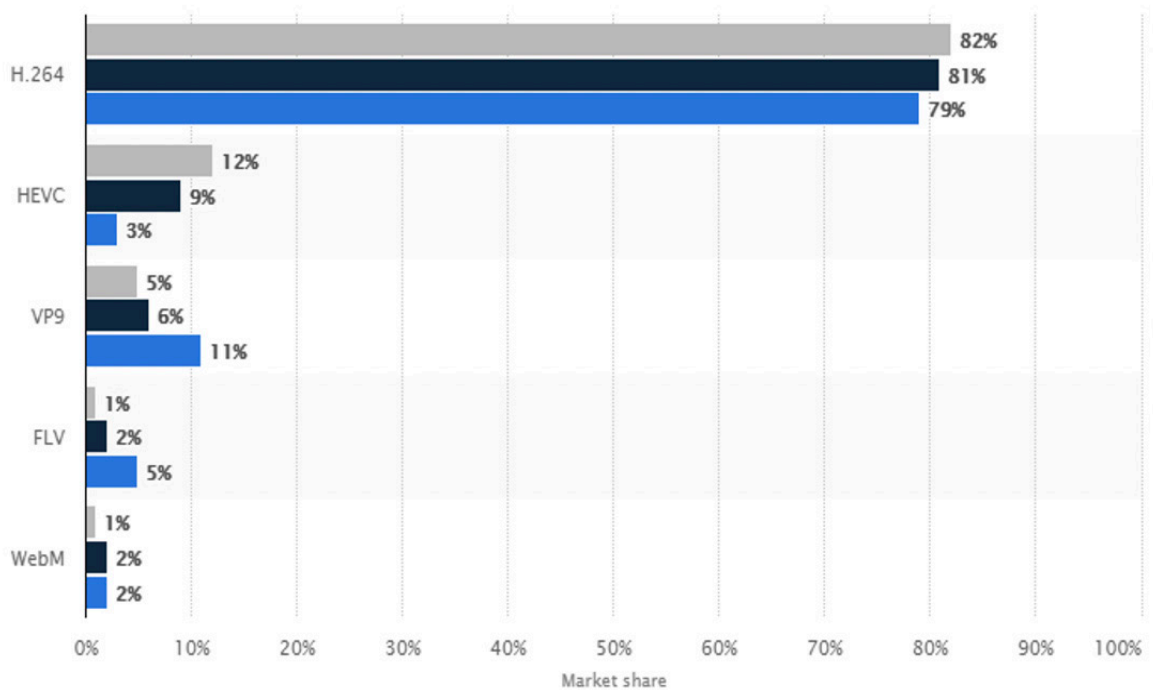


Figure 9: Market adoption of different video codecs by the years 2016, 2017, and 2018 (Liu, 2019).

From Figure 9, many trends can be observed. Firstly, over the years, H.264 has been the most popular video compression standard. Secondly, although inferior to HEVC in terms of compression efficiency, H.264 captured 82% market share in 2018 compared to the 12% market share of HEVC. Another important observation is that the market share of both H.264 and HEVC has increased over the years. One of the major reasons to which the widespread adoption of H.264 can be possibly attributed is its simple licensing structure compared to the more complex licensing structure of HEVC as discussed in the previous subsection.

3.4 Licensing Strategy

While the technical features of a video com-

pression standard allow it to achieve a certain level of performance, its deployment strategy is an important factor in ensuring the market penetration of a video compression standard. In this regard, the cases of the deployment strategies of H.264 and HEVC present an interesting comparison. For example, as discussed in the previous subsections that despite HEVC's richer features compared to H.264, HEVC still has not been able to penetrate the market nearly as well as H.264. One of the reasons for this could be the differences in the licensing strategies of H.264 and HEVC. The licensing/royalty structures of both H.264 and HEVC are summarized in Table 2.

Table 1: Performance of H.264 and HEVC for lossless compression of still images (Cai et al., 2012)

Video	Resolution		Compression ratio	
	H.264		HEVC	
Traffic	2560x1600		2.28	2.16
PeopleOnStreet	2560x1600		2.29	2.21
Kimono	1920x1080		2.35	2.32
ParkScene	1920x1080		1.93	1.96
FourPeople	1280x720		2.64	2.55
Johnny	1280x720		2.85	2.78
RaceHorses	832x480		1.82	2.00
BQMall	832x480		2.05	2.08
BQSquare	416x240		1.42	1.69
BlowingBubbles	416x240		1.33	1.59
Average			2.10	2.13

From Table 1, several trends can be observed. Overall, HEVC achieves a compression ratio of 2.13 which is slightly better than the compression ratio of 2.10 achieved by H.264. This slight improvement in performance can be attributed to the more flexible intra-prediction technique used in HEVC. In terms of resolution, HEVC compresses smaller resolution images much better compared to H.264. For example, for the resolution images BQSquare and BlowingBubbles, HEVC achieves compression ratios of 1.69 and 1.59 compared to 1.42 and 1.33

achieved by H.264. On the other hand, higher resolution images are much better compressed using H.264. For example, for the 2560x1600 resolution images Traffic and PeopleOnStreet, H.264 achieves compression ratios of 2.28 and 2.29 compared to 2.16 and 2.21 achieved by HEVC.

The performance comparison of H.264 and HEVC for the lossy image compression scenario is shown in Figure 8. Unlike the lossless image compression scenario, for lossy image compression, HEVC outperforms H.264 for test images of all resolutions.

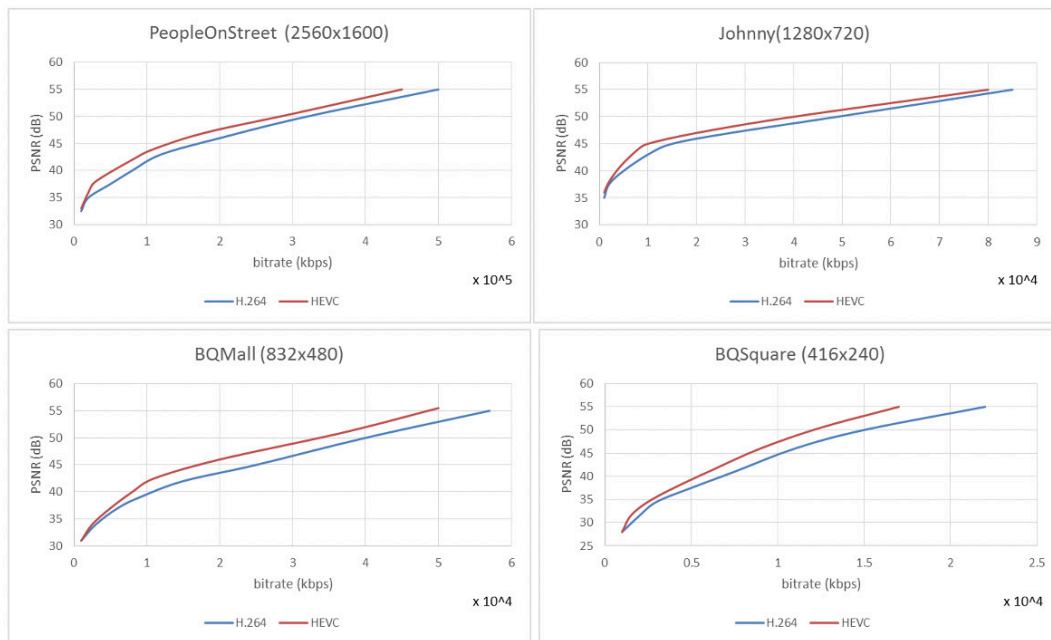


Figure 8: RD performance of HEVC and H.264 for PeopleOnStreet, Johnny, BQMall, and BQSquare test sequences.

HEVC was developed with the aim of providing twice the compression efficiency of the previous standard, H.264. Although the compression efficiency results vary depending on the content type and encoder parameters, at consumer-typical video distribution bit rates, HEVC is generally able to compress the video twice as efficiently as H.264.

At an identical level of visual quality, HEVC can compress video to a file that is about half the size (or half the bit rate) of H.264, or when compressed to the same file size or bitrate that H.264, HEVC offers a much better visual quality.

3.2 Image Compression Performance

In this section, the performances of H.264 and HEVC standards are compared for compression still images under two scenarios: lossless compression and lossy compression. While comparing the performances of H.264 and HEVC, it is important to understand the evaluation criteria which has been used to compare the two standards. Performance under lossless image compression is evaluated with using compression ratio as a metric. Compression ratio can be defined as the ratio between the uncompressed image size and the compression image size i.e.

$$\text{Compression Ratio} = \frac{\text{uncompressed image size}}{\text{compressed image size}} \quad (1)$$

For lossy image and video compression, it is important to evaluate both the quality of video and the data rate. While the quality is evaluated using the Peak Signal-to-Noise Ratio (PSNR) (Equation (2)), the data rate is generally represented using bits per second (bps).

$$PSNR = 10 \log_{10} \frac{R^2}{MSE} \quad (2)$$

In Equation (2), R represents the maximum fluctuation in the image. For an 8-bit image, $R = 255$. Mean Squared Error (MSE) can be computed between two images (or frames, in case of videos) I_1 and I_2 of resolution $M \times N$ pixels, using Equation (3).

$$MSE = \frac{\sum_{M,N} [I_1(m,n) - I_2(m,n)]^2}{M \times N} \quad (3)$$

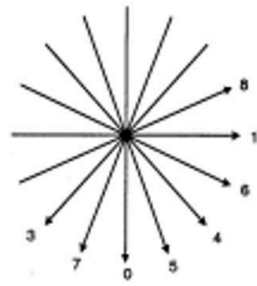
In a typical RD curve, the vertical axis represents the quality (PSNR) while the horizontal axis represents the bitrate. When comparing the performance of two encoders, RD curves representing the two encoders are plotted first. Then, there are two ways of comparing the performance of the two encoders. Either by fixing the data rate and then comparing the quality of the two encoders

or by fixing the quality and then comparing the data rate for the two encoders. The encoder which provides better quality for a given data rate or less data rate for a given quality is considered more efficient.

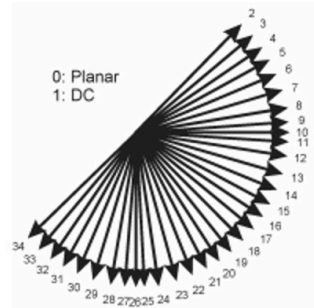
The results of lossless image compression using H.264 and HEVC are shown in Table 1 (Cai et al., 2012).

Similarly, for Intra prediction, H.264 uses a maximum of 9 modes including eight directional modes (Figure 7a) and one DC mode. On the other hand, HEVC uses a total of 35 modes. Among these, 33

are directional modes (Figure 6b) while the remaining two are Planar and DC modes. The Intra prediction modes of H.264 and HEVC are shown in Figure 7 (Wiegand *et al.*, 2003; Sullivan *et al.*, 2012).



The 8 directional prediction modes in H.264
(a)



The 33 directional prediction modes in HEVC
(b)

Figure 7: The intra prediction modes available in H.264 and HEVC (Wiegand *et al.*, 2003; Sullivan

3.1.3 Transform Coding

As discussed in Section 2, transform coding is based on three steps. In the first step, a transform like Discrete Cosine Transform (DCT), Discrete Sine Transform (DST) etc. is applied so that information is compacted in only a few transform coefficients. In the next stage, a quantization technique is used to discard the visually less-important coefficients while an entropy coding technique is then used to finally assign more bits to less frequent symbols and less bits to the more frequent ones. In terms of transform, there are two considerations. The transform block size and the transform type. As for transform block size, the H.264 uses a fixed size of . On the other hand, in HEVC, the transform block also follows a quadtree structure and the size of a transform block can be either of the following: , , or . Hence, HEVC allows for a more flexible transformation of data. However, again, the flexibility of HEVC comes at the cost of additional computational complexity. In terms of the transform type, H.264 use a DCT type integer transform while HEVC uses integer types of both DCT and DST transforms. However, the use of the DST style integer transform in HEVC is restricted to block size.

For quantization, both H.264 and HEVC use the

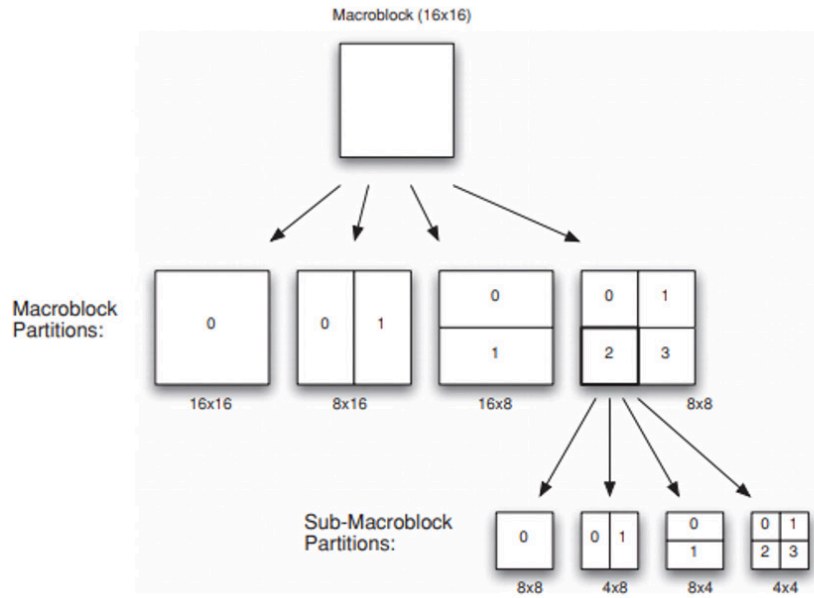
same Uniform Reconstruction Quantization (URQ) (Gupta, Khanna, & Chaudhry, 2013) technique which uses a Quantization Parameter (QP) value for controlling the amount of quantization. The range of QP values in both H.264 and HEVC fall between 0 and 51. Increasing the QP value by 6 nearly doubles the quantization step size in both H.264 and HEVC. Moreover, HEVC also allows the uses of fixed quantization tables. Hence, the quantization process in both H.264 and HEVC is very similar and its impact on the compression efficiency and computational complexity of the two standards is also similar.

For entropy coding, H.264 uses two types of coders: CABAC and CAVLC. On the other hand, HEVC only allows the use of CABAC. However, the CABAC algorithm in HEVC is better than that in H.264. The CABAC used by HEVC provides better throughput speed compared to HEVC and is more suitable for parallel processing architectures. Similarly, in terms of compression efficiency, the CABAC algorithm used HEVC is better than that of H.264. Finally, in terms of context memory requirement, the CABAC algorithm in HEVC requires less context memory compared to the CABAC algorithm used in H.264. Hence, it can be concluded that the entropy coding mechanism in HEVC is better than that of H.264.

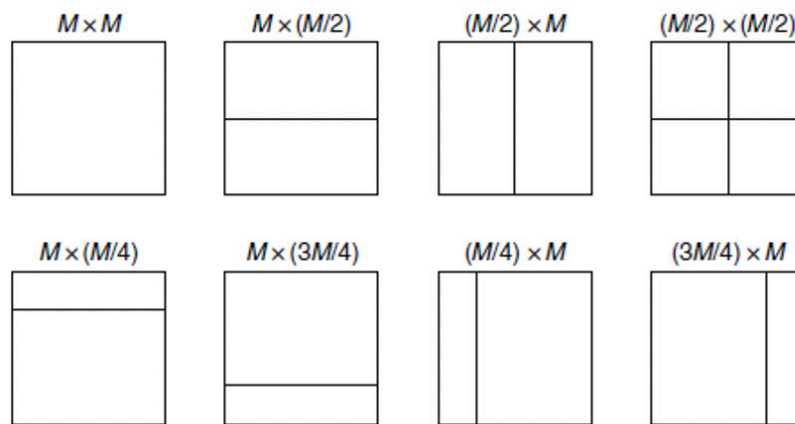
3.1.2 Predictive Coding

Both H.264 and HEVC employ Inter Prediction technique to exploit temporal redundancy between the blocks of different frames and Intra Prediction technique to exploit spatial redundancy between the blocks of the same frame.

However, for inter prediction, H.264 can split an MB into six different partitions to achieve this while HEVC allows the splitting of a CB into many different partitions. The partition sizes allowed in H.264 and HEVC are shown in Figure 6 (Richardson, 2010; Sze, Budagavi, & Sullivan, 2014).



(a) Allowed macroblock partition sizes for Inter prediction in H.264.



(b) Allowed splitting of coding blocks of $M \times M$ size into prediction blocks in HEVC.

Figure 6: Available block partition sizes in H.264 and HEVC (Richardson, 2010; Sze et al., 2014).

3. DISCUSSION

3.1. Technical Comparison

In the following subsections, the major technical features of both H.264 and HEVC compression standards are reviewed.

3.1.1 Block Structure

The basic coding unit in the H.264 video compression standard is a macroblock (MB). An MB has a fixed size of 16x16 pixels. On the other hand, the basic coding unit in HEVC is called a Coding Tree Unit (CTU). The size of a CTU can be configured to 16x16, 32x32, or 64x64. The block structures of

H.264 and HEVC are shown in Figure 4. A CTU contains a luma Coding Tree Block (CTB) and two chroma CTBs. Each sized CTB can be either used as the same size Coding Block (CB) or it can be broken down into square shaped smaller CBs using a quadtree structure (Figure 4c). For example, for a 16x16 CTB, the possible CB sizes are: 16x16, 8x8, 4x4, 2x2. In fact, 2x2 is the smallest allowable size for a CB in HEVC. The H.264 and HEVC block structures are shown in Figure 4 (Sullivan et al., 2012). An MB has a fixed size while a CTB can be broken down into smaller CBs using a quadtree structure. This gives HEVC more flexibility over H.264 but evaluating the extra number of CBs adds to the computational complexity of HEVC and it slows down the encoding process of HEVC.

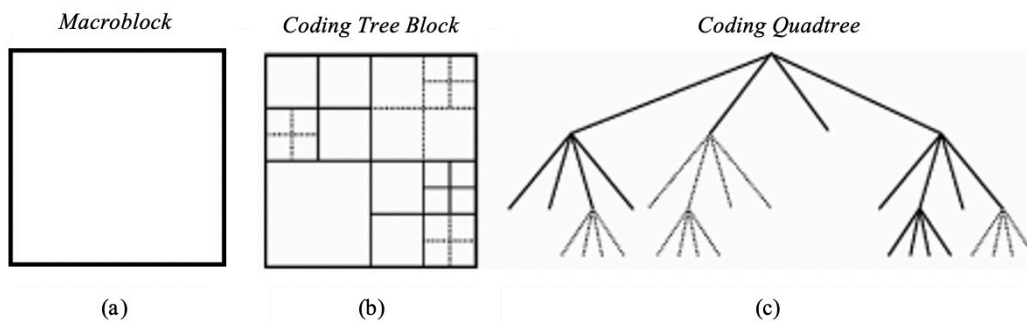


Figure 4: (a) An H.264 macroblock, (b) an HEVC Coding Tree Block subdivided into Coding Blocks. (c) Quadtree structure

From Figure 4, it is clear that an MB has a fixed size while a CTB can be broken down into smaller CBs using a quadtree structure. This gives HEVC more flexibility over H.264 but evaluating the extra number of CBs adds to the computational complexity of HEVC and it slows down the encoding process of HEVC. As shown in Figure 5 (Hruska, 2013), on the left

side, the traditional H.264 standard is used, and each macroblock size is fixed. On the right side, the HEVC standard, the size of the code unit is determined by the regional information. From the contrast of the image, we can see the improvement of the video quality and the skin of the more delicate character HEVC presents, which is much better than H. 264.

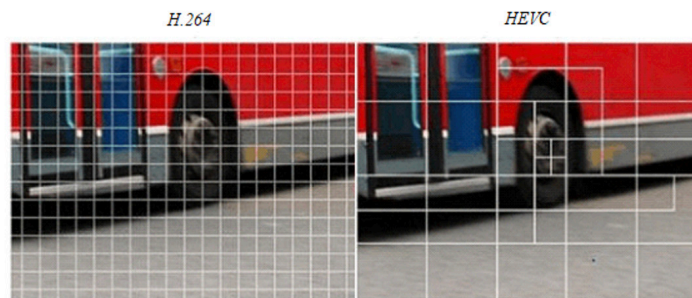


Figure 5: Illustration of block structure of H.264 vs HEVC (Hruska, 2013).

2. RELATED WORK

The H.264 and High Efficiency Video Coding (HEVC) are among the most popular video compression standards (Zhang & Mao, 2019). Encoders conforming to each of these standards offer unique advantages over the other. For example, Pourazad, Doutre, Azimi, & Nasiopoulos (Pourazad, Doutre, Azimi, & Nasiopoulos, 2012) found that while compressing videos, HEVC provides 30 – 50% more compression efficiency compared to H.264. Xu et al. (Xu et al., 2015) found that the main reason for the better compression performance of HEVC over H.264 is the enhanced and improved coding tools (such as the quad-tree block structure) used by HEVC. Nguyen and Marpe (Nguyen & Marpe, 2012) found that for still images, HEVC provides, on average, 30% more compression efficiency compared to H.264. One of the reasons for such improved performance could be the use of larger block sizes by HEVC. Similarly, in terms of computational complexity, Yan et al. (Yan et al., 2013) found that the HEVC encoder is several times more complex compared to H.264. Again, this can be attributed to the exhaustive use of efficient coding tools by HEVC. Video encoders which are capable of high compression efficiency are generally very slow. Much of the research in the field of video compression has focused on finding a solution to this problem. Many fast encoding solutions have been proposed for H.264 (e.g., (Yang, Po., & Lam, 2004; Yin, Tourapis, & Boyce, 2003; Kim, Shih, & Kuo, 2006; Pan, Lim, Rahardja, Lim, Li, Wu, & Wu, 2005)), H.264/MVC (Ho & Oh, 2007) (e.g., (Khattak, 2013; Gul & Khattak, 2018)), H.264/SVC (Vetro, Wiegand, & Sullivan, 2011) (e.g., (Yeh, Fan, Chen, & Li, 2010; Lu & Martin, 2013; Jung, Baek, Park, & Ko, 2010)), HEVC (e.g., (Tan, Ko, & Rahardja, 2016; Belghith, Kibeya, Loukil, Ayed, & Masmoudi, 2016; Jou, Chang, & Chang, 2015; Lee, Hang, Kim, Jeong, & Choi, 2015)), MV-HEVC (Hannuksela, Yan, Huang, & Li, 2015) (e.g., (Khan & Khattak, 2017)), and 3D-HEVC (Tech, Chen, Müller, Ohm, Vetro, & Wang, 2016) (e.g., (Chiang, Peng, Wu, Deng, & Lie, 2019; Zhang, Yang, Chang, Zhang, & Gan, 2017; Shen, An, Zhang, Hu, & Chen, 2015; Fu, Zhang, Su, Tsang, & Chan, 2015)). However, with the development of each new standard, new

challenges related to the issue of computational complexity arise. Hence, research in low-complexity video coding is expected to continue until a radical new and computationally less complex approach is taken for video coding.

In the literature, some studies can be found which compare different video compression standards. For example, Pourazad et al. (Pourazad et al., 2012) compared the performance of H.264 and HEVC. Similarly, Grois, Marpe, Mulayoff, Itzhaky, & Hadar (Grois, Marpe, Mulayoff, Itzhaky, & Hadar, 2013) compare the performance of H.264, HEVC, and VP9 (which is an open source video codec). However, these studies are limited to either reviewing the technical features available in each video compression standard or reviewing the compression performance of each compression standard. Similarly, Koumaras, Kourtis, & Martakos (Koumaras, Kourtis, & Martakos, 2012) confirm that HEVC can achieve twice the compression efficiency of H.264. In terms of comparison of the H.264 and HEVC, some works in the literature compare specific features offered by both the compression standards. For example, Lv, Wang, Xie, Jia & Gao (Lv, Wang, Xie, Jia & Gao, 2012) compare the sub-pixel interpolation filters available in both H.264 and HEVC. Similarly, some works in the literature compare the performance of H.264 and HEVC under different operating environments. For example, Garcia & Kalva (Garcia & Kalva, 2014) evaluate the performance of the two video compression standards in mobile environments and find that the gains of HEVC against H.264 are less impressive in mobile environments with lower video bitrates and resolutions.

While the above studies provide an insight into the compression and complexity performances of HEVC and H.264, the two standards need to be compared in a broader sense. For example, even though HEVC outperforms H.264 in terms of compression efficiency, it has not been able to penetrate the market as successfully as H.264 has (Liu, 2019). The reason for this cannot be explained by only considering the compression efficiency of the two standards. Hence, in this paper, a more comprehensive comparison of the two video compression standards is presented which takes into consideration both the technical and non-technical aspects of the two video compression standards.

main techniques which achieve this in successive steps are: transform, quantization, and entropy coding. Among these, transform is used to represent the frame/block differences (received after the predictive coding stage), in such a way that the energy is compacted in only a few transform coefficients. These transform coefficients are later quantized using a quantization technique. The quantization step allows to discard many of the transform coefficients and hence leaving only a small number of coefficients to encode (Richard-

son, 2010). Finally, an entropy coder is used to code the transformed and quantized coefficient (Richardson, 2010). The idea behind entropy coding is to use reduce the overall number of bits by allocating smaller codes to more probable symbols and larger codes to fewer probable symbols (Richardson, 2010). Context Adaptive Binary Arithmetic Coding (CABAC) and Context Adaptive Variable Length Coding (CAVLC) are two widely used entropy coders for video compression.

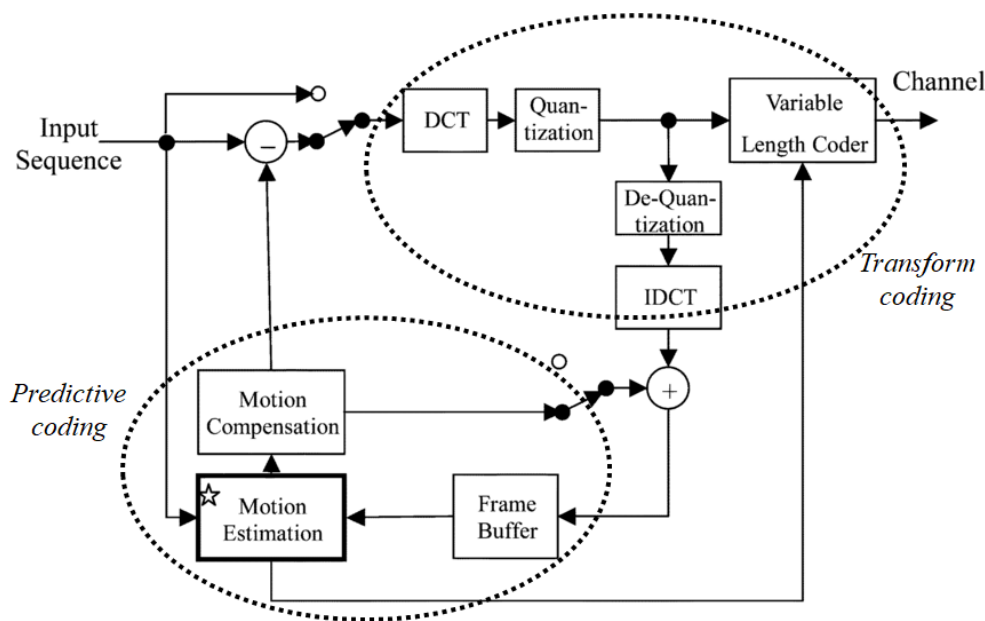


Figure 3: A generic hybrid video encoder (Kuo, Chung, & Shih, 2006).

The main contribution of this paper is that it provides a comparison of the H.264 and HEVC video compression standards from a unique perspective i.e., it reviews both the technical aspects as well as the deployment aspects of both H.264 and HEVC. Among the technical aspects, it reviews the encoding tools/features and the compression performance for the case of still images. Among the deployment aspects, it reviews the licensing strategies as well as the market penetration of both

H.264 and HEVC.

The rest of the paper is organized as follows: in Section 2, related work is reviewed. In Section 3, a discussion of the comparison of both H.264 and HEVC is presented. The discussion is divided into several subsections, including technical comparison, image compression performance, market adoption, licensing structure, and upcoming video compression standards. Finally, conclusions are presented in Section 4.

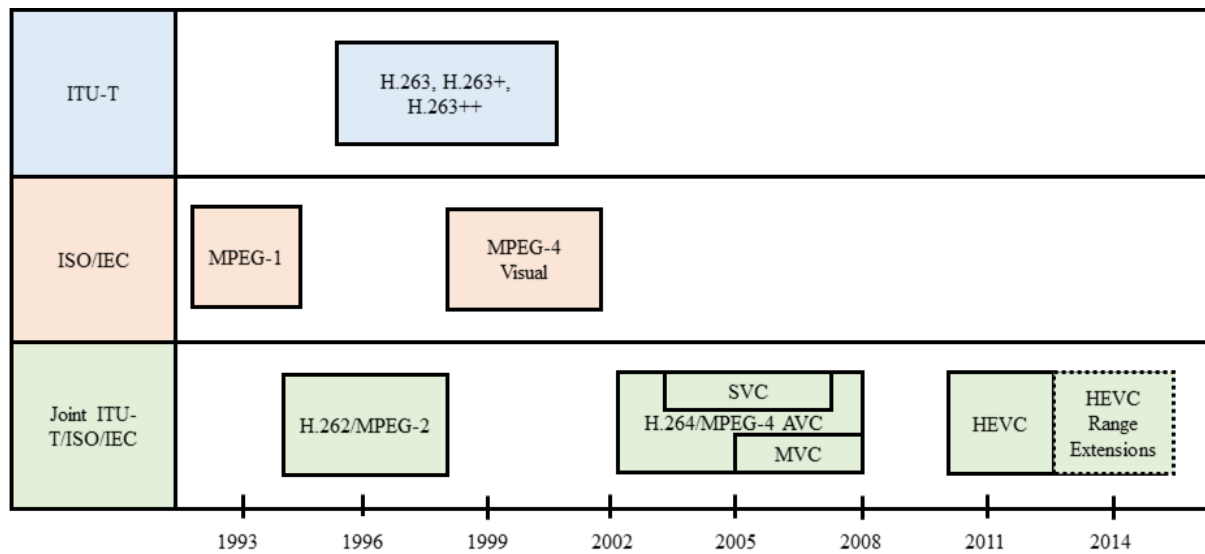


Figure 2: A history of video compression standards (Khattak, 2014).

It can be seen from Figure 2 that in the last two decades, the two standardization bodies of ISO/IEC and ITU-T have combined their efforts in developing joint standards. The last two of their jointly developed standards are the H.264 (Wiegand, Sullivan, Bjontegaard, & Luthra, 2003) and the High Efficiency Video Coding (HEVC) (Sullivan, Ohm, Han, & Wiegand, 2012) standards. Advanced Video Coding (MPEG-4 AVC) or H.264 is a video compression standard based on block-oriented motion compensation (Dominguez & Villegas, 2014). It is widely used in Blu-ray discs, Internet sources such as videos on iTunes Store and YouTube, Web software, as well as HDTV terrestrial, cable and satellite broadcasts (Diehl & Karmasin, 2013). On the other hand, the High-Efficiency Video Coding (HEVC) combines original technologies with advanced techniques to significantly improve bit flow, establish a better connection between delay and complexity of the algorithm and improve coding quality, leading to better optimizations considerably (Jiang & Nooshabadi, 2017). Both the H264-AVC and HEVC compression standards implement a hybrid video coding approach based on spatial redundancies and temporal redundancies contained in a video sequence

(Kovács & Nagy, 2014; Pastuszak & Abramowski, 2016). In hybrid video coding, two video compression techniques, predictive coding and transform coding, are combined. A generic hybrid video encoder is shown in Figure 3 (Kuo, Chung, & Shih, 2006). The idea behind predictive coding is that there is spatial redundancy within a video frame and temporal redundancy between the frames of a video. Hence, instead of coding each video block separately, information from already coded blocks of the same frame should be used to predict information in a current block (Richardson, 2010). Similarly, instead of coding each frame separately, information from one frame should be used to predict information in another frame (Richardson, 2010). A simple technique to achieve this is based on block differences and frame differences. That is, only the block or frame differences are encoded. This way, the amount of information, which is encoded, is reduced. Modern video compression standards achieve predictive coding using techniques such as motion estimation and motion compensation as shown in Figure 3. On the other hand, the idea behind transform coding is to reduce any existing psychovisual and coding redundancy while compressing videos (Richardson, 2010). The three

INTRODUCTION

Communication is an important aspect of human life. Humans have always found a way to communicate with each other. Among the forms of communication, visual communication has always been a popular mode of communication for humans. One reason for this could be that it allows human beings to understand the context of communication in a better way compared to speech communication only. The rapid advancements in telecommunication technologies have given birth to newer means of visual communication. For example, today, millions of people use their mobile phones to capture and share videos. There are over 170 million mobile video users in the USA alone (Statista, 2019). Similarly, a number of online video sharing and broadcasting services have emerged (e.g. YouTube, Netflix, and Facebook etc.). All these developments have made video communication more interesting for users and, hence, the number of users who use online video sharing or broadcasting services is ris-

ing with every passing day. For example, it is estimated that the number of viewers who watch online videos will grow from over 2.6 billion in 2019 to over 3.1 billion in 2023 (Verna, 2019). While video is one of the most interesting mediums of online communication, it is also the most data-intensive medium. For example, it is estimated that, currently, around 80% of all internet traffic is based on video (Roesler, 2019). For example, storing a one-minute raw High Definition (HD) video requires more than 8 GB of storage space (DR, 2019). If the same video is required to be transmitted in real-time, it would require a substantially high bandwidth which may not be available in many scenarios. Hence, most of the times, when a video is captured, it is compressed before storage or transmission (Segall, Katsaggelos, Molina, & Mateos, 2004). At the receiver side, the compressed bit-stream is decompressed to view the video. So, almost all the digital videos that we see online today, are the compressed and decompressed versions of the raw videos. The video compression phenomenon is illustrated in Figure 1.

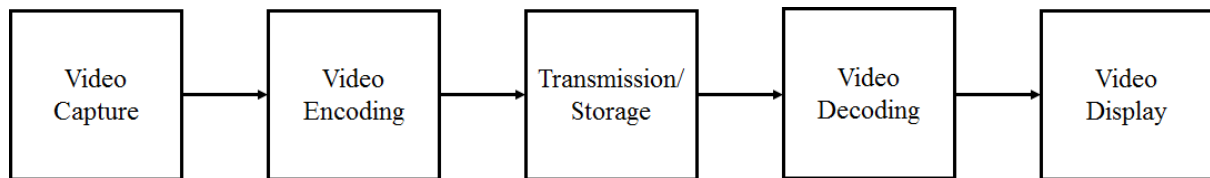


Figure 1: The video compression and decompression process (Richardson, 2010).

Video compression technologies are reducing and eliminating redundant video data so that a digital video file can be efficiently sent over a network and stored on computer disks. With efficient compression techniques, a significant reduction in file size can be achieved with little or no adverse effects on visual quality (Shi & Sun, 2008). The quality of the video, however, may be affected if the file size is further lowered by increasing the compression level for a given compression technique (Hernández & Schwarz, 2018).

Many different techniques can be used to compress videos. Since many different vendors of video technology (e.g., camera and television manufacturers etc.) exist, it is important that there exists a standard which defines the compression technique. In such a way, a video captured using a device from one vendor will be able to be played on a device from another vendor since both the capture (and encoding) device and display (and decoding) de-

vice will conform to one compression scheme. Without standardization, video captured using device from one manufacturer would not be able to play on a device from another manufacturer (Bhaskaran & Konstantinides, 1997). Hence, many video compression standards have been developed over the years. In this respect, the two main standardization bodies are the Motion Picture Experts Group (MPEG) of the International Standardization Organization/International Electro-Technical Commission (ISO/IEC) and Video Coding Experts Group (VCEG) of the International Telecommunication Union – Telecommunication (ITU-T). While in the beginning, both these groups competed each other by working on competing standards, lately, the two groups have joined resources and combined efforts in order to develop joint video compression standards. A pictorial depiction of the history of video compression standards developed by the two organizations is shown in Figure 2 (Khattak, 2014).



المملكة العربية السعودية
جامعة الحدود الشمالية (NBU)

مجلة الشمال للعلوم الأساسية والتطبيقية (JNBAS)

طباعة - ردمد: 1658-7022 / الكتروني - ردمد: 1658-7014

www.nbu.edu.sa
http://jnbas.nbu.edu.sa

مجلة الشمال
للعلوم
الأساسية والتطبيقية
دورية علمية محكمة

جامعة الحدود الشمالية

1658-7022
1658-7014



دراسة للمقارنة بين معياري ضغط الفيديو: H.264 و ترميز الفيديو عالي الكفاءة

محمد عبدالمنان بار

(قدم للنشر في 1440/05/13 هـ ؛ وقبل للنشر في 1442/01/15 هـ)

ملخص: تُستخدم تقنيات ضغط الفيديو لتقليل عدد وحدات البت المطلوبة لوصف بيانات الفيديو. هذه التقنيات تم تعييرها لتسمح بالتشغيل البيئي، الداخلي، بين الأجهزة المختلفة. لقد تم تطوير العديد من معايير ضغط الفيديو على مدار العقود القليلة الماضية. يقدم هذا البحث دراسة عامة على أحدث معيارين لضغط الفيديو وهما (H.264) ونظام ترميز الفيديو عالي الكفاءة (HEVC). تناقش هذه الدراسة بشكل خاص السمات الرئيسية والاختلافات في تقنيات الضغط المستخدمة من قبل المعيارين. تتوصل هذه الدراسة الى انه في حين يوفر H.264 ترميزاً أسرع من HEVC، يوفر HEVC أداءً ضغطاً أفضل بكثير مقارنة بـ H.264 وخاصة في حالة الضغط المفقود (Lossy compression). ومن المتوقع أن تركز أبحاث تقنيات ضغط الفيديو مستقبلاً على تطوير حلول ترميز منخفضة التعقيد وعلى الاستفادة من تقنيات الذكاء الاصطناعي لضغط الفيديو بشكل أسرع وأكثر كفاءة.

كلمات مفتاحية: ضغط الفيديو، كفاءة الضغط، سرعة الترميز، تعقيد الوقت، H.264، ترميز الفيديو عالي الكفاءة.

JNBAS ©1658-7022 . (1441هـ/2020م) نشر بواسطة جامعة الحدود الشمالية. جميع الحقوق محفوظة.

* للمراسلة:

أستاذ مساعد، قسم الهندسة الكهربائية، كلية الهندسة، جامعة الحدود الشمالية، ص ب: 1321، رمز بريدي: 91431، المدينة عرعر -، المملكة العربية السعودية.

e-mail: m.abarr@nbu.edu.sa



jnbas.nbu.edu.sa

DOI: 10.12816/0056076



KINGDOM OF SAUDI ARABIA
Northern Border University (NBU)
**Journal of the North for Basic and Applied Sciences
(JNBAS)**

p- ISSN: 1658 - 7022 / e- ISSN: 1658 - 7014

www.nbu.edu.sa
<http://jnbas.nbu.edu.sa>



Journal of the North
for Basic and
Applied Sciences

Peer-Reviewed Scientific Journal

Northern Border University
www.nbu.edu.sa

Volume 5
Issue 2
2020

A Comparative Study between two Video Compression Standards: the H.264 and the High Efficiency Video Coding

Mohammad A. Barr

(Received 20/01/2019; Accepted 03 /09 /2020)

Abstract: Video compression techniques are used to reduce the number of bits required to represent video data. These techniques are standardized to allow inter-operability between different devices. Many video compression standards have been developed over the last few decades. This article presents an overview of the two latest video compression standards, the H.264 and the High Efficiency Video Coding (HEVC). The major features and strengths and weaknesses of the two standards are particularly discussed. It is found that while H.264 provides faster encoding than HEVC, HEVC provides much better compression performance compared to H.264. The performance gains of HEVC are more prominent in case of lossy compression. Moreover, it is found that despite better compression performance, due to its complicated royalty structure, HEVC lags significantly behind H.264 in terms of deployment. Lastly, it is concluded that, in future, research in video compression techniques will focus on developing low-complexity encoding solutions and on leveraging artificial intelligence techniques for fast and efficient video compression.

Keywords: Video Compression, Compression Efficiency, Encoding Speed, Time Complexity, H.264, High Efficiency Video Coding.

1658-7022© JNBAS. (1441 H/2020). Published by Northern Border University (NBU). All Rights Reserved.



jnbas.nbu.edu.sa

DOI: 10.12816/0056076

* **Corresponding Author:**

Assistant Professor, Dept. of Electrical Engineering, College of Engineering -, Northern Border University, P.O. Box: 1321, Postal Code: 91431-, City Arar, Kingdom of Saudi Arabia.

e-mail: m.abarr@nbu.edu.sa

of radiogenic nature such as cheralite and zircon. While the pegmatite of Gabal El-Dob are of normal radioactivity in eU (av. 4.20 ppm) and eTh (av. 7.20 ppm).

ACKNOWLEDGEMENTS

Authors would like to express their sincere thanks to Prof. Abdalla, H.M., Professor of Exploration Geochemistry, NMA, for his valuable comments added during revising the manuscript.

REFERENCES

- Abu El-Leil, I., Tolba, S. I., Shahin, T. M. (2015). Mineralogical studies of placer Wadi deposits of Gabal El-Dob area, North Eastern Desert, Egypt: A good preliminary tool for prospecting ores in Arabian-Nubian Shield. *Int. Jour. Innov. Sci., Engineering & Technology*, 2(10), 68-93.
- Asran, A. M., El-Mansi, M. M., Ibrahim, M. E. & Abdel Ghani, I. M. (2013). Pegmatites of Gabal El-Urf, Central Eastern Desert, Egypt. *The 7th Inter. Conf. Geol. Afr.*, Assuit Univ., Egypt. IV, 1-22.
- Bishady, A. M., Attawiya, M. Y., Attia, G. M. & El-Nahas, A. A. (1999). Petrographical and geochemical studies on Abu Zawal pegmatites and their host rocks, Central Eastern Desert, Egypt. *The 4th Inter. Conf. on The Geol. of the Arab World (GAW-4)*, Cairo Univ., Egypt. 1, 222-245.
- Draz, O. M., El-Alfi, S. M. & Esmail, E. M. (2017). Mineralogical and radiometrical studies of Gabal El-Dob area, Central Eastern Desert, Egypt. *Current Science International*, 6(1), 103-120.
- El-Mansi, M. M. & Dardier, A. M. (2005). Contribution to the geology and radioactivity of the older granitoids and younger granites of Gabal El-Urf-Gabal Abu Shihat area, Eastern Desert, Egypt. *Delta Jour. Sci.*, 29, 1-17.
- El-Sherif, A. M. (2015a). Mineralogical and radioactive characterization of Gabal El-Urf pegmatites, Central Eastern Desert, Egypt. *Al-Azhar Bull. Sci.*, 26 (2-D), 85-96.
- El-Taher, M. A. (1978). *Relation between Geology and Radioactivity of Some Basement Rocks to The North of Qena-Safaga Asphaltic Road, Eastern Desert, Egypt*. M.Sc. Thesis, Fac. Sci., Al-Azhar Univ., Egypt, 101p.
- Habib, M. E. (1982). Landsat investigation of mineralized granites in the area between Gabals El-Urf and El-Erediya due to west of Safaga, Egypt. *The 8th International Symposium on Machine Processing of Remotely Sensed Data, LARS/Purdue Univ., west Lafayette, U.S.A.*, 441-446.
- Hedrick, J. B. (1985). Rare-earth elements and yttrium, In Mineral facts and problems. *Bureau of Mines Bull., U.S. Department of Interior, Washington D.C.*, 675, 647-664.
- Hedrick, J. B. (2004). Rare Earths in selected U.S. defense applications. *40th Forum on The Geology of Industrial Minerals*, Bloomington, Indiana, 13p.
- Khaleal, F. M. (2014). Granites of Gabal El-Dob area and associated pegmatites, Central Eastern Desert, Egypt: Geochemistry and spectrometry. *Nucl. Sci. Scient. Jour.*, 3, 15-25.
- Long, K. R., Van Gosen, B. S., Foley, N. K. & Cordier, D., 2010. The principal rare earth elements deposits of the United States-A summary of domestic deposits and a global perspective. *U.S. Geol Surv., Scientific Investigations Report 2010-5220*, 96p.
- Lumpkin, G. R. (1998). Rare-element mineralogy and internal evolution of the Rutherford #2 pegmatite, Amelia County, Virginia: A classic locality revisited. *Canad. Mineral.*, 36(2), 339-353.
- Moharam, A. F. (2004). Uranium distribution in the Um Samra-Um Bakra granitic plutons and associated pegmatites, Central Eastern Desert, Egypt. *Proceeding of the 7th Arab Conf. on the Peaceful Uses of Atomic Energy, II*, 311-335.
- Matolin, M. (1991). Construction and use of spectrometric calibration pads, Laboratory of gamma-ray spectrometry. *A report to the government of the Arab Republic of Egypt*, 4, 030-03.
- Pan, Y. & Breaks, F. W. (1997). Rare earth elements in fluorapatite, Separation Lake area, Ontario: Evidence for S-type granite-rare-element pegmatite linkage. *Canad. Mineral.*, 35(3), 659-671.

uranium and presence of radioactive minerals.

The monzogranites around Gabal Abu Kharif, Gabal El-Dob and Gabal El-Urf are moderately of high radioactivity due to the presence of allanite, zircon and titanite minerals where the average of eU (5 ppm) and average eTh (11.50 ppm).

The syenogranites from Gabal El-Urf can be generally described as slightly radioactive rocks in which average eU (11.80 ppm), whereas average eTh (20.40 ppm). The relative increase in eU and eTh in the rocks are due to the presence of cheralite, monazite and zircon mineral.

The radiometric investigations indicate that the concerned pegmatite of Wadi Abu Zawal is high in eU and eTh where the eU content has an average of 1017 ppm, while eTh content average is 432.40 ppm. These averages are also higher than those recorded for the Egyptian uraniferous pegmatite (33 and 28 ppm for U and Th respectively, Moharam, 2004). The analyses show that the studied pegmatite is uraniferous since the high eU and eTh can be attributed to U and Th-mineralization and presence of minerals of radioactive nature such as uranophane, beta-uranophane, thorianite, uranopolycrase, monazite and zircon. These minerals are also well suited for U-series disequilibrium dating.

The pegmatite of Gabal El-Urf is enriched in eU and eTh relative to its hosting granites. The average values of eU and eTh contents are 37.2 and 94.4 ppm respectively which reflect the uraniferous nature of the pegmatite. The high eU and eTh can be attributed to presence of accessory minerals of radiogenic nature such as meta-autunite and zircon. While the pegmatite of Gabal El-Dob is of normal radioactivity where it has 4.2 and 7.2 ppm as averages of eU and eTh respectively.

The quartz veins of Gabal Abu Kharif are moderately radioactive rocks due to the presence of pyrochlore and uranopolycrase minerals where eU average is 22.3 ppm and eTh average is 2.33 ppm. The analyses show that the studied pegmatite is uraniferous since the high eU and eTh can be attributed to U and Th-mineralization and presence of minerals of radiogenic nature such as uranophane, beta-uranophane, thorianite, uranopolycrase, monazite and zircon. These minerals are also well suited for U-series disequilibrium dating.

The pegmatite of Gabal El-Urf is enriched in eU and

eTh relative to their hosting granites. The average values of eU and eTh contents are 37.2 and 94.4 ppm respectively, reflect also the uraniferous nature of the pegmatite, since the high eU and eTh can be attributed to presence of accessory minerals of radiogenic nature such as meta-autunite and zircon. While the pegmatite of Gabal El-Dob is of normal radioactivity where average of eU is 4.20 ppm and the average of eTh is 7.20 ppm.

The quartz veins of Gabal Abu Kharif are moderately radioactive rocks due to the presence of uranopolycrase minerals where the average of eU is 22.3 ppm and the average of eTh is 2.33 ppm.

6. CONCLUSIONS

The rock types of Gabal El-Dob area are arranged as follows starting with the oldest: 1) Metavolcanics, 2) Older granites, 3) Dokhan volcanics, 4) Younger gabbro, 5) Younger granites and 6) Post granitic dykes, pegmatites and quartz veins.

The younger granitic rocks are subdivided according to their field relations and petrographical characteristics into monzogranites, syenogranites and alkali feldspar granites. The monzogranites is slightly radioactive due to the presence of allanite and titanite minerals. The syenogranites can generally be described as of higher radioactivity rocks due to the presence of zircon mineral while alkali feldspar granites are slightly radioactive due to presence of radioactive zircon mineral.

Radioactive pegmatites are commonly encountered in the studied area and are found as large to smaller bodies. They are of zoned and unzoned types. The zoned pegmatites of Wadi Abu Zawal are formed of an outer zone of blocky feldspars with subordinate biotite clusters that envelop an inner core of massive quartz which exists as disconnected pods. The pegmatite rocks present at three localities at Wadi Abu Zawal, Gabal El-Urf and Gabal El-Dob. The pegmatite of Wadi Abu Zawal is high in eU (av. 1017 ppm) and eTh (av. 432.40 ppm) that can be attributed to U and Th mineralization and presence of minerals of radiogenic nature such as uranophane, beta-uranophane, thorianite, uranopolycrase, monazite, bastnaesite and zircon.

The pegmatite of Gabal El-Urf is enriched in eU (av. 37.20 ppm) and eTh (av. 94.40 ppm) relative to their hosting granites due to presence of accessory minerals

Table (3): Radioelement distribution of the younger granites and pegmatites, Gabal El-Dob area.

Radioelements		Monzo granites	Syeno granites	Alkali feldspar granites	Abu Zawal pegmatite	El-Urf pegmatite	El-Dob pegmatite	Quartz veins
eU (ppm)	Rang	1-9	4-29	1-4	96-3102	18-80	2-8	14-25
	Avg	5	11.80	3	1017.2	37-20	4.20	22.30
eTh (ppm)	Rang	8-16	11-34	4-12	43-854	62-164	4-12	1-3
	Avg	11.50	20.40	8	432	94.40	7.20	2.33
K (%)	Rang	2.15-4.09	2.83-4.11	3.6-4.42	3.95-4.64	8-9.25	3.73-6.62	0.72-2
	Avg	3.34	3.40	3.88	4.32	8.58	5.46	1.23
eTh/eU	Rang	0.07-14	1.17-3.25	1.75-4	0.24-0.85	2.05-5.33	1.13-3.50	0.09-0.12
	Avg	3.57	2.25	2.88	0.49	2.92	1.99	0.09

The eU-eTh-K ternary diagram shows that most of the granitic rocks (Figure 8) and pegmatitic rocks (Figure 9) of Gabal El-Dob area lies around eTh/

eU=3 where particular enrichment occur in eTh relative to eU (more than three times). The pegmatitic rocks of Wadi Abu Zawal and quartz veins of Gabal Abu Kharif lies below eTh/eU=3 due to increasing of

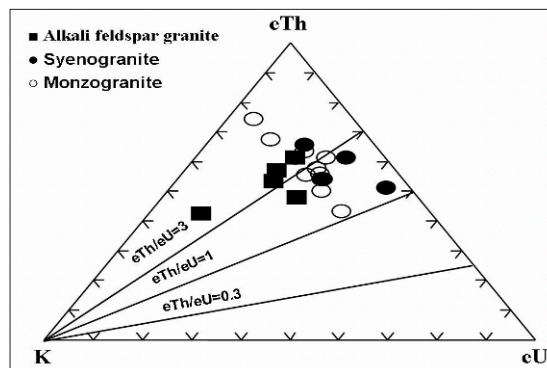


Figure 8: eTh-K-eU diagram of the studied younger granites

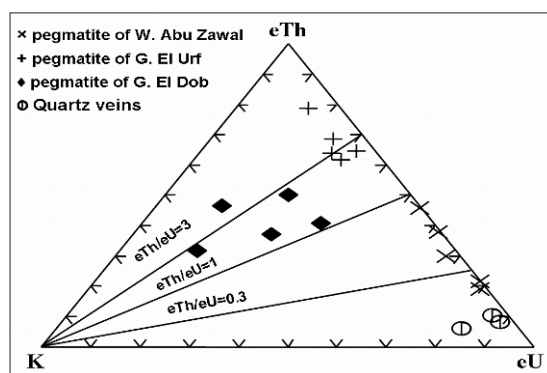


Figure 9: eTh-K-eU diagram of the studied pegmatites.

some uranopolyrase mineral are present as inclusions in apatite minerals (Table 2 No.11).

Fluorite (CaF_2) occurs in different geological environments. It is recorded in the younger granites of Gabal Abu Kharif and Gabal El-Dob. It has a close geochemical association with U, Th and REE's. Fluorite crystals are colourless and have irregular form. It acquires a deep violet coloration at the contact with radioactive minerals. X-ray diffraction analysis (Figure 7b) and The EDX semi-quantitative analyses (Table 2 No.12) confirmed the presence of fluorite.

4.2.4. Sulphides Minerals

Pyrite (FeS_2) is the main sulphide mineral in the study area. The occurrence of such sulphide minerals induce reducing conditions favorable for the precipitation of radioactive mineralization. Pyrite occurs as anhedral crystals with pale brass-yellow with metallic luster. It is recorded in the radioactive pegmatites of Wadi Abu Zawal. X-ray diffraction detected the pattern of pyrite mineral (Figure 7c). EDX semi-quantitative analysis shows some uranopolyrase inclusions in pyrite mineral (Table 2 No.13).

4.2.5. Oxides And Silicates Minerals

Zircon (ZrSiO_4) is characterized by bi-pyramidal prismatic crystals from granites of Gabal Abu Kharif and the pegmatite of Wadi Abu Zawal (Figure 5k). The X-ray diffraction analysis detected the presence of zircon (Figure 7k). EDX semi-quantitative analysis of zircon shows inclusions of thorianite mineral (Table 2 No.14).

Hematite (Fe_2O_3) have dark brown colour and present in anhedral forms (Figure 5l). X-ray diffraction analysis detected the presence of hematite mineral associated with

goethite mineral (Figure 7e). The EDX semi-quantitative analysis of hematite mineral shows hematite has inclusions of xenotime mineral (Table 2 No.15).

Rutile (TiO_2) is a common accessory mineral in igneous rocks. The majority of rutile of Wadi Abu Zawal area is euhedral to subhedral prismatic, tabular and elongated grains with brownish colour (Figure 5m). The X-ray diffraction analysis detected the presence of rutile mineral (Figure 7f). EDX semi-quantitative analysis data are listed in Table (2 No.16).

Titanite (CaTiSiO_5) is characterized by its prismatic shape with yellowish brown colour (Figure 5n). This mineral is present in the granites of Gabal El-Dob and pegmatite of Wadi Abu Zawal. XRD data (Figure 7g) and the EDX semi-quantitative analyses show some inclusions of thorianite mineral in titanite (Table 2 No.17).

Garnet is represented by spessartine mineral ($\text{Mn}_3\text{Al}_2\text{Si}_3\text{O}_{12}$). Crystals of spessartine are of deep honey colours, transparent to translucent with vitreous luster. It was confirmed by X-ray diffraction (Figure 7h) and EDX semi-quantitative analysis (Table 2 No.18).

5. RADIOACTIVITY

The radiometric evaluation of U concentration by γ -ray spectrometry is usually carried out using one or more of the intermediate decay products in the U decay series. The most important of these γ -emitters are ^{226}Ra in the ^{238}U series and ^{227}Ra in the ^{235}U series and ^{228}Ra in the ^{232}Th series. Radiometric measurements of the gamma ray emitted from radium in U and Th is expressed as eU (U equivalent) and eTh (Th equivalent). The purpose is to determine the contents of eU and eTh to display to what extent the mineral composition affects the radioactivity of the various rocks (Table 3).

Apatite $[Ca_5(PO_4)_3(OH, F, Cl)]$ is a common phosphate accessory mineral recorded in the pegmatites of Wadi Abu Zawal. The mineral occurs either as rounded to subrounded crystals (Figure 5i) or as elongated crystals

(Figure 5j), of white to yellow colour with vitreous to greasy luster. Fluoro-apatite mineral was identified by X-ray diffraction (Figure 7a). The EDX semi-quantitative analysis and ESEM image revealed that

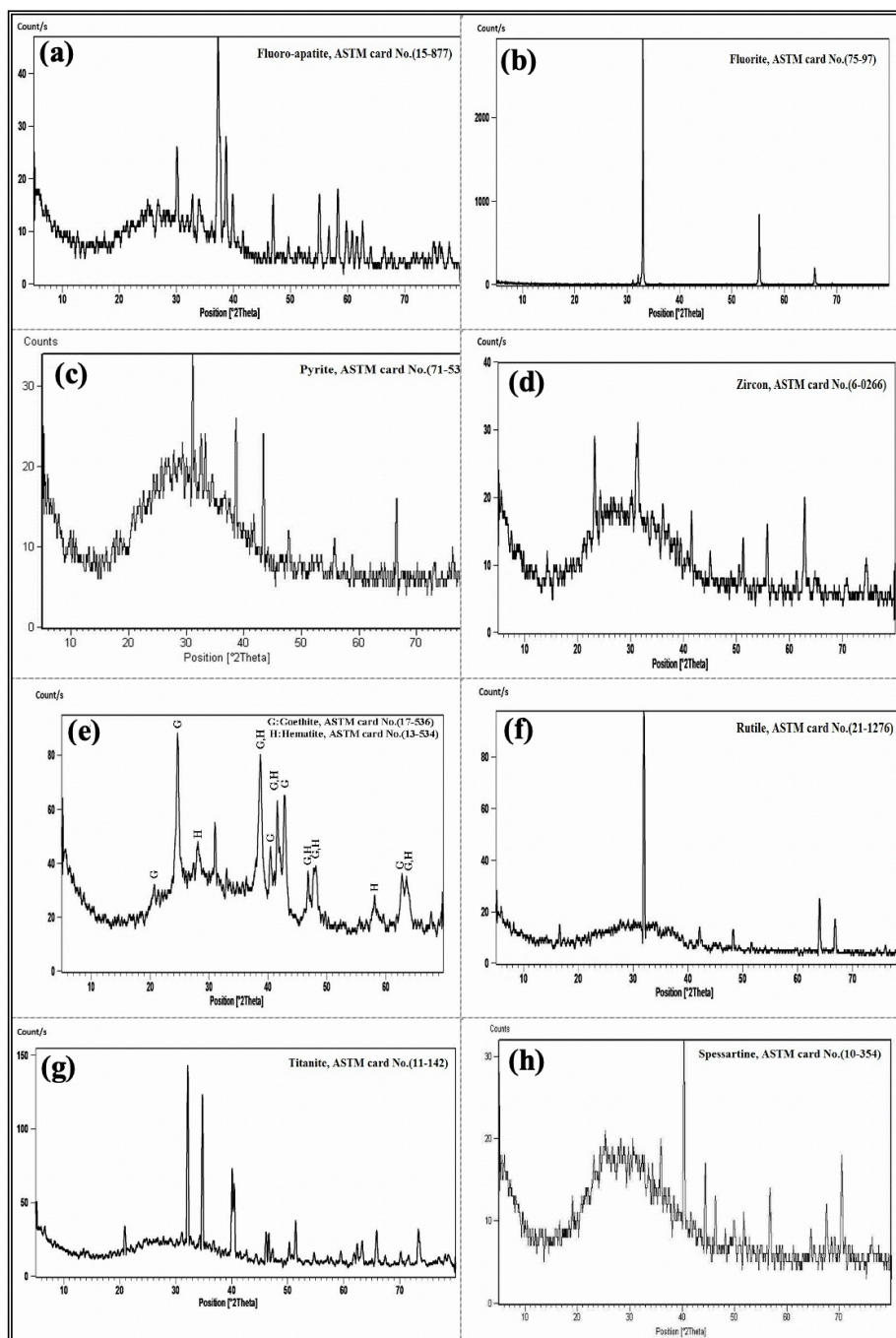


Figure 7: X-ray diffraction patterns of:
 (a) Fluoro-apatite, (b) Fluorite, (c) Pyrite, (d) Zircon, (e) Hematite associated with goethite, (f) Rutile, (g) Titanite and (h) Spessartine.

Meta-autunite [$\text{Ca}(\text{UO}_2)_2(\text{PO}_4)_{2.2} \cdot 6\text{H}_2\text{O}$] is formed as a result of autunite dehydration. It is present as soft and yellow small crystallites (Figure 5b) with vitreous to pearly luster. It is recorded for the first time in the pegmatite of Wadi Abu Zawal and identified by X-ray diffraction analyses (Figure 6b) and the EDX semi-quantitative analysis data (Table 2 No.2).

4.2.2. Thorium Mineral

Thorianite (ThO_2) is one of the most common thorium oxide mineral in the pegmatite of Wadi Abu Zawal. Thorianite is a hard heavy mineral with orange colour (Figure 5c). The identification of thorianite was carried out by using both of XRD (Figure 6c) and EDX semi-quantitative analyses (Table 2 No.3).

4.2.3. U, Th and REE Bearing Minerals

Monazite [$(\text{Ce}, \text{La}, \text{Th}, \text{Nd}, \text{Y})\text{PO}_4$] is a rare earth phosphate mineral present in Wadi Abu Zawal. It exhibits yellow colours with vitreous or resinous luster. According to EDX semi-quantitative analyses (Table 2 No.4), monazite can be classified into two types, the first one of Th-poor monazite, the second one is Th rich monazite. Th-poor monazite might be used to fingerprint its potential sources which comprise allanite and titanite as well as leaching or replacement of fluorapatite (Pan and Breaks, 1997). Monazite mineral is confirmed by XRD analysis (Figure 6d) and EDX semi-quantitative analyses (Table 2 No.4).

Cheralite [$(\text{Th}, \text{Ca}, \text{Ce})(\text{PO}_4, \text{SiO}_4)$] is regarded as Ca-rich monazite-Ce mineral found in the pegmatites of Gabal El-Urf. It is iso-structural with monazite. It occurs as anhedral crystals with brown colours (Figure 5d). The XRD analysis (Figure 6e) and EDX semi-quantitative data confirm the presence of cheralite mineral (Table 2 No.5).

Allanite [$(\text{Ce}, \text{Ca}, \text{Y})(\text{Al}, \text{Fe})_3(\text{SiO}_4)_3 \cdot \text{OH}$] is one of the epidote groups which can incorporate significant amounts of LREE. It occurs as an accessory mineral found in Gabal El-Dob granites and the pegmatite

of Wadi Abu Zawal. Allanite is present as yellowish brown grains (Figure 5e). It was confirmed by EDX analysis technique (Table 2 No.6).

Bastnaesite [$(\text{Ce}, \text{La}, \text{Nd})(\text{CO}_3)\text{F}$] is an uncommon REE-bearing carbonate mineral formed by the replacement crystals after allanite (Long, Van Gosen, Foley & Cordier, 2010). Its yttrium content is generally very low at about 0.05 % (Hedrick, 1985). In addition to being found in carbonatites, bastnaesite is known as an accessory mineral in some alkaline igneous rocks and in some hydrothermal deposits (Hedrick, 2004). It is found in Wadi Abu Zawal as transparent to translucent mineral present in composite grains with rutile and spessartine in black colour and confirmed by X-ray diffraction analysis (Figure 6f). EDX analysis shows that bastnaesite contains 35.20% of Ce_2O_3 and 29.61 of Nd_2O_3 (Table 2 No.7).

Uranopolycrase [$(\text{U}^{4+}, \text{Y})(\text{Ti}, \text{Nb})_2\text{O}_6$] is a very rare radioactive mineral that belongs to the polycrase group of minerals including euxenite-polycrase and yttracrasite. It is a metamict mineral recorded in the pegmatites of Wadi Abu Zawal and Gabal Abu Kharif. Radioactive uranopolycrase occurs as black colored anhedral crystals with adamantine luster and grayish brown streak (Figure 5f). X-ray diffraction and EDX (Table 2 No.8) confirmed the presence of uranopolycrase mineral in these pegmatites (Figure 6g).

Fergusonite [$(\text{Y}, \text{Er})(\text{Nb}, \text{Ta}, \text{Ti})\text{O}_4$] occurs as an accessory mineral in the granitic rocks of Gabal El-Urf, and is often combined with one or more Y, Th, Nb, Ta, Ti oxide accessory mineral (Lumpkin, 1998). It occurs as subhedral grains with brown (Figure 5g) or black colours (Figure 5g). The EDX semi-quantitative analysis of fergusonite is shown in Table (2 No.9).

Pyrochlore [$(\text{Na}_{0.5}\text{Sm}_{1.5})(\text{Ti}, \text{Sb})\text{O}_7$] is recorded for the first time in the wolframite bearing quartz veins of Gabal Abu Kharif and is mainly composed of Sb and Sm. Pyrochlore mineral is associated with the metasomatic end stages of magmatic intrusions. Pyrochlore crystals are of a reddish brown colour (Figure 5h) and resinous luster. It is identified by X-ray diffraction analyses (Figure 6h) and EDX semi-quantitative analysis (Table 2 No.10).

Table (2): Semi-quantitative EDX analysis data of the studied minerals.

Oxide	1	2	3	4	5	6	7	8	9	10	11	12	13	14	15	16	17	18
SiO ₂	15.75	10.87	16.27	5.59	5.24	14.34	3.14	6.34	6.86	19.95	5.10	3.32	5.65	13.30	4.36	---	4.10	40.38
Al ₂ O ₃	---	6.84	---	---	0.52	6.78	---	---	6.15	13.99	---	---	2.94	3.54	3.48	---	0.58	28.08
TiO ₂	---	---	---	---	---	---	---	29.68	---	---	13.80	---	20.83	2.83	1.28	95.02	35.52	---
Fe ₂ O ₃	---	7.17	---	---	---	7.97	---	4.57	8.94	4.45	3.84	0.38	9.66	0.83	22.94	2.78	4.77	15.83
MnO	---	---	---	---	---	---	---	---	---	---	---	---	---	---	---	---	---	12.37
CaO	6.14	14	---	---	0.46	7.69	---	4.52	1.62	---	20.79	58.09	3.47	---	0.61	---	7.77	1.11
MgO	---	---	---	---	---	---	---	---	---	1.35	---	---	---	---	---	---	---	---
Na ₂ O	---	---	---	---	---	---	---	---	---	---	---	---	---	---	---	---	---	---
K ₂ O	---	1.54	---	---	---	---	---	---	---	3.74	0.27	---	---	---	---	---	---	2.23
P ₂ O ₅	---	14.34	---	30.09	28.09	---	---	---	---	---	14.17	---	---	---	26.03	---	---	---
SO ₃	---	---	---	---	---	---	---	---	---	---	---	---	12.29	---	---	---	---	---
F ₂ O	---	---	---	---	---	---	3.46	---	---	---	---	38.21	---	---	---	---	---	---
UO ₂	60.91	45.23	11.33	---	2.68	0.96	---	19.06	---	---	16.99	---	19.98	8.93	1.38	2.20	3.73	---
ThO ₂	14.21	---	72.40	15.49	17.61	1.98	---	---	---	---	---	---	---	35.34	1.13	---	43.54	---
ZrO ₂	---	---	---	---	---	---	---	---	---	---	---	---	---	35.23	---	---	---	---
Sb ₂ O ₃	---	---	---	---	---	---	---	---	---	56.11	---	---	---	---	---	---	---	---
As ₂ O ₃	---	---	---	---	---	---	---	---	---	0.41	---	---	---	---	---	---	---	---
Nb ₂ O ₃	---	---	---	---	---	---	---	26.55	38.12	---	15.95	---	15.70	---	---	---	---	---
TaO	---	---	---	---	---	3.53	---	---	3.47	---	---	---	---	---	---	---	---	---
Y ₂ O ₃	---	---	---	---	---	---	---	9.28	24.50	---	9.07	---	9.49	---	32.95	---	---	---
La ₂ O ₃	---	---	---	8.28	7.74	10.75	15.67	---	---	---	---	---	---	---	---	---	---	---
Ce ₂ O ₃	---	---	---	22.07	21.24	23.91	35.20	---	---	---	---	---	---	---	---	---	---	---
Eu ₂ O ₃	---	---	---	---	0.79	---	---	---	---	---	---	---	---	---	---	---	---	---
Nd ₂ O ₃	---	---	---	12.58	11.76	13.19	29.61	---	---	---	---	---	---	---	---	---	---	---
Sm ₂ O ₃	---	---	---	2.85	3.87	3.06	5.77	---	---	---	---	---	---	---	2.01	---	---	---
Pr ₂ O ₃	---	---	---	3.05	---	3.73	4.03	---	---	---	---	---	---	---	---	---	---	---
Gd ₂ O ₃	---	---	---	---	---	2.12	3.12	---	---	---	---	---	---	---	3.81	---	---	---
Er ₂ O ₃	---	---	---	---	---	---	---	---	5.99	---	---	---	---	---	---	---	---	---
Yb ₂ O ₃	---	---	---	---	---	---	---	---	4.36	---	---	---	---	---	---	---	---	---

(1) Uranophane, (2) Meta-autumite, (3) Thorianite, (4) Monazite, (5) cheralite, (6) Allanite, (7) Bastnaesite, (8) Uranopolyrase, (9) Fergusonite, (10) Pyrochlore, (11) Apatite+uranopolyrase inclusion, (12) Fluorite, (13) Pyrite+uranopolyrase, (14) Zircon+thorianite inclusion, (15) Hematite+xenotime inclusion, (16) Rutile, (17) Titanite+thorianite inclusion and (18) Spessartine.

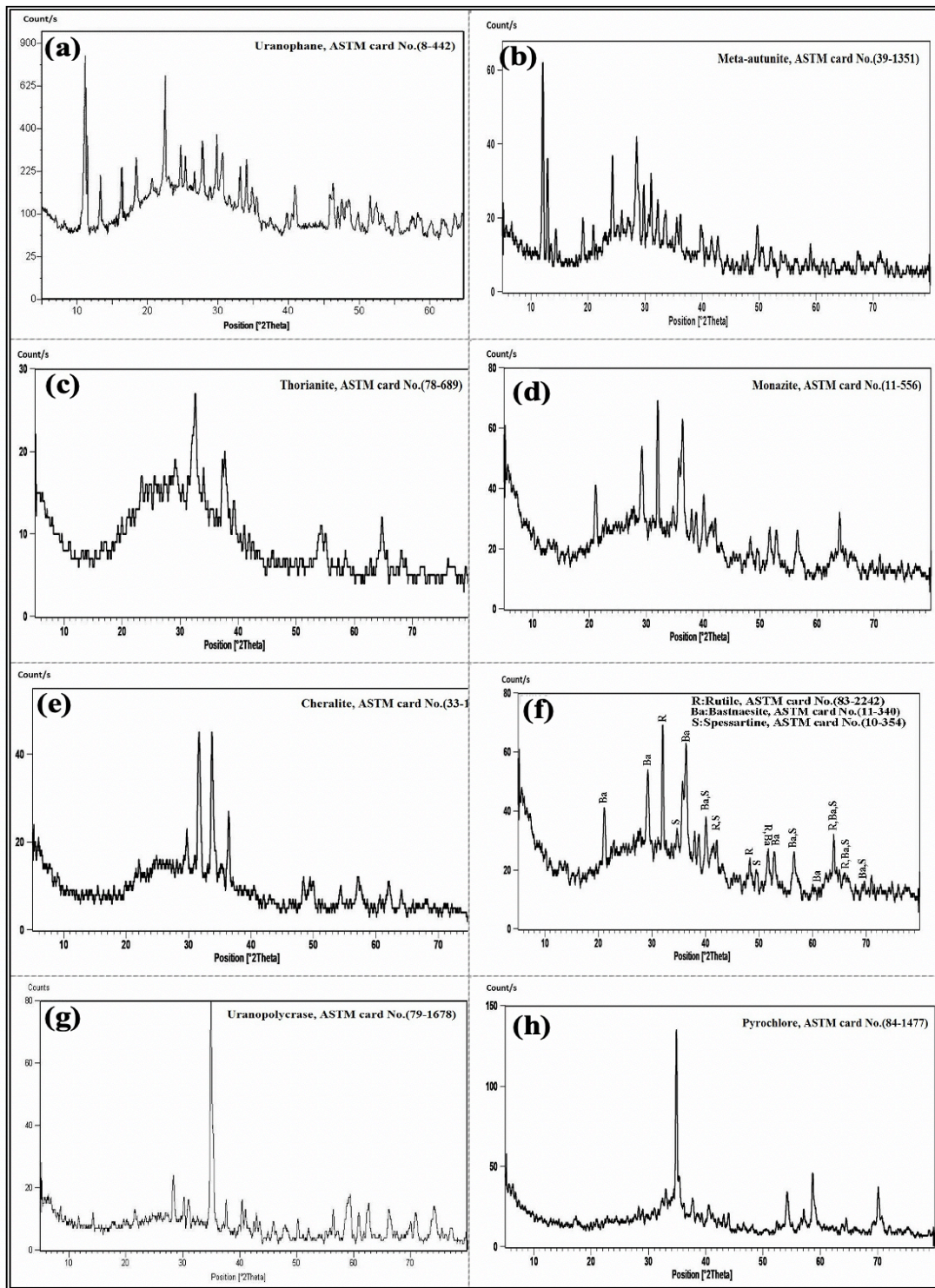


Figure 6: X-ray diffraction patterns of:
(a) Uranophane, (b) Meta-autunite, (c) Thorianite, (d) Monazite, (e) Cheralite,
(f) bastnaesite associated with spessartine and rutile, (g) Uranopolycrase and (h) Pyrochlore.

4.2.1. Uranium Minerals

Uranophane $[Ca (UO_3)_2(SiO_2)_2(OH)_2, 5H_2O]$ is present as massive radiating aggregates of canary yellow colour (Figure 5a) as well as dense microcrystalline masses in the pegmatite

of Wadi Abu Zawal. The crystals exhibit poorly developed faces and do not afford good morphological measurements. It is also identified by X-ray diffraction analyses (Figure 6a) and the EDX semi-quantitative analysis data (Table 2 No.1).

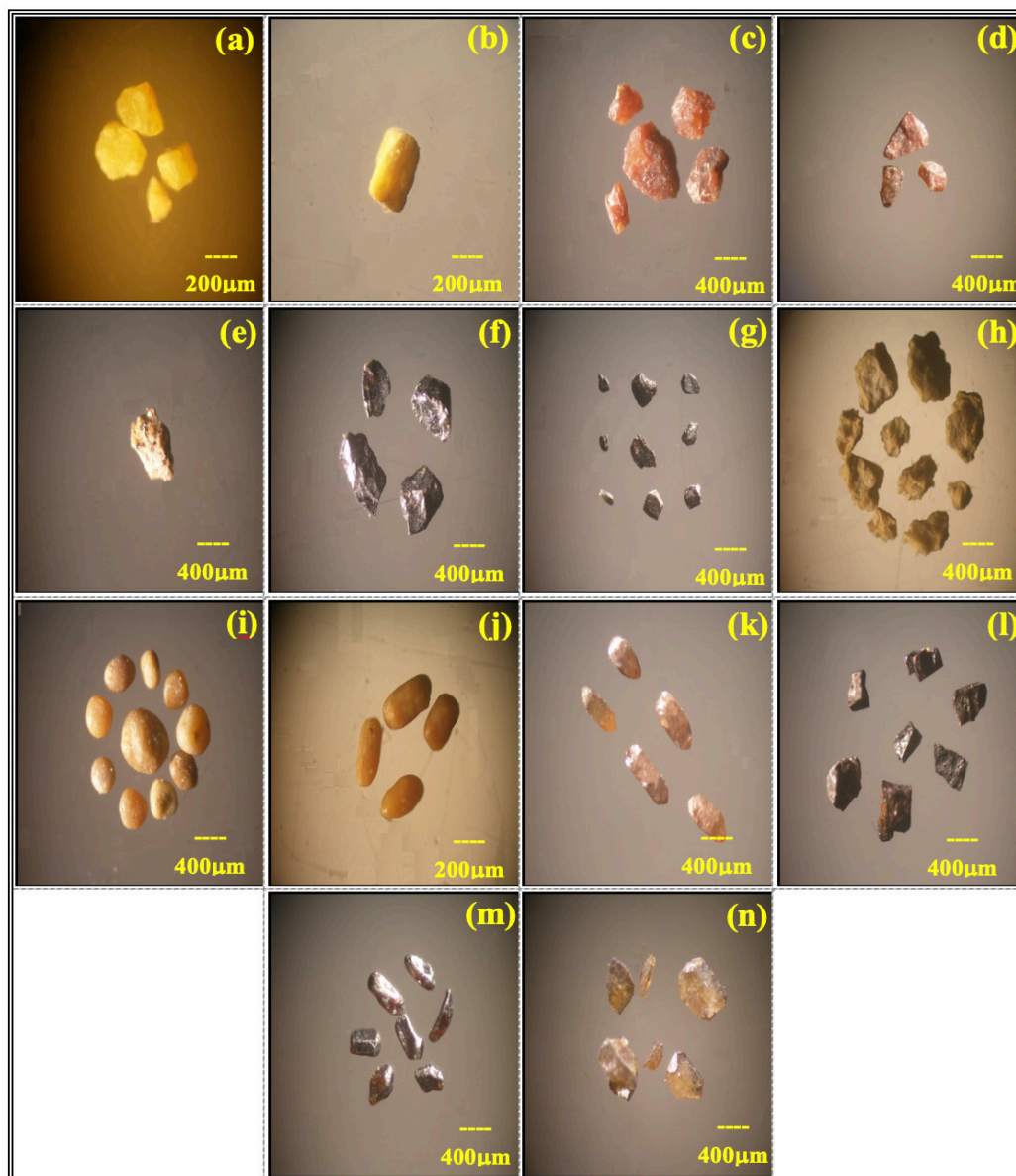


Figure 5: Binocular microscope photomicrographs showing:

- (a) Uranophane, (b) Meta-autunite, (c) Thorianite, (d) Cheralite, (e) Allanite, (f) Uranopolycrase,
- (g) black fergusonite, (h) Pyrochlore, (i) Rounded fluoro-apatite, (j) Elongated fluoro-apatite, (k) Zircon,
- (l) Hematite, (m) Rutile and (n) Titanite.

In Gabal El-Urf, two types of unzoned pegmatite are present; perthitic pegmatite and albitic pegmatite. The perthitic pegmatites are composed of alkali feldspar and quartz (granitic composition). The alkali feldspar is present as megacrysts of string perthite (Figure 4e) and quartz present as megacrysts enclosing finer crystals of perthite. Also albitic pegmatite is composed of albite and quartz. The albite present as megacrysts enclosing skeletal quartz

exhibiting graphic texture (Figure 4f).

4.2. Mineralogical Investigations

Five main groups of the accessory heavy minerals are actually identified as uranium, thorium, U-Th and REE bearing minerals, sulphides as well as oxides and silicate mineral groups. The distribution of these minerals in the investigated granitic and associating pegmatites are summarized in Table (1).

Table (1) Distribution of accessory heavy minerals in the investigated granitic and associating pegmatites.

Rock Minerals	Monzo granites	Syeno granites	Alkali feldspar granites	Abu Zawal Pegmatite	El-Urf Pegmatite	Quartz Veins
Uranophane	-	-	-	+++	-	-
Meta-autunite	-	-	-	+++	-	-
Thorianite	-	-	-	+++	-	-
Monazite	-	++	-	+++	-	-
Cheralite	-	-	-	-	+++	-
Allanite	+	-	-	+++	-	-
Bastnaesite	-	-	-	+++	-	-
Uranopolyrase	-	-	-	+++	-	+
Fergusonite	-	++	-	-	-	-
Pyrochlore	-	-	-	-	-	+++
Apatite	-	-	-	+++	-	-
Fluorite	-	-	+++	-	-	-
Pyrite	+	-	-	+++	-	-
Zircon	+	+++	+++	-	+++	-
Rutile	-	-	-	-	-	-
Titanite	+++	-	-	-	-	-
Hematite	+++	-	-	-	-	-
Spessartine	+++	-	-	-	-	-

(-) Absent (+) Present in few (++) Abundant (+++) Very abundant

4.1.2. Pegmatites

As mentioned before, there are two types of pegmatite; the first is the zoned pegmatite and the second is an unzoned pegmatite type.

The zoned pegmatites of Wadi Abu Zawal display three zones. The first zone is pegmatitic quartz composed of megacrysts of quartz, followed by

the middle zone pegmatitic plagioclase composed of megacrysts of plagioclase associating with megacryst of perthite (Figure 4a). The outer zone is formed of mica. The accessory minerals are apatite, rutile and pyrite and enclose traces of radioactive minerals such as uranophane (Figure 4b), beta-uranophane (Figure 4c), thorianite and uranopolycrase (Figure 4d).

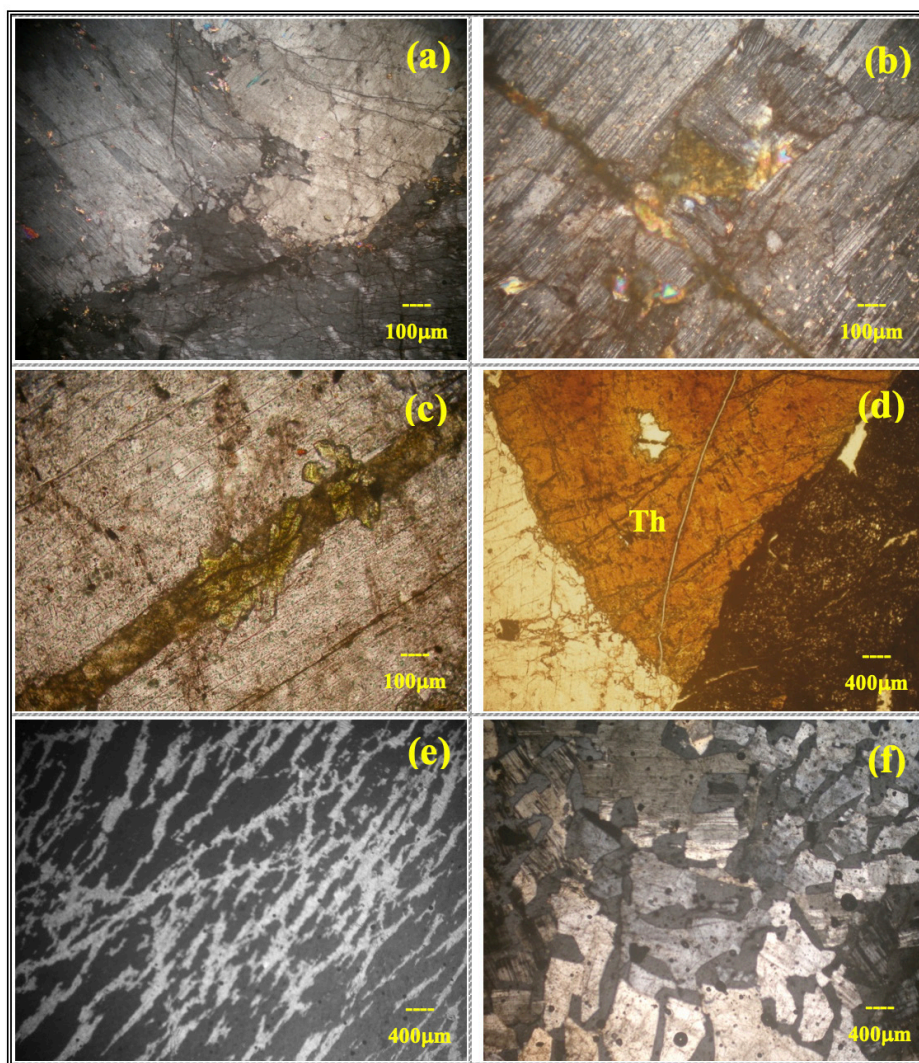


Figure 4: Crossed Nicol photomicrographs in the studied pegmatites showing:

- a): Pegmatitic crystals of plagioclase with perthite in pegmatite of Wadi Abu Zawal.
- b): Uranophane mineral associating albite in pegmatite of Wadi Abu Zawal.
- c): Fractures in plagioclase megacryst filled with beta-uranophane in pegmatite of Wadi Abu Zawal.
- d): Coarse crystals of thorianite (Th) with contact iron oxides in pegmatite of Wadi Abu Zawal.
- e): Pegmatitic crystal of string perthite in pegmatite of Gabal El-Urf.
- f): Pegmatitic crystals of albite with skeletal quartz exhibiting graphic texture in pegmatite of Gabal El-Urf.

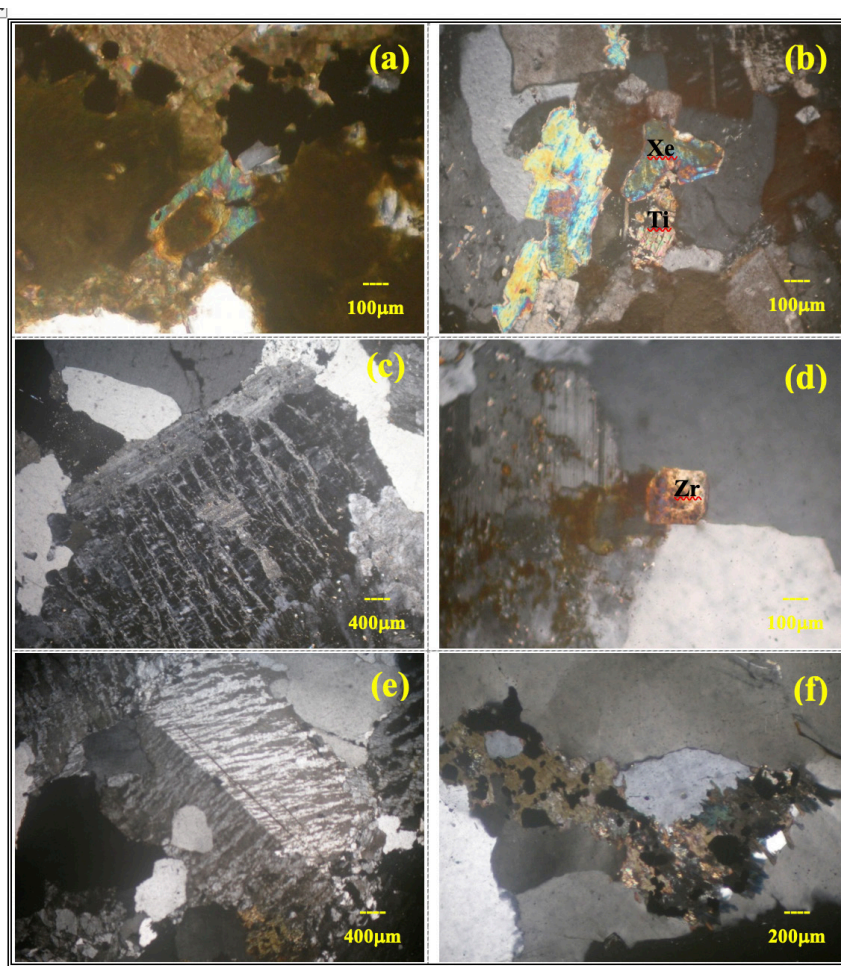


Figure 3: Crossed Nicol photomicrographs in the studied younger granites showing:

- a): Zoned crystal of allanite mantled by epidote in monzogranite.
- b): Fractured crystal of xenotime (Xe) associating titanite (Ti) and quartz in monzogranite.
- c): Subhedral crystal of perthite mantled by plagioclase in syenogranite.
- d): Partially metamict zircon included in quartz in syenogranite.
- e): Subhedral crystal of orthoclase perthite in alkali feldspar granite.
- f): Riebeckite associating arfvedsonite and quartz in alkali feldspar granite.

The syenogranite is mainly composed of quartz, alkali feldspar and plagioclase. Alkali feldspars are present as perthite mantled by plagioclase (Figure 3c). Plagioclase occur as euhedral blade-like crystals of albite and oligoclase (An_{10-12}) exhibiting their characteristic albitic twinning. Quartz occurs as anhedral to subhedral crystals filling the interstitial spaces between the other constituents and associating the feldspars. Zircon is the sole accessory mineral present as well-formed zoned crystal included in quartz (Figure 3d).

The alkali-feldspar granite is essentially composed of alkali feldspars and quartz with rare crystals of plagioclase

and alkaline amphibole represented by riebeckite and arfvedsonite. Alkali feldspar is the sole constituting feldspar present as anhedral crystals of string perthite and as subhedral crystals of orthoclase perthite (Figure 3e). Perthite is also present as patchy perthite. Quartz is present as anhedral crystals associating the main constituents or as skeletal crystals enclosed in the perthite crystal, it also participates the alkali feldspars forming the well-known graphic texture. The alkalinity of the rocks is indicated by the presence of riebeckite and arfvedsonite (Figure 3f). Accessory minerals are only zircon which is present as well formed zoned crystals associating perthite crystals and it is faintly metamict.

with about 200 m in length and about 200 m in width. It is zoned and composed of rosy feldspar with mica in the outer zone and cored by quartz. No anomalous radioactive measurements are recorded in this pegmatite.

Quartz veins occur as small veins or lenses but mostly as veinlets and fracture fillings. They cut all the exposed rocks in the study area. Two sets of wolframite-bearing quartz veins are found directed NE-SW and E-W directions at Gabal Abu Kharif (Figure 2f).

Acidic dykes are relatively of great extensions and cut both the older and younger granites. They are mostly trending in two main directions NNE-SSW and NW-SE and dipping WSW or NE.

Basic dykes are mainly injected in the older granitoids, Dokhan volcanics and younger granites. They are mostly trending in NW-SE direction with vertical or steep dips to the NE.

3. SAMPLING AND METHODOLOGY

Thirty eight representative samples of younger granites, pegmatites and quartz veins from Gabal El-Dob area were subjected to radiometric analyses including: monzogranites (ten samples), syenogranites (five samples), alkali-feldspar granites (five samples), pegmatite of Wadi Abu Zawal (five samples), pegmatite of Gabal El-Urf (five samples), pegmatite of Gabal El-Dob (five samples) and quartz veins (three samples). The samples were subjected to petrographical, mineralogical studies and radiometrical analyses. The mineralogical investigation was carried out using a stereomicroscope for the obtained heavy mineral fractions.

Physical concentrates of heavy liquids using bromoform (sp.gr. 2.81 gm/cm³) was used to concentrate the heavy minerals. The interesting heavy minerals were picked under binocular microscope to obtain pure mineral samples for X-ray diffraction (XRD) as well as environmental scanning electron microscope (ESEM) investigation. The XRD technique

was used to identify the unknown minerals using PHILIPS diffractometer model PW 3710/31. The ESEM model (PHILIPS XL 30) fitted with energy dispersive X-ray (EDX) unit was used. The EDX analysis is considered as semi-quantitative analysis. For the radiometric study, plastic containers, cylindrical in shape, were filled with about 300-400 gm of the crushed sample, and then sealed well and left undisturbed for at least 4 weeks for radon accumulation establishing equilibrium within the radon decay series before counting with gamma ray spectrometer for the determination of eU, eTh and K, (Matolin, 1991). All of the previously mentioned analyses were carried out in the Laboratories of the Nuclear Materials Authority of Egypt (NMA).

4. PETROGRAPHIC AND MINERALOGIC CHARACTERISTICS

4.1. Petrographical Characteristics

4.1.1. Younger Granites

As mentioned before, the younger granites are categorized as monzogranite, syenogranite and alkali feldspar granites.

The monzogranite is essentially composed of quartz, alkali feldspars and plagioclase associated together with biotite and muscovite minerals. Zircon, titanite, allanite, apatite and opaque minerals are accessory minerals. The secondary minerals are chlorite, sericite and epidote. Alkali feldspars occur as euhedral to subhedral tabular crystals of orthoclase and orthoclase perthite exhibiting carlsbad twinning. Plagioclase exists as subhedral crystals of oligoclase (An₁₀₋₁₄); exhibiting albitic and pericline twinning. Quartz is present as anhedral individual crystals and as polycrystalline fine crystals. Biotite, muscovite and chlorite are characterized by wide scope of accessory minerals represented by allanite mantled by epidote (Figure 3a), zircon, xenotime associated with titanite (Figure 3b) and apatite in addition to the opaque minerals.

The Dokhan volcanics of intermediate to felsic members are represented by porphyritic andesite, dacite, rhyodacite and trachyte. They occur as elongated masses trending nearly E-W at Gabal Fatirah and capping the metavolcanics and older granites. These rocks are intruded by the younger granites of Gabal Abu Kharif. Dokhan volcanics at Wadi Fatirah El-Beidah are strongly fractured and occasionally affected by macro and minor faults.

The younger gabbroic rocks at Wadi Abu Zawal are of low to moderate relief and occurs as small rounded or elongated bodies. They are of blocky appearance and characterized by black to gray color showing rhythmic layering. They intrude the older granites and the younger granites of Gabal El-Urf with sharp intrusive contact.

The younger granites are mainly represented by three mountains; Gabal El-Urf, Gabal El-Dob and Gabal Abu Kharif. They form oval to elongate plutons extending in the N-S and NNE-SSW directions and bounded by major faults of the same direction. Based on field relationships and petrographic studies, these younger granites can be easily differentiated into three main phases: monzogranites, syenogranites and alkali feldspar granites.

Monzogranite represents the first phase and occurs as elongated body forming a NNE-SSW trending mass with rugged summit and some parallel serrated peaks at Wadi Fatirah El-Beidah, Wadi Abu Zawal and the outer area of Gabal El-Dob, Gabal El-Urf and Gabal Abu Kharif. The monzogranite is characterized by bouldery appearance (Figure 2b) and spherical exfoliation and presence of taffoni structure. The second phase is represented by syenogranite and is exposed at Gabal El-Urf as an elongated mass. It is characterized by well-developed joint pattern either vertical or horizontal. It is highly sheared and dissected by numerous faults (Figure 2c).

Alkali feldspar granites outcrop as the last phase and occur as high topographic elliptical to semi-rounded masses at Gabal Abu Kharif (Figure 2d) and Gabal El-Dob. Gabal Abu

Kharif alkali feldspar granites intrude the older granitoids and the monzogranite. The rocks are invaded by veins of various composition. Some quartz veins are occasionally mineralized with wolframite.

Gabal El-Dob younger granites occurs as a small lenticular mass ($0.8 \times 0.6 \text{ km}^2$) trending NNE-SSW. It is of zonal composition ranging from monzogranite in the outer rim to alkali feldspar granite at the core. Gabal El-Dob includes an old gold mine as well as wolframite mine. Joints and exfoliated weathering surfaces are well developed

The post granitic dykes and veins represent the last igneous activity in the study area. Swarms of acidic and basic dykes are invading all pre existing rocks. They are differentiated into pegmatites, quartz veins, acidic and basic dykes. Pegmatitic rocks occur as rounded, elongated, lenticular and irregular shaped bodies varying in size from few meters to hundreds of meters. They are of zoned and unzoned types. The zoned pegmatites are formed of an outer zone of blocky feldspars with subordinate biotite clusters that envelop an inner core of massive quartz. The pegmatitic rocks are encountered at three localities; Wadi Abu Zawal, Gabal El-Urf and Gabal El-Dob.

Abu Zawal pegmatite body is intruded in the older granitoids. It is an elongated dyke-like body. It is of zoned type showing milky quartz and feldspars at the inner core and white mica in the outer rim. It contains black radioactive minerals as disseminations and fracture fillings (Figure 2e). The pegmatite of Wadi Abu Zawal shows anomalous radioactive measurements among the other pegmatite bodies recorded in the studied area.

The pegmatites of Gabal El-Urf are unzoned pegmatite present as dykes cut the host granodiorite. The dykes are segmented by faults. They are composed of rosy feldspars and quartz with subordinate mica.

The pegmatite body at the east of Gabal El-Dob cut the host monzogranites and is considered the largest pegmatite body in the study area

El-Sherif (2015a) studied the mineralogical and radioactive characteristics of the pegmatitic rocks at Gabal El-Urf area and concluded that the studied pegmatites are affected by magmatic and hydrothermal processes that enriched with rare metals mineralization accompanied by event of an intensive tectonic structure.

Finally, Draz, El-Alfi & Esmail (2017) studied the mineralogy of the stream sediments and hard rocks of Gabal El-Dob area and classified heavy the mineral assemblages found into two main groups; the opaque iron minerals (magnetite, hematite, goethite and pyrite) and non-opaque minerals (garnet, rutile, zircon, sphene, fluorite, chalcocite, atacamite, biotite, Cu minerals, Mn minerals and green silicates).

The present paper aims to study the mineralogy that affect the radioactivity of both the younger granitic and pegmatitic rocks of Gabal El-Dob area.

2. GEOLOGICAL SETTING

Detailed field mapping of the basement rocks and

structural observations, as well as, the petrographical studies revealed that, the chronological sequence of the rock types of Gabal El-Dob area (Figure 1) is arranged tectono-stratigraphically beginning with oldest as follows: 1) Metavolcanics, 2) Older granites, 3) Dokhan volcanics, 4) Younger gabbro, 5) Younger granites and 6) Post granitic dykes, pegmatites and quartz veins.

The metavolcanics are the oldest rock types. They occur at the south western part of Gabal Abu Kharif as low hills and dissected by mafic and felsic dykes of different attitudes. They are represented by metabasalt, meta-andesite, and metapyroclastics.

The older granites cover about 40% of the study area. They are medium-, to coarse-grained with gray color and show gneissic texture. They are fractured, jointed and possesses foliation along their margin. They are characterized by the bouldery appearance, cavernous weathering, exfoliation and monumental shapes (Figure 2a). The older granites are represented by quartz diorite and granodiorite.

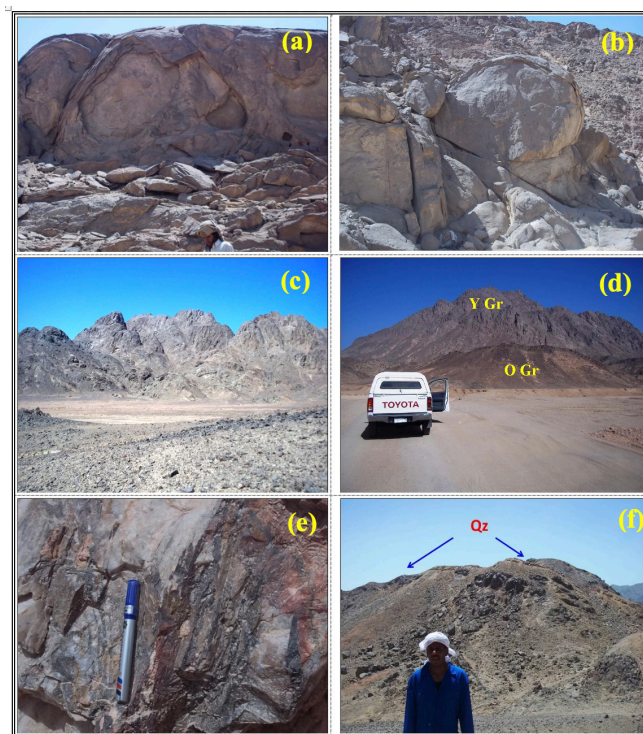


Figure 2: Photographs showing:

- a) Older granitoids showing exfoliation and cavernous weathering of Gabal El-Dob area (looking N).
- b) Bouldery weathering in the younger granites at Gabal El-Dob (looking N).
- c) Highly sheared younger granites dissected by numerous faults, Gabal El-Urf (looking NE).
- d) Intrusive sharp contact between the older (O Gr) and the younger granites (Y Gr) of Gabal Abu Kharif area (looking N).
- e) Black radioactive minerals disseminated in fractures, Wadi Abu Zawal pegmatite.
- f) Wolframite-bearing quartz veins (Qz) intrude in Gabal Abu Kharif granite (looking N).

1. INTRODUCTION

Gabal El-Dob area is located at the Northern Eastern

Desert between Latitudes $26^{\circ} 40'$ and $26^{\circ} 50'$ N and Longitudes $33^{\circ} 20'$ and $33^{\circ} 30'$ E covering an area of about 265 Km² (Figure 1).

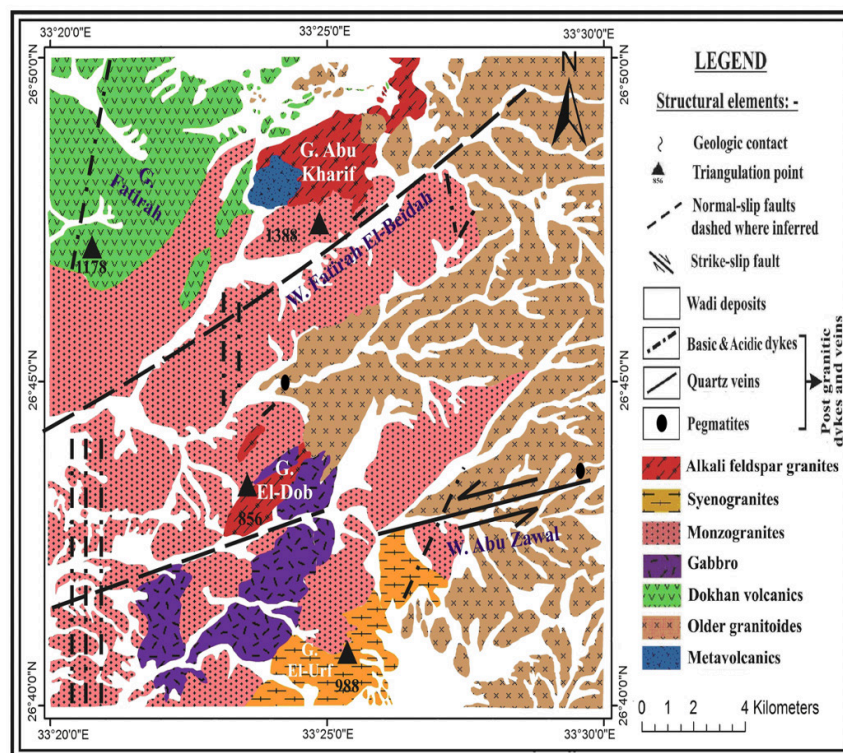


Figure 1 : Geologic map of Gabal El-Dob area, North Eastern Desert, Egypt

Abu El-Leil, Tolba & Shahin (2015) recorded some occurrence of mineralizations such as gold, wolframite, cassiterite and banded iron formation (BIF). They stated that the gold mineralization is encountered in quartz veins occurring in the granodiorite of Abu Zawal gold mine. The wolframite and cassiterite belong to quartz veins origin associated within the post granitic magmatism of Gabal Abu Kharif old mine.

The area was studied by many researches since it was discovered by El-Taher (1978). Several geologic, mineralogic and radiometric studies were carried out in order to explore the uranium mineralizations.

Habib (1982) detected numerous bright signatures in Gabal El-Missikat, Gabal El-Erediya and Gabal El-Urf which reflect numerous hydrothermal alteration halos around mineralized quartz veins.

Bishady, Attawiya, Attia & El-Nahas (1999) stated that the radioactive and heavy minerals encountered in Abu Zawal pegmatites are thorite, columbite, monazite and

xenotime in association with allanite.

El-Mansi and Dardier (2005) studied the geology and radioactivity of Gabal El-Urf-Gabal Abu Shihat area. They recorded dissemination of metallic black and waxy yellow minerals (samarskite, axinite, fergusonite, betafite and uranophane) in the unzoned pegmatite pockets dominate along the southwestern corner of Gabal Abu Shihat alkali-feldspar granites.

Asran, El-Mansi, Ibrahim & Abdel Ghani (2013) recorded two anomalies at the north and south of Gabal El-Urf area and recorded radioactive minerals as uranophane, thorianite, columbite, euxenite, betafite and non-radioactive minerals as allanite, fluorite, zircon, rutile, hematite and magnetite.

Khaleal (2014) studied the geochemistry and spectrometry of Gabal El-Dob alkali granite and associated pegmatites and concluded that El-Dob granites have relatively high uranium and thorium contents.



المملكة العربية السعودية
جامعة الحدود الشمالية (NBU)

مجلة الشمال للعلوم الأساسية والتطبيقية (JNBAS)

طباعة - ردمد: 1658-7022 / الكتروني - ردمد: 1658-7014

www.nbu.edu.sa
http://jnbas.nbu.edu.sa

مجلة الشمال
للعلوم
الأساسية والتطبيقية
دورية علمية محكمة

جامعة الحدود الشمالية
المسجلة في المحكمة
1658-7022
1658-7014



تأثير التركيب المعدني على إشعاعية صخور الجرانيت الحديث والجمائيت لمنطقة جبل الدُّب، شمالي الصحراء الشرقية، مصر

دعاء انور مصطفى¹، محمود هاني شلبي¹، إبراهيم عبد الناجي سالم²، سمير محمد علي² وأنس مالك الشريف³

1. هيئة المواد النووية ص.ب. 530 المعادي، القاهرة، مصر.
2. قسم الجيولوجيا، كلية العلوم، جامعة طنطا، مصر.
3. كلية الهندسة، جامعة الحدود الشمالية، المملكة العربية السعودية.

(قدم للنشر في 1440/01/27 هـ ؛ وقبل للنشر في 1441/06/26 هـ)

ملخص: تقع منطقة جبل الدُّب شمالي الصحراء الشرقية المصرية بين خطي عرض 26° 50'، 26° 40' شمالاً وخطي طول 30° 33'، 33° 20' شرقاً وتبلغ مساحتها حوالي 265 كيلومتراً مربعاً، تحتوي المنطقة على هذه الوحدات الصخرية ترتيباً من الأقدم إلى الأحدث؛ الصخور البركانية المتحولة، الدخان البركاني، الجابرو الحديث، الجرانيت القديم والجرانيت الحديث إضافة إلى قواطع ما بعد الجرانيت وتشمل الجمائيت، عروق الكوارتز والقواطع القاعدية والهامضية. يتواجد الجرانيت الحديث بالمنطقة في العديد من الجبال كابوخريف والدُّب والغرف وبعض الكتل الصخرية المنتشرة بوادي فطيرة البيضاء وابو زؤل، وتم تصنيف هذا الجرانيت بناء على الدراسات البتروجرافية له إلى صخور المونوزجرانيت، السيانوجرانيت وجرانيت الفلسيار القلوي، كذلك توجد في المنطقة بعض القواطع الصخرية والتي تتمثل في صخور الجمائيت والتي تكون قاطعة لصخور الجرانيت القديم والحديث وتتواجد بوادي ابو زؤل وجبلي العُرف والدُّب وتكون حاوية للمعادن المشبعة.

أمكن تقسيم المعادن الثقيلة الشائعة في منطقة جبل الدُّب إلى معادن اليورانيوم، معادن الثوريوم، المعادن الحاوية لليورانيوم والثوريوم والعناصر الأرضية النادرة، معادن الكبريتيدات ومعادن الأكاسيد والسيليكاتية.

بدراسة تأثير التركيب المعدني على النشاط الإشعاعي للمنطقة وجد ان صخور الجمائيت هي الأكثر تمعدناً حيث أن بجمائيت ابو زؤل هو الأعلى إشعاعياً ولكن بتركيزات متفاوتة وذلك نظراً لإحتوائه على معادن اليورانيوم، الثوريانيت، المونازيت، الألائيت، الباستانيزيت، اليورانوبوليكريز وغيرها من المعادن الحاملة لليورانيوم، يليه بجمائيت جبل العُرف نظراً لإحتوائه على معدني الشيراليت والزرقون. كما وجد أن صخور الجرانيت الحديث تظهر نشاطاً إشعاعياً ملحوظاً خصوصاً في صخور السيانوجرانيت الذي يظهر أعلى تركيزات إشعاعية نسبياً بالمنطقة مقارنةً بباقي أنواع الجرانيت الحديث الأخرى.

كلمات مفتاحية: جبل الدب، وادي أبو زؤل، جبل العرف، الجمائيت، معادن، النشاط الإشعاعي.

JNBAS ©1658-7022 . (1441هـ/2020م) نشر بواسطة جامعة الحدود الشمالية. جميع الحقوق محفوظة.

* للمراسلة:

أستاذ، كلية الهندسة، جامعة الحدود الشمالية، ص ب: 1321، رمز بريدي: 91431، عرعر، المملكة العربية السعودية.

e-mail: anas.alshareef2@nbu.edu.sa



jnbas.nbu.edu.sa

DOI: 10.12816/0056075



KINGDOM OF SAUDI ARABIA
Northern Border University (NBU)
Journal of the North for Basic and Applied Sciences
(JNBAS)

p- ISSN: 1658 - 7022 / e- ISSN: 1658 - 7014

www.nbu.edu.sa
http://jnbas.nbu.edu.sa



Journal of the North
for Basic and
Applied Sciences

Peer-Reviewed Scientific Journal

Northern Border University

www.nbu.edu.sa

Volume 5
Issue 2
2020

Effect of The Mineralogical Composition on The Radioactivity of The Younger Granites and Pegmatites at Gabal El-Dob Area, Northern Eastern Desert, Egypt

Doaa A. Moustafa¹, Mahmoud H. Shalaby¹, Ibrahim A. Salem², Samir M. Ali² & Anas M. El-Sherif^{*3}

1. Nuclear Materials Authority, P.O. Box 530 Maadi, Cairo, Egypt

2. Geology Dept., Fac. Sci., Tanta Univ., Egypt

3. College of Eng., Northern Border Univ., Saudi Arabia

(Received 08/10/2018; Accepted 20 /02 /2020)

Abstract: Gabal El-Dob area is located at the Northern Eastern Desert of Egypt. The late pan-African El-Dob pluton is one of the well exposed granitic batholith at the Northern part of Eastern Desert of Egypt. It comprises starting from oldest: metavolcanics, older granites, Dokhan volcanics, younger gabbro and younger granites. All rock types of Gabal El-Dob area are cross-cut by various pegmatites, quartz veins, acidic and basic dykes. The younger granites can be differentiated into three main phases: monzogranites, syenogranites and alkali feldspar granites. They form oval to elongate plutons extending in the N-S and NNE-SSW directions.

Pegmatitic rocks are exposed at Wadi Abu Zawal, Gabal El-Urf and Gabal El-Dob nearby or enclosed in the granitic rocks and present as dykes or vein like bodies.

X-ray diffraction analysis (XRD) as well as Environmental Scanning Electron Microscope (ESEM) was used in the mineralogical studies of the various rocks of Gabal El-Dob area which clarified that the common heavy minerals can be classified into: 1) uranium minerals, 2) thorium minerals 3) U, Th and REE bearing minerals 4) sulphides minerals and 5) oxides and silicate minerals.

Wadi Abu Zawal pegmatites are considered as the most radioactive and uranium mineralized rocks due to presence of uranophane, meta-autunite, thorianite, monazite, cheralite, allanite, bastnaesite and uranopolyrase.

Keywords: Gabal El-Dob, Wadi Abu Zawal, Gabal El-Urf, Pegmatites, Mineralogy, Radioactivity.

1658-7022© JNBAS. (1441 H/2020). Published by Northern Border University (NBU). All Rights Reserved.



jnbas.nbu.edu.sa

DOI: 10.12816/0056075

* Corresponding Author:

Professor, College of Engineering, Northern Border University, P.O. Box: 1321, Postal Code: 91431, Ar'ar, Kingdom of Saudi Arabia.

e-mail:anas.alsharef2@nbu.edu.sa

Manuscripts in English Language

CONTENTS

Manuscripts in English Language

- **Effect of The Mineralogical Composition On the Radioactivity of the Younger Granites and Pegmatites at Gabal El-Dob Area, Northern Eastern Desert, Egypt**
Doaa A. Moustafa, Mahmoud H. Shalaby, Ibrahim A. Salem, Samir M. Ali & Anas M. El-Sherif 82

- **A Comparative Study between two Video Compression Standards: The H.264 and the High Efficiency Video Coding**
Mohammad A. Barr..... 100

- **Dynamic Behavior of Static VAR Compensator during Faults of Grid Including Wind Power Plant**
E. Touti 116

- **Association of Body Mass Index, Age, and Gender with Bone Mineral Density in Patients Referred to King Fahad University Hospital**
Osama A M Kheiralla, Arafat M Goja, Adel O Bakheet, Ali Al-Ghamdi & Syed M Sadath 132

- **Nutritional Status of Breast Cancer Female Patients**
Ekram R. Soliman, Isis A. Nawar, Heba G. Elsheredy & Mariam A. Ginena 142

Citation from a book of more than one author:

Timothy, N., Stepich, D., & James, R. (2014/1434 H) *Instructional technology for teaching and learning*. Riyadh, Kingdom of Saudi Arabia: University of King Saud Publications.

Citation from Periodicals:

Al Nafaa, A. H. (1427 H). Effect of driving off-road on wild vegetation parks: A study in environmental protection, in the center of the Kingdom of Saudi Arabia. *Saudi Journal of Life Sciences*, 14(1), 35-72.

Citation from M.A. or Ph.D. Thesis:

AlQadi, I. A. (1429 H). *Natural Plants in a Coastal Environment between Rassi Tanoura and Elmalouh in the Eastern Region: A Study in Botanical Geography and the Protection of Environment*. Unpublished Ph.D. Dissertation, College of Arts for Girls, Dammam, Kingdom of Saudi Arabia: King Faisal University.

Citation from Internet References:

Citing an online book:

Almazroui, M. R. & Madani, M. F. (2010). *Evaluation of performance in Higher Education Institutions*. Digital Object Identifier (doi:10.xxxx/xxxx-xxxxxxx-x), or the Hypertext Transfer Protocol (http://www...), or the International Standard Book Number (ISBN: 000-0-00-000000-0) must be mentioned.

Citing an article in a periodical:

Almadani, M. F. (2014). The definition of debate in reaching consensus. *The British Journal of Educational Technology*, 11(6), 225-260. Digital Object Identifier (doi:10.xxxx/xxxx-xxxxxxx-x) or the Hypertext Transfer Protocol (http://onlinelibrary.wiley.com/journal/10.1111), or the International Standard Serial Number of the journal (ISSN: 1467- 8535) must be mentioned.

15. It is the researcher's responsibility to translate into English the Arabic bibliography.

Example:

الجبر، سليمان. (1991م). تقويم طرق تدريس الجغرافيا ومدى اختلافها باختلاف خبرات المدرسين وجنسياتهم وتخصصاتهم في المرحلة المتوسطة بالمملكة العربية السعودية. *مجلة جامعة الملك سعود- العلوم التربوية*، 3(1)، 143-170.

Al-Gabr, S. (1991). The evaluation of geography instruction and the variety of its teaching concerning the experience, nationality, and the field of study in intermediate schools in Kingdom of Saudi Arabia (*in Arabic*). *Journal of King Saud University- Educational Sciences*, 3(1), 143-170.

16. Numerals should be the original Arabic numbers (0, 1, 2, 3 ...) in the manuscript.

Required Documents

Researchers are required to submit the following:

1. An electronic copy of their submissions in two formats: Microsoft Word Document (WORD) and Portable Document Format (PDF), to be sent to the following email:

s.journal.nbu@gmail.com

&

s.journal@nbu.edu.sa

2. The researcher's CV, including his/her full name in Arabic and English, current work address, email, and academic rank.
3. The researcher must fill out and submit the application for publishing in the Journal of the North, along with the Pledge Statement that his/her submission has not been published before or has not been submitted for publishing elsewhere.

NB

1. The submissions received by the Journal of the North will not be returned whether they are published or not.
2. The published papers reflect only the author's points of view.
3. All accepted manuscripts devolve their property to *the Journal of the North for Basic and Applied Sciences (JNBAS)*.

PUBLICATION INSTRUCTIONS FOR AUTHORS

Submission Guidelines

1. Manuscript must not exceed 35 pages of plain paper (A4).
2. Manuscript must have a title and an abstract in both Arabic and English on one page; the abstract should not be more than 250 words. The manuscript should include, in both languages, keywords that indicate the field of specialization. The keywords are written below each summary and should not be more than six.
3. The author(s) name(s), affiliation(s) and address(es) must be written immediately below the title of the article, in Arabic and English.
4. The Arabic manuscript is typed in Simplified Arabic, in 14-font size for the main text, and 12-font size for notes.
5. The English manuscript is typed in Times New Roman, in 12- font size for the main text, and 9-font size for notes.
6. The manuscript is typed only on one side of the sheet, and line spacing should be single. Margins should be 2.5 cm (or 1.00 inches) on all four sides of the page.
7. The manuscript must have the following organization:
 - Introduction:** It should indicate the topic and aims of the research paper, and be consistent with its ideas, information and the established facts. The research problem(s) and importance of the literature review should also be introduced.
 - Body:** The manuscript body includes all necessary and basic details of research approach, tools and methods. All stated information should be arranged according to priority.
 - Findings and Discussion:** Research findings should be clear and brief, and the significance of these findings should be elucidated without repetition.
 - Conclusion:** It is a brief summary of the research topic, findings, recommendations and suggestions.
8. Figures, diagrams and illustrations should be included in the main text and consecutively numbered and given titles, with explanatory notes beneath them.
9. Tables should also be included in the main text, consecutively numbered and given titles at the top, with explanatory notes below.
10. Footnotes should be added at the bottom of each page, when necessary. They are to be indicated by numbers or asterisks, in 12-font size for Arabic and 9-font size for English.
11. The Journal of the North does not publish research and measurement tools (instruments). However, they must be included in the submission(s).
12. Citations must follow the American Psychological Association (APA) reference style in which both the author's name and year of publishing are mentioned in the main text, i.e. (name, year). Numbering the references inside the main text and adding footnotes are not allowed.

Researchers' documentation must be as follows:

 - For single author, the author's family name, followed by a comma, and the publishing year, such as (Khayri, 1985). Page numbers are indicated in the main text in case of quotations, such as (Khayri, 1985, p. 33).
 - If a manuscript has two authors, they must both be cited as shown previously, e.g. (AL-Qahtani & AL-Adnani, 1426 H).
 - If there are multiple (more than two) authors, their family names must be mentioned the first time only, e.g. (Zahran, Al-Shihri, & Al-Dusari, 1995); if the researcher is quoting the same work several times, the family name of the first author followed by "et al." [for papers in English] and by "وأخرون" [for papers in Arabic] must be used, e.g. (Zahran et al., 1995) / (1995 زهران وأخرون). Full publishing data must be mentioned in the bibliography.
13. Hadith documentation must follow the following example: (Sahih Al-Bukhari, vol.1, p.5, hadith number 511).
14. The bibliography, list of all the sources used in the process of researching, must be added in alphabetical order using the author's last name according to the APA reference style (6th edition) in 12-font size for Arabic and 9-font size for English.

The bibliography should be organized as follows:

Citation from books:

Citation from a one-authored book:

Shotton, M. A. (1989). *Computer education? A study to computer dependency*. London, England: Taylor & Francis.

Journal of the North for Basic and Applied Sciences (JNBAS)

About the Journal

The Journal of the North is concerned with the publication of original, genuine scholarly studies and researches in Basic and Applied Sciences in Arabic and English. It publishes original papers, review papers, book reviews and translations, abstracts of dissertations, reports of conferences and academic symposia. It is a biannual publication (May and November).

Vision

The journal seeks to achieve leadership in the publication of refereed scientific papers and rank among the world's most renowned scientific periodicals.

Mission

The mission of the journal is to publish refereed scientific researches in the field of Basic & Applied Sciences according to well-defined international standards.

Objectives

1. Serve as a scholarly academic reference for researchers in the field of Basic & Applied Sciences.
2. Meet the needs of researchers, publish their scientific contributions and highlight their efforts at the local, regional and international levels.
3. Participate in building a knowledge community through the publication of research that contributes to the development of society.
4. Cover the refereed works of scientific conferences.

Terms of Submission

1. Originality, innovation, and soundness of both research methodology and orientation.
2. Sticking to the established research approaches, tools and methodologies in the respective discipline.
3. Accurate documentation.
4. Language accuracy.
5. The contribution must be unpublished or not submitted for publication elsewhere.
6. The research extracted from a thesis/dissertation must be unpublished or not submitted for publishing elsewhere and the researcher must indicate that the research submitted for publishing in the journal is extracted from a thesis/dissertation.

Correspondence

Editor-in-Chief
Journal of the North for Basic and Applied Sciences (JNBAS),
Northern Border University, P.O.Box 1321, Arar 91431,
Kingdom of Saudi Arabia.
Tel: +966(014)6615499
Fax: +966(014)6614439
email: s.journal@nbu.edu.sa & s.journal.nbu@gmail.com
Website: <http://jnbas.nbu.edu.sa>

Subscription & Exchange

Scientific Publishing Center,
Northern Border University,
P.O.Box. 1321, Arar 91431,
Kingdom of Saudi Arabia.



Journal of the North for Basic and Applied Sciences (JNBAS)

Peer-Reviewed Scientific Journal

Published by

**Scientific Publishing Center
Northern Border University**

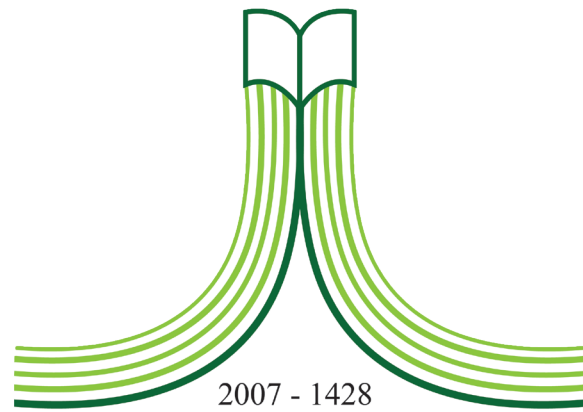
**Vol. (5), Issue (2)
November 2020 – Rab'II 1442 H**

Website & Email

<http://jnbas.nbu.edu.sa>

s.journal@nbu.edu.sa & s.journal.nbu@gmail.com

p-ISSN: 1658- 7022 / e-ISSN: 1658- 7014



جامعة الحدود الشمالية
NORTHERN BORDER UNIVERSITY
Kingdom of Saudi Arabia



IN THE NAME OF ALLAH
THE MOST GRACIOUS, THE MOST MERCIFUL